PREPARATION OF NOVEL FIBER COATINGS FOR SOLID PHASE MICROEXTRACTION OF FLAVONOIDS

A Thesis Submitted to

the Graduate School of Engineering and Sciences of

İzmir Institute of Technology

in Partial Fulfillment of the Requirements for the Degree of

DOCTOR OF PHILOSOPHY

in Chemistry

by Meral ESEN

July 2014

İZMİR

We approve the thesis of **MERAL ESEN**

Examining Committee Members:

Prof. Dr. Ahmet E. EROĞLU
Department of Chemistry, İzmir Institute of Technology

Prof. Dr. Figen TOKATLI
Department of Food Engineering, İzmir Institute of Technology

Prof. Dr. Nil ERTAŞ
Department of Chemistry, Ege University

Prof.Dr. Serdar ÖZÇELİK
Department of Chemistry, İzmir Institute of Technology

Assist. Prof.Dr. Hasan ERTAŞ
Department of Chemistry, Ege University

14 July 2014

Prof.Dr. Ahmet E. EROĞLU
Supervisor, Department of Chemistry
İzmir Institute of Technology

Assoc.Prof. Dr. Ali ÇAĞIR
Co-Supervisor, Department of Chemistry
İzmir Institute of Technology

Prof.Dr. Ahmet E. EROĞLU
Head of the Department of Chemistry

Prof.Dr. R. Tuğrul SENGER
Dean of the Graduate School of
Engineering and Sciences

ACKNOWLEDGEMENTS

It would not have been possible to write this doctoral thesis without the help and support of the kind people around me, to only some of whom it is possible to give particular mention here.

I would like to express my deepest gratitude to my supervisor Prof.Dr. Ahmet E. EROĞLU for his suprevision, continous support he provided me during my studies in İYTE.

I specially express thanks to the members of the thesis committee, Prof. Dr. Nil ERTAŞ, Prof. Dr. Serdar ÖZÇELİK, Prof.Dr. Figen TOKATLI, and Assist. Prof. Hasan ERTAŞ for their valuable comments. I would like to thank again Assoc. Prof.Dr. Ali ÇAĞIR for his suggestions to complete my research.

This thesis would have remained a dream had it not been for my friend, Dr. Ayşegül ERDOĞAN. I cannot find words to express my gratitude because of her endless help and excellent suggestions to complete my reserach. She always stands by me.

I would like to show my greatest appreciation to Dr. Hüseyin Özgener, I cannot thank him enough for his tremendous support and help. I feel motivated and encouraged every time I attend his meeting. Without his encouragement and guidance this project would not have materialized.

I am grateful to my dad Mustafa KARACA and Polat Bulanık for his endless help in the experimental setup design, and for their genius ideas.

Special thanks to İYTE MAM for their help in performing SEM analysis, Esra TUZCUOĞLU YÜCEL for FTIR analysis.

Moreover, I am thankful to my colleagues and room mates; Esen DÖNERTAŞ, Merve DEMİRKURT for their friendship and inner support.

And last, but by not the least, I wish to thank my family for the support they have given. Without the support and confidence of my parents and my husband Hasan ESEN would never have been able to achive what I have. I do really appreciate my brother Mehmet KARACA for sharing his experiences with me, for listening to my complaints and frustrations and for believing in me.

ABSTRACT

PREPARATION OF NOVEL FIBER COATINGS FOR SOLID PHASE MICROEXTRACTION OF FLAVONOIDS

Many plant species contain flavonoids which are widely utilized in food, pharmaceutical and cosmetics industries as additives. Literature studies show that most of the earliest drugs were of plant origin. Application of flavonoids in many fields necessitates the development of new extraction and determination methods in various samples.

In this study, three different types of solid phase microextraction (SPME) coatings were produced. The first one is baicalin- and imidazole-functionalized silica fibers via sol-gel method. Both manual and dip-coating were employed. The fibers were examined by SEM and the results show that dip-coating produced more homogeneous coatings. The second one is polystyrene templated monolithic silica. Then, it was functionalized with baicalin and imidazole groups. The last solid phase microextraction coating is molecularly imprinted silica. In this case, a sol-gel process was used to synthesize molecularly imprinted silica with tetraethoxysilane (TEOS) as the crosslinking agent, aminopropytriethoxysilane (APTES) as a functional monomer, quercetin as the template molecule, and $AlCl_3$ as a Lewis acid. Characterization of baicalin-functionalized monolithic silica and molecularly imprinted silica was achieved by SEM, FTIR, TGA and elemental analysis. SPME process was followed by HPLC-DAD at 335 nm after separation of flavonoids on a Zorbax Eclipse XDB-C18 (5μm, 4.6x150mm) column at 25.0°C with gradient elution using methanol and water (containing 0.10% acetic acid). Functionalized silica fibers were utilized in solid phase microextraction of apigenin, apigetrin, eriodictyol, isoquercitrin, luteolin, and quercetin. The results demonstrated that higher extraction efficiency can be obtained with baicalin-functionalized monolithic silica and molecularly imprinted silica coated fibers.

ÖZET

FLAVONOİDLERİN KATI FAZ MİKROEKSTRAKSİYONU İÇİN YENİ FİBER KAPLAMALARININ HAZIRLANMASI

Flavonoid içeren çok sayıda bitki gıda, ilaç ve kozmetik endüstrisinde yaygın olarak kullanılmaktadır. Literatür çalışmaları ilk ilaçların bitkisel kaynaklı olduğunu göstermektedir. Flavonoidlerin farklı alanlardaki uygulamaları yeni ekstraksiyon ve tayin yöntemlerinin geliştirilmesini gerektirmektedir.

Bu çalışmada, üç farklı katı faz mikroekstraksiyon (SPME) kaplaması üretilmiştir. İlk olarak, sol-gel yöntemi ile sentezlenen baikalin- ve imidazol- grupları ile işlevselleştirilmiş kaplamalar yer almaktadır. Bu fiberler hem manuel kaplama hem de sol-jel kaplama cihazı (dip coater) kullanarak üretilmiştir. Fonksiyonelleştirilmiş silika fiberler taramalı elektron mikroskobu ile karakterize edilmiştir ve elde edilen sonuçlara göre sol-jel kaplama cihazı ile yapılan kaplamalarda homojen kaplamalar elde edilmiştir. İkinci tip kaplamapolistiren kalıp yöntemi ile sentezlenen monolitik silikayı içermektedir. Monolitik silika daha sonra baikalin- ve imidazol- grupları ile işlevselleştirilmiştir. Son katı faz mikroekstraksiyon kaplaması moleküler baskılama yöntemi ile hazırlanan silikadır. Moleküler baskılanmış silika sol-jel yöntemi ile, çapraz bağlayıcı olarak tetraethoxysilane (TEOS), fonksiyonel monomer olarak aminopropyltriethoxysilane (APTES), kalıp molekül olarak kuersetin ve Lewis asit olarak $AlCl_3$ kullanılmıştır. Baikalin ile işlevselleştirilmiş monolitik silika ve moleküler baskılı silikanın karakterizasyonu SEM, FTIR, TGA ve elemental analiz yöntemleri ile yapılmıştır. SPME prosesinden sonra flavonoidler HPLC-DAD kullanarak Zorbax Eclipse XDB-C18 (5µm, 4.6x150mm) kolonunda 25ºC'de gradient elüsyon ile ayrılmış ve 335 nm'de tayin edilmiştir. Hazırlanan SPME kaplamaları apigenin, apigetrin, eriodictyol, izokuersetin, luteolin, and kuersetinin katı faz mikroekstraksiyonunda kullanılmıştır. Sonuçlar, baikalin ile işlevselleştirilmiş monolitik silika ve moleküler baskılı silika ile kaplanan fiberler ile yüksek ekstraksiyon verimi elde edilebileceğini göstermiştir.

TABLE OF CONTENTS

LIST OF FIGURES ix

LIST OF TABLES xiii

LIST OF ABBREVIATIONS xiv

CHAPTER 1. INTRODUCTION 1

1.1. Flavonoids 1

1.2. Extraction of Flavonoids 5

1.3. Solid Phase Microextraction (SPME) 6

1.3.1. Types of SPME 7

1.3.2. Solid Phase Microextraction Coatings 10

1.3.3. Monolithic Microextraction Coatings 13

1.3.4. Solid Phase Microextraction of Flavonoids 16

1.4. HPLC Analysis of Flavonoids 18

1.5. UV Detection of Flavonoids 19

1.6. Plants Used for the Extraction of Flavonoids 20

1.6.1. *Laurus nobilis* 20

1.7. Aim of This Study 22

CHAPTER 2. EXTRACTION OF FLAVONOIDS: METHOD DEVELOPMENT 23

2.1. Experimental 23

2.1.1. Preparation of Stock Solutions 23

2.1.2. Plant Material 23

2.1.3. Chemicals and Reagents 23

2.1.4. Instrumentation and Apparatus 27

2.1.5. Extraction of Flavonoids 28

2.1.5.1. Ultrasonic Extraction 28

2.5.1.2. Soxhlet Extraction 28

2.5.1.3. Magnetic Stirring 28

2.2. Results and Discussion 29

2.2.1. Elemental Analysis 29
2.2.2. UV Spectra of Flavonoids 29
2.2.3. HPLC Analysis 32
2.2.4. Analytical Performance of the Method 36

CHAPTER 3. NOVEL SOLID PHASE MICROEXTRACTION COATINGS FOR FLAVONOIDS PART I: SOL-GEL COATINGS 41
3.1. Experimental 41
3.1.1. Chemicals and Reagents 41
3.1.2. Preparation of SPME Fiber 41
3.1.3. Chloro- and Amine- Coating of Bare Silica Fiber 46
3.1.4. Imidazole- and Baicalin- Functionalization of SPME Fibers 46
3.2. Results and Discussion 48
3.2.1. Characterization of SPME Fibers 48
3.2.1.1. SEM Results 48

CHAPTER 4. NOVEL SOLID PHASE MICROEXTRACTION COATINGS FOR FLAVONOIDS PART II: MONOLITHIC SILICA 68
4.1. Experimental 68
4.1.1. Chemicals and Reagents 68
4.1.2. Synthesis of Polystyrene Templated Monolithic Silica 73
4.1.2.1. Synthesis of Polystyrene Macropore Template 73
4.1.2.2. Synthesis of Silica Monolith 75
4.1.2.3. Imidazole Functionalization of Silica Monolith 76
4.1.2.4. Baicalin Functionalization of Silica Monolith 78
4.1.2.5. SPME Fiber Coating with Imidazole- and Baicalin-Functionalized Monolithic Silica 79
4.2. Results and Discussion 81
4.2.1. Characterization of Polystyrene Nanosphers 81
4.2.1.1. SEM images 81
4.2.2. Characterization of Monolithic Silica, and Functionalized Monolithic Silicas 84
4.2.2.1. SEM images 84
4.2.2.2. FTIR Results 90

4.2.2.3. Elemental Analysis 92
4.2.2.4. Thermal Gravimetric Analysis 93
4.2.3. SPME of Flavonoids by Baicalin-Functionalized Monolithic Silica Fibers 94

CHAPTER 5. NOVEL SOLID PHASE MICROEXTRACTION COATINGS FOR FLAVONOIDS PART III: MOLECULARLY IMPRINTED SILICA ... 97
5.1. Experimental 97
5.1.1. Reagents and Solutions 97
5.1.2. Preparation of MIS SPME Fiber 97
5.2. Results and Discussion 102
5.2.1. Characterization 102
5.2.1.1. SEM Images 102
5.2.1.2. Elemental Analysis 106
5.2.1.3. FTIR Analysis 106
5.2.2. SPME of Flavonoids 108

CHAPTER 6. CONCLUSION 110

REFERENCES 113

LIST OF FIGURES

Figure **Page**

Figure 1.1. Basic flavonoid structure 2
Figure 1.2. Structures of the various classes of flavonoids 3
Figure 1.3. Summary of microextraction techniques. 7
Figure 1.4. Solid-phase microextraction and related microextraction techniques 9
Figure 1.5. SPME extraction modes: direct extraction, and headspace extraction 10
Figure 1.6. Chemical reactions involved in sol-gel coating of fused silica fiber. 11
Figure 1.7. HPLC profile for 28 different polyphenols on a C18 column. 19
Figure 1.4. *Laurus nobilis* Bay Laurel (*Laurus nobilis*) flower buds and leaves. 21
Figure 1.5. Geographical distribution of Laurus nobilis in Turkey 22
Figure 2.1. UV spectra of apigenin, apigetrin, and catechin in methanol. 30
Figure 2.2. UV spectra of eriodictyol, and luteolinin methanol. 31
Figure 2.3. UV spectra of quercetin, and isoquercitrinin methanol. 32
Figure 2.4. HPLC chromatogram of apigenin, apigetrin, and eriodictyol. 34
Figure 2.5. HPLC chromatogram of isoquercitrin, luteolin, and quercetin. 35
Figure 2.6. HPLC chromatogram of flavonoids 36
Figure 2.7. HPLC chromatogram of methanolic extract 36
Figure 2.8. Calibration plots of the standards 37
Figure 3.1. Dip coater 47
Figure 3.2. The reaction scheme for the preparation of imidazole- and baicalin-functionalized silica fibers. 47
Figure 3.3. Experimental setup for the synthesis of baicalin- and imidazole-functionalized SPME fibers. 48
Figure 3.4. SEM images of bare fiber at varous maginifications. 49
Figure 3.5. SEM images of manually single layer coated sol-gel based chloro-functionalized (no PDMS) SPME fibers. 50
Figure 3.6. SEM images of manually double layer coated sol-gel based chloro-functionalized (no PDMS) SPME fiber. 51
Figure 3.7. SEM images of manually double layer coated sol-gel based chloro-functionalized SPME fibers at various magnifications. 52

Figure 3.8. SEM images of manually double layer coated sol-gel based chloro-functionalized (with PDMS) SPME fiber (from a different parts of a fiber)..... 53
Figure 3.9. SEM images of manually coated 1-vinylimidazole modified SPME fibers after single layer coating of sol-gel based chloro-functionalization (no PDMS) at various magnifications. 54
Figure 3.10. SEM images of manually coated 1-vinylimidazole modified SPME fibers after double layer coating of sol-gel based chloro-functionalization (no PDMS) at various magnifications..... 55
Figure 3.11. SEM images of manually coated 1-vinylimidazole modified SPME fibers after single layer coating of sol-gel based chloro-functionalization (with PDMS) at various magnifications..... 56
Figure 3.12. SEM images of manually coated 1-vinylimidazole modified SPME fibers after double layer coating of sol-gel based chloro-functionalization (with PDMS) at various magnifications. 57
Figure 3.13. SEM images of manually coated 1-methylimidazole modified SPME fibers after single layer coating of sol-gel based chloro-functionalization (no PDMS) at various magnifications..... 58
Figure 3.14. SEM images of manually coated 1-methylimidazole modified SPME fibers after double layer coating of sol-gel based chloro-functionalization (no PDMS) at various magnifications. 59
Figure 3.15. SEM images of manually coated 1-methylimidazole modified SPME fibers after single layer coating of sol-gel based chloro-functionalization (with PDMS) at various magnifications. 60
Figure 3.16. SEM images of manually coated 1-methylimidazole modified SPME fibers after double layer coating of sol-gel based chloro-functionalization (with PDMS) at various magnifications. 61
Figure 3.17. SEM images of sol-gel based chloro-functionalized fibers SPME fibers with dip coater: single layer coating..... 62
Figure 3.18. SEM images of of sol-gel based chloro-functionalized fibers with dip coater: double layer coating 63
Figure 3.19. SEM images of sol-gel based chloro-functionalized fibers with dip coater: triple layer coating. 64

Figure 3.20. SEM images of sol-gel based amine-functionalized fibers SPME fibers with dip coater: single layer coating 65
Figure 3.21. SEM images of imidazole-functionalized silica fiber (after triple layer chloride coating silica fiber) at various magnifications. 66
Figure 3.22. SEM images of baicalin-functionalized silica fiber (after triple layer amine coating of silica fiber) at various magnifications..... 67
Figure 4.1. Change in the color of styrene during the extraction with NaOH. 74
Figure 4.2. Set-up for the synthesis of polystyrene nanospheres..... 74
Figure 4.3. Set-up for the synthesis of polystyrene nanospheres..... 75
Figure 4.4. Set-up for the synthesis of silica monolith. 76
Figure 4.5. Reaction scheme for the preparation of imidazole-functionalized silica monolith. 77
Figure 4.6. Experimental setup for the preparation of ionic liquid..... 78
Figure 4.7. Experimental setup for the amine-modification of monolithic silica. 79
Figure 4.8. SEM images of polystyrene nanoparticles (synthesized by magnetic stirring) 82
Figure 4.9. SEM images of polystyrene nanoparticles (synthesized by mechanical stirring) 83
Figure 4.10. SEM images of silica monolith (n-pentane as a cosurfactant) 85
Figure 4.11. SEM images of silica monolith (n-pentane/ethanol mixture as a cosurfactant)..... 86
Figure 4.12. SEM images of baicalin functionalized silica monolith at different magnifications 88
Figure 4.13. SEM images of imidazole functionalized silica monolith at different magnifications 89
Figure 4.14. FTIR spectra of silica monolith, baicalin modified silica monolith, and imidazole modified silica monolith..... 91
Figure 4.15. TGA decomposition curve of monolithic silica, and baicalin-functionalized monolithic silica 95
Figure 4.16. Extraction percentages of flavonoids 95
Figure 4.17. Desorption profile of flavonoids 96
Figure 5.1. Mechanism proposal of MIS-Al synthesis. 101
Figure 5.2. Sem images of MIS prepared with 0.01 M $AlCl_3$ 103
Figure 5.3. Sem images of MIS prepared with 0.1 M $AlCl_3$… 103

Figure 5.4. Sem EDX spectra of MIS prepared with 0.10 M $AlCl_3$ and 0.1 M $AlCl_3$.. 105
Figure 5.5. FTIR sectra of MIS prepared with 0.01 M $AlCl_3$ and 0.1 M $AlCl_3$ 107
Figure 5.6. TGA decomposition curve of MIS prepared with 0.01 M $AlCl_3$ and 0.10 M $AlCl_3$ 1097
Figure 5.7. Extraction percentages of flavonoids 109
Figure 5.8. Desorption profile of flavonoids 109

LIST OF TABLES

Table **Page**

Table 1.1. Structure of flavonoids and their bioavailability in foods 4
Table 1.2. Reagents used in sol-gel solution 12
Table 1.3. Monolithic extraction phases for the solid phase microextraction in the literature 14
Table 1.4. SPME of fibers used in the literature for the determination of flavonoids 17
Table 2.1. The properties of chemicals and reagents. 24
Table 2.2. Elemental composition of *Laurus Nobilis* 29
Table 2.3. Parameters of the analytical curves, LOD and LOQ for flavonoids quantification. 39
Table 2.4. Amounts of flavonoids (mg of flavonoid /g of plant) extracted from *Laurus nobilis*. 40
Table 3.1. The properties of chemicals and reagents. 42
Table 3.4. Elemental composition of chloro-functionalized silica fibers (from SEM EDX results of Figure 3.22). 63
Table 3.5. Elemental composition of chloro-functionalized silica fibers (from SEM EDX results of Figure 3.23). 64
Table 4.1. The properties of chemicals and reagents. 69
Table 4.2. Elemantal composition of monolithic silicas. 92
Table 5.1. The properties of chemicals and reagents. 99
Table 5.2. SEM EDX results of MIS 105
Table 5.3. Elemental composition of MIS in terms of %C, %H, %N, and %S. 106

LIST OF ABBREVIATIONS

Abbreviation	Meaning
APTES	(3-aminopropyl)triethoxysilane or (3-(Triethoxysilyl)propylamine)
APTMOS	(3-aminopropyl)trimethoxysilane or (3-(Trimethoxysilyl)propylamine)
BSTFA	Bis(trimethylsilyl) trifluoroacetamide
CAR	Carboxen
CPTMOS	(3-Chloropropyl)trimethoxysilane
CPTES	(3-Chloropropyl)triethoxysilane
CW/TPR	Carbowax/Templated Resin
DAD	Diode Array Detection
DCM	Dichloromethane of methylenechloride
DMF	Dimethyl formamide
DVB	Divinylbenzene
EDCl	1-(3-dimethylaminopropyl)-3-ethylcarbodiimide hydrochloride
EtOH	Ethanol
FTIR	Fourier Transform Infrared Spectroscopy
F127	Pluronic F127
GC	Gas Chromatography
GC-MS	Gas Chromatography-Mass Spectrometry
HPLC	High-Performance Liquid Chromatography
LOD	Limit of Detection
LOQ	Limit of Quantitation
LPME	Liquid Phase Microextraction
MEPS	Microextraction in a Packed Syringe
MeOH	Methanol
MIP	Molecularly Imprinted Polymer
MIS	Molecularly Imprinted Silica
MTMOS	Methyltrimethoxysilane
PA	Polyacrylate

Abbreviation	Meaning
PDMS	Poly(dimethylsiloxane)
PEG	Polyethylene glycol
PMHS	Poly(methylhydrosiloxane)
SEM	Scanning Electron Microscopy
SPE	Solid-Phase Extraction
SDME	Single-Drop Microextraction
SPDE	Solid-Phase Dynamic Extraction
SPME	Solid-Phase Microextraction
SBSE	Stir Bar Sorptive Extraction
Styrene	Phenylethylene, Vinylbenzene
TEA	Triethylamine
TMOS	Tetramethylorthosilicate (or Tetramethoxysilane)
TEOS	Tetraethylorthosilicate (or Tetraethoxysilane)
TFA	Trifluoroacetic Acid
TFME	Thin Film Microextraction
TGA	Thermo Gravimetric Analysis
TR	Templated Resin
THF	Tetrahydrofuran
UV	Ultraviolet

CHAPTER 1

INTRODUCTION

1.1. Flavonoids

Flavonoids are polyphenolic compounds that produce the flavour of fruits and vegetables as well as the red and blue pigments of plants, and have been used in taxonomic studies of angiosperms (Hrazdina, 1982). Other roles of flavonoids to be performed by plants are modulation of enzymatic activity, insect attraction or repulsion, nectar guides, viral, fungal, and bacterial protection (Andersen and Markham 2006). The core structure consists of a C15 skeleton with two aromatic rings joined by a chromane ring (Aruoma et al., 2003) (Figure 1.1.). Flavonoids are divided into six subgroups: flavones, flavonols, flavanols, flavanones, isoflavones, and anthocyanins, according to the oxidation state of the central C ring (Mumper and Dai 2010) (Figure 1.2.). Table 1.1. summarizes the presence of flavonoids in foods and their structures. The difference in the number and nature of substituent groups attached to the rings within the various classes makes the further differentiation of flavonoids possible (Robards and Antolowich, 1997). Like most plant constituents, flavonoids can exist both as free aglycones and as glycosidic conjugates. The glycosylation renders the flavonoid less reactive, more polar and thus more water soluble, so that this modification can be thought as an essential form of protection in plants to prevent cytoplasmic damage and to store the flavonoids safely in the cell vacuole (Cuyckens et al., 2003; Justesen et al., 1998).

According to the literature studies, flavonoids were involved in disease resistance in plants. For example, phytoalexin is the compound that is produced by the plants in case of infection of microorganisms to prevent them from affecting the disease organisms. Flavonoid compounds were reported as phytoalexins from various plant species. The greater number of flavonoid phytoalexins were primarily isolated from underground parts, such as roots, rhizomes, hypocotyls, or seeds (Iwashina, 2003).

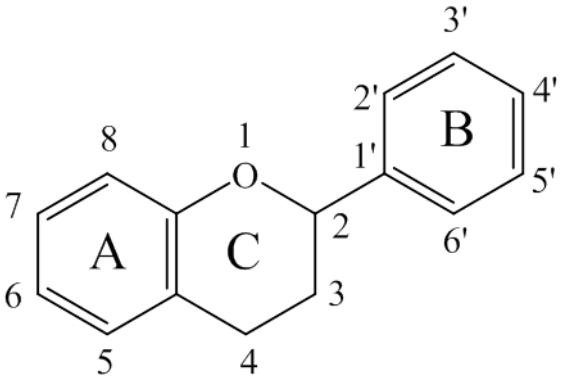

Figure 1.1. Basic flavonoid structure

Another important function of flavonoids is to serve as an ultraviolet (UV) filter in land plants; enhanced levels of flavonoids were observed in plants exposed to strong UV radiation (Monici et al., 1994; Takeda et al., 1994). Monici et al. (1994) investigated the function of kaempferol and pelargonidin as photoprotectors, the results demonstrated that both compounds play a role in plant protection by distinctly different mechanisms. For example, pelargonidin acts as a strong radical scavenger, while kaempferol can be thought as a good screen against UV radiation.

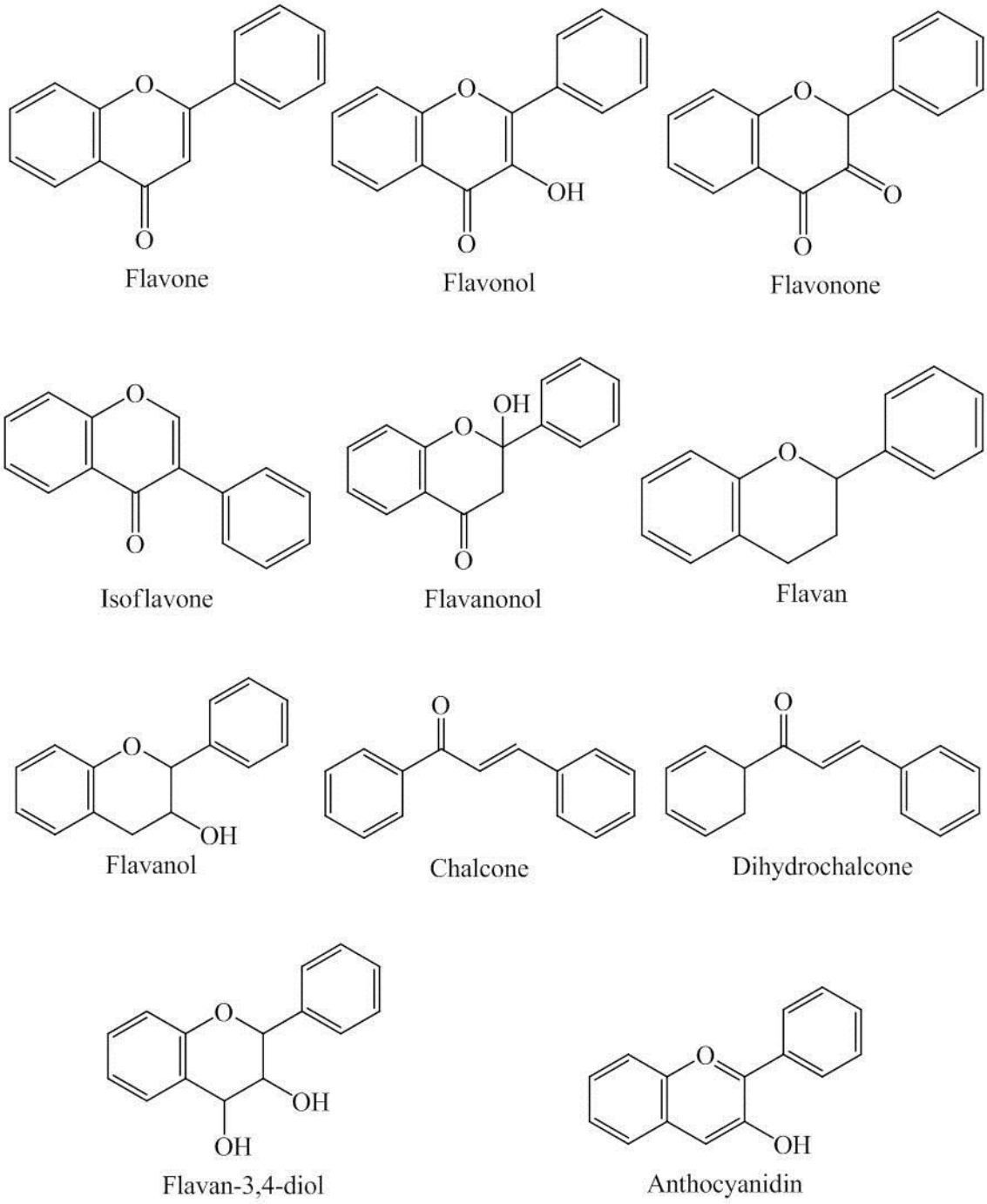

Figure 1.2. Structures of the various classes of flavonoids

(Source: Corradini et al., 2011)

Table 1.1. Structure of flavonoids and their bioavailability in foods (Source: D'Archivio et al., 2007).

Flavanoids	Examples	Structure	Food
Flavonols	Quercetin	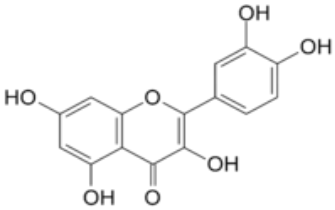	Onion, Broccoli, Buckwheat tea, Apple
Flavanols	Catechin	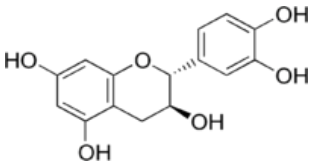	Red wine, black tea
	Epigallocatechin gallate	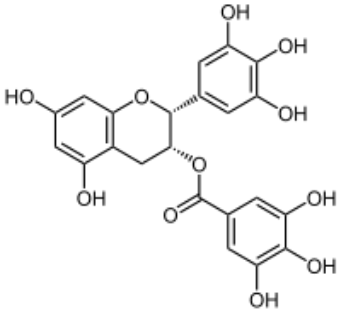	Green tea
	Proanthocyanidin	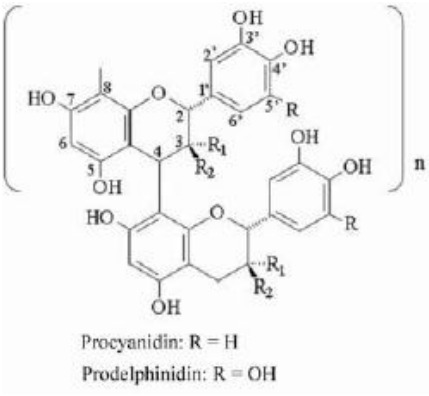	Grapeseed
Flavanones	Hesperidin	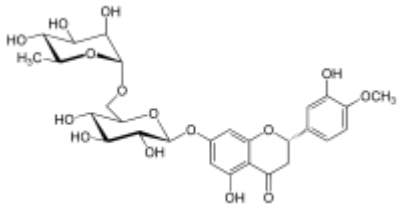	Orange juice
	Naringenin	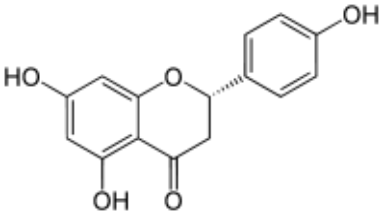	Orange juice, Grapefruit juice

(cont. on next page)

Table 1.1. (cont.).

Flavanoids	Examples	Structure	Food
Flavones	Apigenin	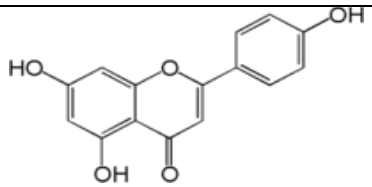	Mandarin
	Daidzein	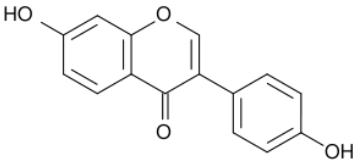	Soy milk, Soy extract, Soy nuts
	Genistein	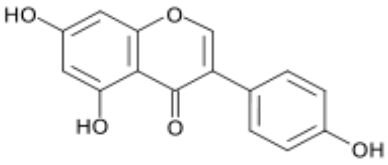	Soy milk, Soy extract, Soy nuts
Isoflavones	Glycitein	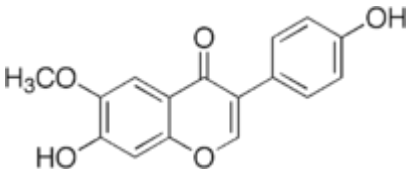	Soy milk
Anthocyanins	Cyanidin	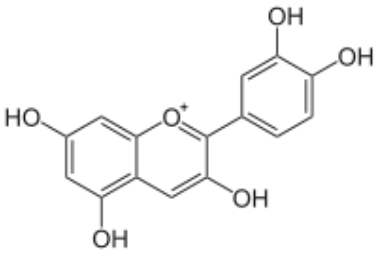	Berry fruits (black currant, raspberry, blackberry, *etc.*)

1.2. Extraction of Flavonoids

Flavonoids can be degraded by enzyme action once plant material is fresh or nondried. Therefore, use of dry, lyophilized, or frozen samples is advisable (Andersen and Markham, 2006). In the case of dry sample, the sample is generally ground into powder for the homogenization of the sample material. The flavonoid type defines the solvent used for the extraction step. Polarity becomes an important parameter in the extraction. Generally, less polar flavonoids like isoflavones, flavanones, methylated flavones, and flavonols are extracted with chloroform, dichloromethane, diethyl ether, or ethyl acetate; however flavonoid glycosides and more polar aglycones are extracted

with alcohols or alcohol–water mixtures. Aqueous alcoholic solutions are appropriate as glycosides of flavonoids have increased water solubility compared with their aglycone analogs. The majority of the extraction has still performed with simple direct solvent extraction. Soxhlet apparatus has also found use in the extraction of flavonoids to remove lipids with hexane, then extraction is continued with ethyl acetate or ethanol to obtain flavonoids. However, this process can decompose the heat –sensitive compounds.

Sequential solvent extraction isused commonly procedure. The less polar flavonoids and flavonoid aglycones can be extracted with dichloromethane, and then the polar flavonoids and flavonoid glycosides can be extracted with alcohol, for example.

In many cases, water can extract flavan-3-ols (catechins, proanthocyanidins), but the extraction solvent defines the composition of the extract. Hussein et al., 1990 explained that methanol is the best solvent for catechins and 70% acetone for procyanidins.

Acidified alcoholic solutions are utilized for anthocyanins. Acetic acid or trifluoroacetic acid (TFA) are the examples and the acidification of alcoholic solutions (Andersen and Markham, 2006), as attached acyl groups can be lost by the use of mineral acid.

Usually, extraction is carried out with magnetic stirring or shaking. Ultrasound-assisted extraction is a quick process, and it allows to use the mixtures of immiscible solvents. Sergenti et al., 2000 used the solvent system, for example, hexane with methanol–water (9:1), for the Brazilian plant *Lychnophora ericoides* (Asteraceae) ones.

1.3. Solid Phase Microextraction (SPME)

It is to emphasize that the isolation of desired compounds from complex matrixes (e.g. plants) is important in terms of the analysis reliability and accuracy. For this reasons, solid phase microextraction is an attractive sample preaparation technique due to its being automation, high-throughput performance, online coupling with analytical instruments, and low-cost operation through less solvent consumption. Microextraction techniques have the advantages over the traditional extraction techniques like liquid-liquid extraction. Figure 1.3. summarizes the microextraction techniques which have been used in the sample preparation techniques.

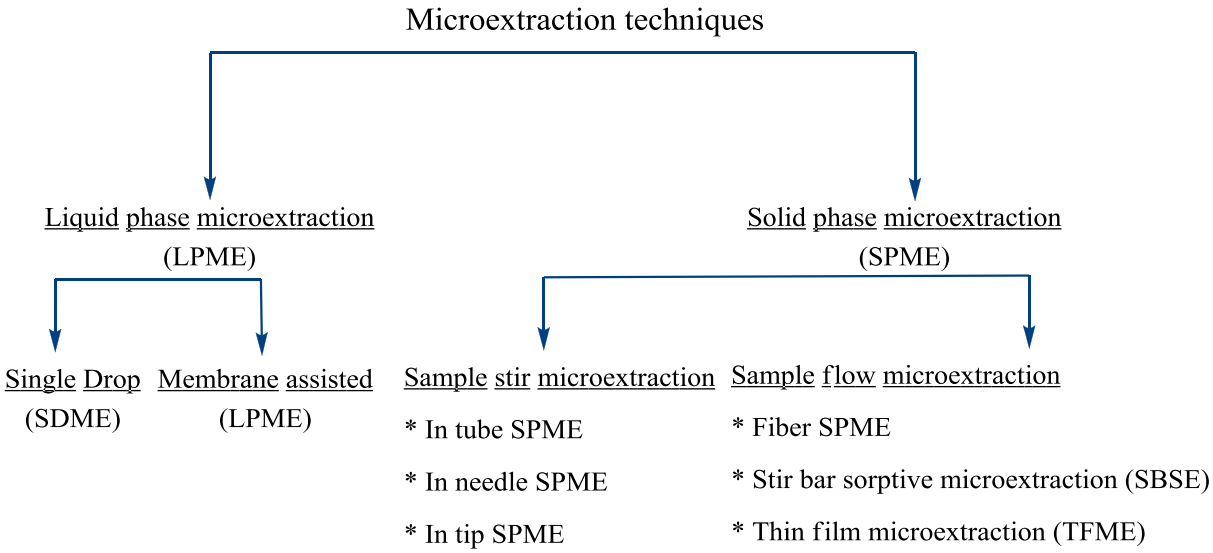

Figure 1.3.Summary of microextraction techniques
(Source: Pawliszyn J., 1999).

.

Microextraction techniques are illustrated briefly in Figure 1.4. These methods are performed with minimum amounts of solvent. Hence, it makes the extraction process carried out with minimal amount of toxic solvent.

Fiber SPME is one of the microextraction techniques that is based on that fused-silica fiber coated with a suitable stationary phase. Once the coated fibers are dipped into the analyte solution, the desired analytes partition from the sample matrix into the polymeric stationary phase coated on the surface of the fiber takes place until the equilibrium is reached. Fiber SPME has been utilized routinely in combination with GC and GC-MS for a wide variety of of volatile and semivolatile organic compounds. HPLC, CE and LC-MS techniques are applied to analyze weakly volatile or thermally labile compounds.

1.3.1. Types of SPME

Two types of fiber SPME extraction modes are applied: direct extraction, and headspace extraction (Figure 1.4., and 1.5.). These are either performed manually or automatically and used in combination with any GC, GC-MS, HPLC, LC-MS. Direct extraction mode is used for the extraction of nonvolatile analytes, and the coated fiber is immersed in liquid samples. Carbowax, PDMS, Polyvinylbenzene, Carboxen, or

templated resins coatings are the examples for the commercial available fibers (Table 1.2.). However, head-space extraction mode is used in the extraction of volatile and semivolatile analytes from the vapor phase above gaseous, liquid, or solid samples. Mostly nonpolar analytes are extracted with a PDMS, polyacrylate, DVB, and PDMS/DVB fibers, and then they are analyzed in combination with GC and GC-MS.

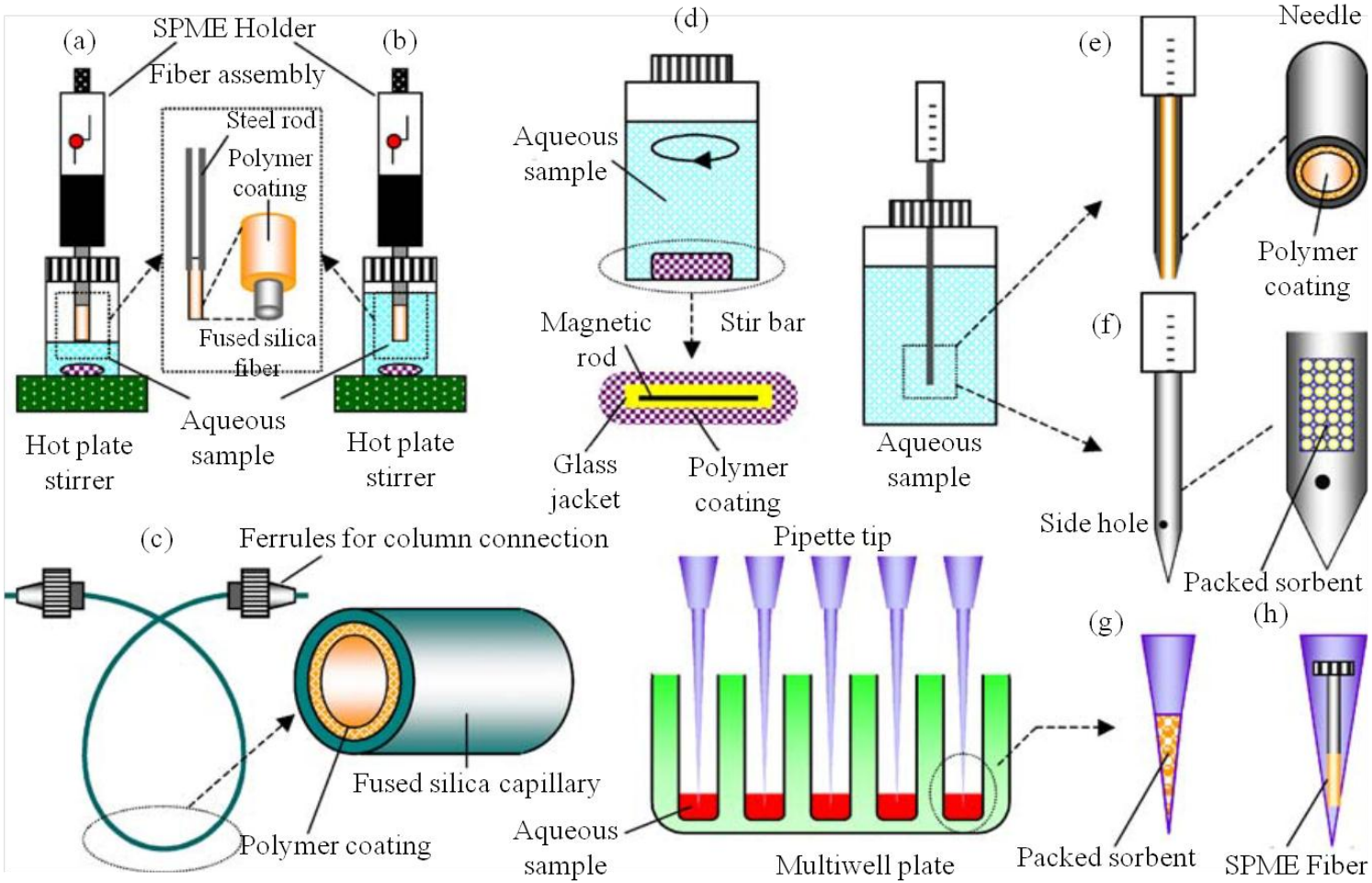

Figure 1.4. Solid-phase microextraction and related microextraction techniques: (a) headspace SPME, (b) direct immersion SPME, (c) in-tube SPME, (d) SBSE, (e) SPDE, (f) MEPS, (g) sorbent-packed in-tip SPME, (h) fiber-packed in-tip SPME (Source:Kataoka H., 2010)

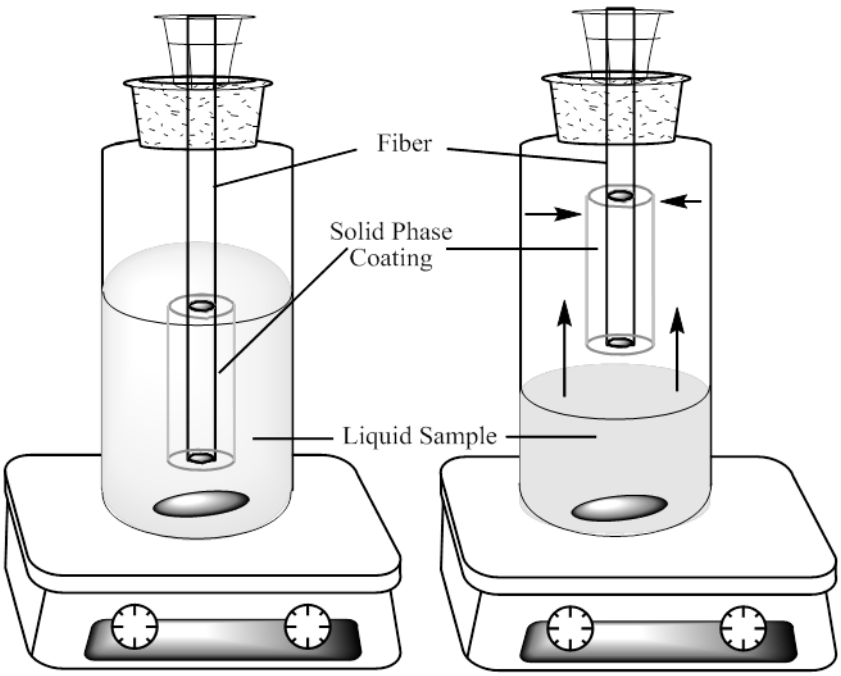

Figure 1.5. SPME extraction modes: (a) direct extraction, and (b) headspace extraction

1.3.2. Solid Phase Microextraction Coatings

Chemical reactions which occur during the sol-gel coating of fused fiber are shown in Figure 1.6. The first one is that hydrolysis of alkoxysilane precursor causes to the formation of reactive silanol groups on the surface. These reactive silanol containing products lead to the production of polycondensation reaction with sol-gel-reactive species which are readily present in the sol-gel solution in order to form a three-dimensional network of sol-gel polymer. Since the polycondensation reactions take place, the visco-elastic properties of the sol solution undergo progressive changes, and after a certain period of time then, it leads to the formation of a gel. The gel formed has a three dimensional porous polymeric network with the solvent trapped inside the pores of the gel. To create a surface-bonded stationary phase, the chain of the chemical events involved in this sol-gel process has a potential ability. Table 1.2. summarizes the role of sol-gel solution components that the coating is effectively used in the production of a surface bonded stationary phases.

Hydrolysis of the precursor:

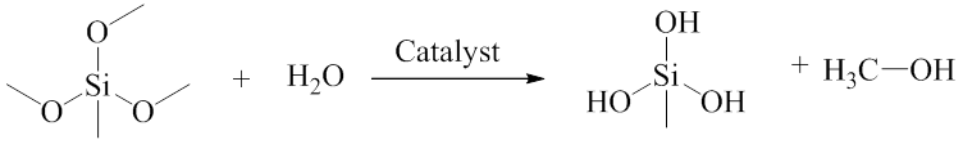

Polycondensation of the hydrolyzed products into sol-gel network:

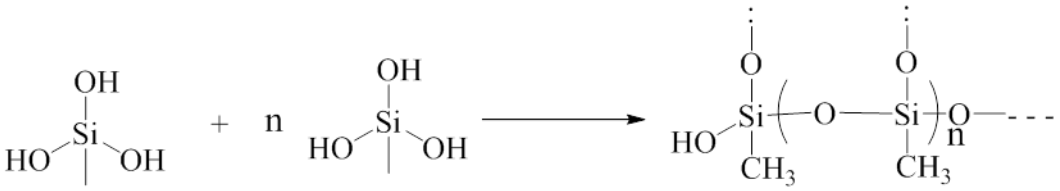

Chemical bonding of the growing sol-gel network onto the fiber surface:

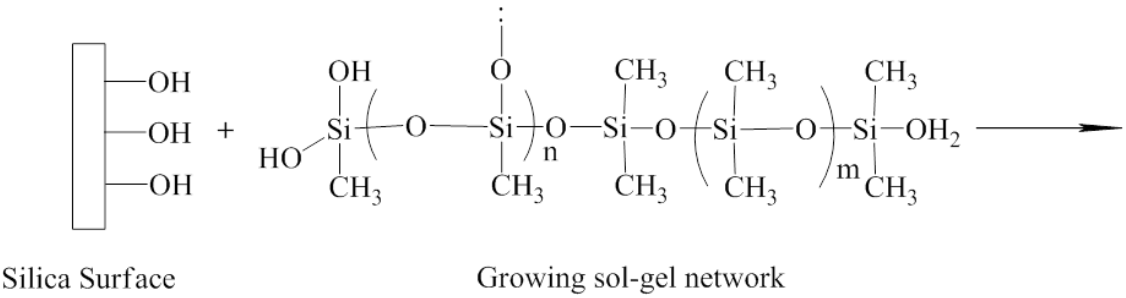

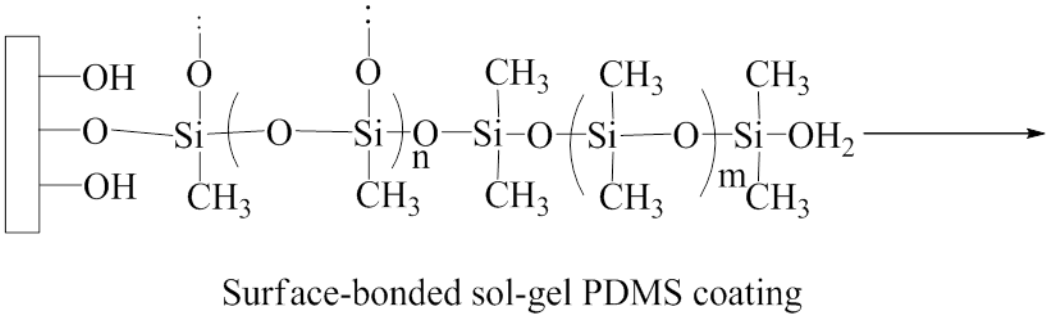

Figure 1.6 . Chemical reactions involved in sol-gel coating of fused silica SPME fiber.

Table 1.2. Reagents used in sol-gel solution
(Source: Pawliszyn J., 1999).

Sol-gel solution reagents	**Chemical Name**	**Role in the sol-gel solution**
Sol-gel precursor	Methyltrimethoxysilane	• Source for the inorganic part of the sol-gel coating, and delivers it by hydrolytic polycondenstaion reaction. • Provides active silanol groups on the sol-gel coating to allow its chemical bonding to the fiber surface.
Organic polymer with sol-gel-active functional groups	1) Hydroxy-terminated polydimethylsiloxane (PDMS), 2) Poly(ethylene-propylene) glycol (PEG)	• Provides organic part for the sol-gel organic-inorganic hybrid coating by polycondensation reactions with the hydrolyzed products of the precursor.
Deactivating reagent	Poly(methylhydroxysilane)	• Supplies desired level of high-temperature derivatization of silanol groups on the sol-gel coating, and hence the control of the organic-inorganic hybrid coating polarity can be controlled. • Derivatization reaction occurs during thermal conditioning of fiber after completion of the sol-gel coating process.
Sol-gel catalyst	Trifluoroacetic acid (TFA)	• Two roles in sol-gel process: 1) Catalyst for the sol-gel process, 2) Source of water for the hydrolysis of the precursor (generally 5% of water). • The sol-gel process to be carried out in organic solvent-rich environment with controlled amount of water is supplied.

1.3.3. Monolithic Microextraction Coatings

Monolith microextraction coatings have become more popular because of their increased mass-transfer kinetics and the controllable porous structure (Vuckovic 2013). Table 1.3. summarizes the monolithic extraction phases for the microextraction techniques in the literature. As it can be seen from the literature works, the majority of the monolith coatings are based on the preparation of molecularly imprinted polymer coatings by radical polymerization. Polymerization solution contains polymerization solvent, template, functional monomer, and cross-linker. The proprties of the polymer relies on the composition of the polymer solution. These coatings were assisted either by UV radiation (Xu et al. 2011), microwave radiation (Xu et al. 2013, Jin et al. 2012 and 2013), and thermally induced radical polymerization (Djozan et al. 2007, Djozan and Baheri 2007, Djozan et al. 2009, Khorrami et al. 2011, Prasad et al. 2011, Wang et al. 2012, Zhang et al. 2006 and 2012). Literature studies indicates that these monolith microextraction coatings have found widespread use in the analysis of biologically important samples (e.g. beverage, lake water, wheat bran, serum, human blood plasma, cerebro-spinal fluid samples, pearl water, milk, poly(ethylene terephthalate) (PET) bottles, human saliva, various street-drugs).

Table 1.3. Monolithic extraction phases for the solid phase microextraction in the literature

Extraction phase	Analyte / Sample	Detection	Reference/Year
monolithic dimethyl phthalate (DMP) imprinted polymer SPME fiber	DMP, dibutyl phthalate, di-n-octylo-phthalate in beverage samples	HPLC-UV	Y.F. Jin, Y.P Zhang, M.X. Huang, L.Y. Bai, M.L. Lee, 2013.
microwave-assisted preparation of monolithic bisphenol A imprinted polymeric SPME fiber:	diethylstilbestrol, hexestrol in tap water, sewage and urine samples	HPLC-UV	S. Xu, X. Zhang, Y. Suna, D. Yua, 2013.
monolithic olivetol imprinted polymer SPME fiber	olivetol, phenol and m-toluidine in lake water and wheat bran samples	HPLC-UV	Y.F. Jin, N. Chen, R.Q. Liu, Y.P Zhang, L.Y. Bai, J. Chen, 2012.
monolithic epinephrine imprinted polymer SPME fiber	dopamine, epinephrine, and norepinephrine in urine and serum samples	CE	X. Zhang, S. Xu, J.M. Lim, Y. Lee, 2012.
sulfadimidine-imprinted monolithic polymer-based SPME fiber	sulfadimidine, sulfamerazine, sulfadiazine, and sulfadimethoxine in pearl water and milk	HPLC-UV	L. Wang, G. Shao, F. Gan, 2012.
acetaldehyde-imprinted monolithic SPME fiber	acetaldehyde from head-space of beverages stored in poly(ethylene terephthalate) (PET) bottles	GC/MS	A.R. Khorrami, E. Narouenezhad, 2011.

(cont. on next page)

Table 1.3. (cont.).

Extraction phase	Analyte / Sample	Detection	Reference/Year
poly(methacrylic acid-co-ethylene glycol dimethacrylate) monolithic frit	hexanal and heptanal in biological samples (human urine and serum)	HPLC-UV	H. Xu, S. Wang, G. Zhang, S. Huang, D. Song, Y. Zhou, G. Long, 2011.
tryptophan imprinted micro-solid phase extraction fiber	D- and L-tryptophan in Astymin capsule, human blood plasma, and cerebro-spinal fluid samples	voltammetric analyzer/stripping voltammeter	B.B. Prasad, M.P. Tiwari, R. Madhuri, P.S. Sharma, 2011.
ametryn-imprinted polymer SPME fiber	persistent triazine herbicides in tap water, rice, maize and onion	GC/MS	D. Djozan, M. Mahkam, B. Ebrahimi, 2009.
diacetylmorphine-imprinted polymer SPME fiber .	diacetylmorphine, 6-monoacetylcodeine, and 6-monoacetylmorphine in street heroin sample	GC and GC/MS	D. Djozan, T. Baheri, 2007.
poly (methacrylic acid–ethylene glycol dimethacrylate) monolithic frit	2,4-dinitrophenylhydrazine derivatives of several aldehydes in human saliva	HPLC-UV	Feng Y.Q., H.J. Zhang, J.F. Huang, H. Wang, 2006.
monolithic codeine imprinted polymer fiber	codeine in various street-drug samples	GC and GC-MS	D. Djozan, T. Baheri, M.H.P. Azar, M. Mahkam. 2007.

1.3.4. Solid Phase Microextraction of Flavonoids

According to the literature studies, only the commercial fibers are used in the solid phase microextraction of flavonoids (Table 1.3.) From these studies, CW/TPR, PDMS/DVB, PDMS, CAR-PDMS, PA, DVB-CAR-PDMS, and PEG are the examples of SPME fiber coatings in the study of flavonoids. To the best of oır knowledge, there is no study in literature, yet, for the preparation of solid phase microextraction coatings for the flavonoids.

Table 1.4. SPME of fibers used in the literature for the determination of flavonoids

Extraction phase	Analyte	Derivatization	Detection	Reference/Year
50 µm Carbowax/ Templated Resin (CW/TPR).	Myricetin, Quercetin	-	HPLC–UV	Malika A.K., A. Kumara, D.K.Tewaryb, 2009.
100µm Polydimethylsiloxane (PDMS), 65µm polydimethylsiloxane-divinylbenzene (PDMS-DVB), 85µm polyacrylate (PA), 75µm Carboxen-polydimethylsiloxane (CAR-PDMS), 70µm Carbowax-divinylbenzene (CW-DVB), 50/30µm DVB-CAR-PDMS and 60µm Poly(ethylene glycol) (PEG).	cis- and trans-Resveratrol, Piceatannol, Catechin, Epicatechin.	BSTFA	GC-MS	Hernández-Córdoba M., P. Viñas, N. Campillo, N. Martínez-Castillo, 2009.
100 µm Polydimethylsiloxane (PDMS), 65 µm Polydimethylsiloxane–divinylbenzene (PDMS–DVB), 85µm Polyacrylate (PA), and 50µm Carbowax templated poly(divinylbenzene) (CW–TPR).	Genistein, Daidzein	-	HPLC–UV	Brodbelt J.S., M. Satterfield, D. M. Black, 2001.
85 µm Polyacrylate (PA), 100 µm Polydimethylsiloxane (PDMS), 70 µm Carbowax-divinylbenzene (CW-DVB), 75 µm Carboxen-polydimethylsiloxane (CAR-PDMS), and 65 µm Polydimethylsiloxane-divinylbenzene (PDMS-DVB).	Pinocembrin, Pinobanksin, Chrysin		GC-MS	Daher S., and Gülaçar F.O., 2008.

1.4. HPLC Analysis of Flavonoids

For a given type of flavonoids (flavonols, flavones, flavonones, etc.), there are parameters to be optimized that include the stationary phase, solvent, and the solvent gradient. Most of the separations are run on octadecylsilyl bonded (ODS, RP-18, or C18) phases. There are some results with the use of octasilyl bonded (RP-8 or C8) phases but these are not common. Mobile phase as acetonitrile–water or methanol–water mixtures are very common. In addition, mixtures containing small amounts of acid are generally applied to suppress the ionization of the phenolic hydroxyl groups and also to obtain sharper peaks without tailing and are compatible with gradients and UV detection. Tetrahydrofuran, isopropanol, or n-propanol are sometimes used (Andersen and Markham, 2006).

Classes of compound are shown in the upper part of the chromatogram (Figure 1.7.). Flavone C-glycosides have mostly shorter retention times than the corresponding O-glycosides. The unsaturation between positions 2 and 3 makes that flavanones elute before their corresponding flavones (Andersen and Markham, 2006).

The analysis of flavonoids in medicinal and other plants have been listed in a review, and from the methods listed in this review, the majority of the separations includes the use of C_{18} columns (Cimpan and Gocan, 2002).

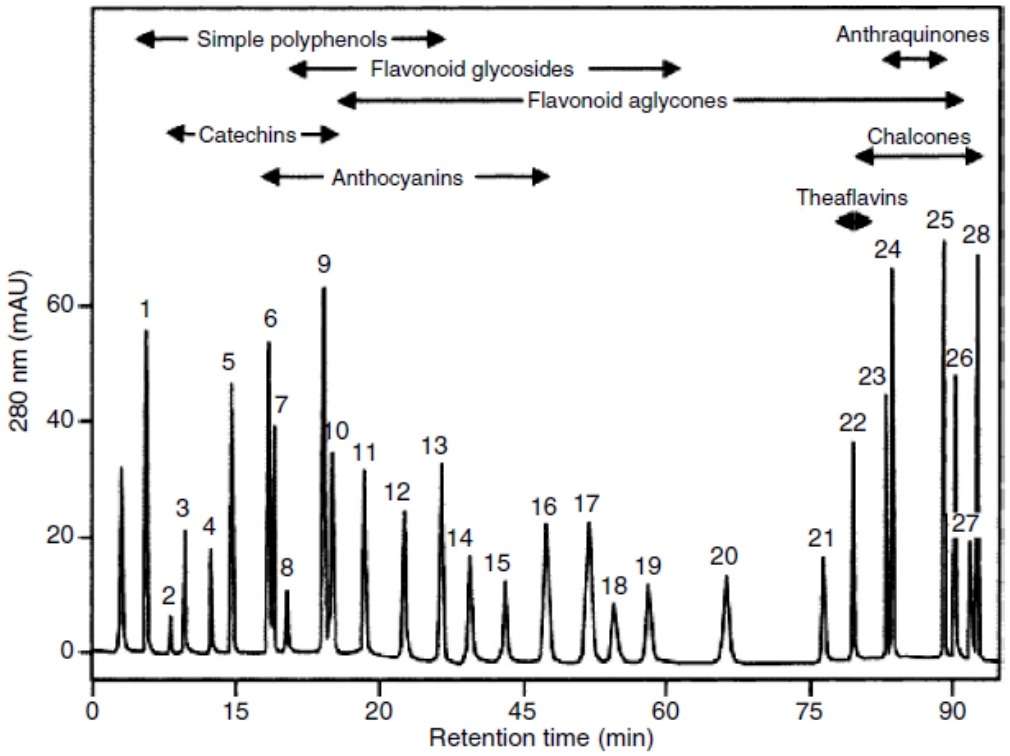

Figure 1.7. HPLC profile for 28 different polyphenols on a C18 column. Numbers show the following standard chemicals: 1, gallic acid; 2, gallocatechin; 3, protocatechuic acid; 4, â-resorcylic acid; 5, chlorogenic acid; 6, caffeic acid; 7, epigallocatechin gallate; 8, sesamol; 9, p-coumaric acid; 10, daidzein-7-O-glucoside; 11, catechin gallate; 12, luteolin-3¢,7-O-diglucoside; 13, o-coumaric acid; 14, luteolin-7-O-glucoside; 15, quercetin-3-O-rutinoside; 16, hesperetin-7-O-rutinoside; 17, myricetin; 18, apigenin-7-O-glucoside; 19, kaempferol-3-O-glucoside; 20, daidzein; 21, quercetin; 22, luteolin; 23, kaempferol; 24, apigenin; 25, flavone; 26, galangin; 27, flavonol; 28, chalcone (Source: Sakakibara et al., 2003).

1.5. UV Detection of Flavonoids

UV spectrophotometry is the most frequently used detection method for HPLC. Flavonoids can be detected by a UV spectrophotometer or a UV diode array detector (UV-DAD) because of having at least two aromatic rings. The presence of these rings possess efficiently absorption of UV light. The characteristics of flavonoids is that having two absorption band in the UV spectrum. The first maximum comes from the A-ring, and lies in the wavelength range of 240-285 nm (Figure 1.1.). The next absorption band lies between 300-560 nm (band II) which relies on the substitution pattern and the

conjugation of the C-ring (Mabry et al. 1970). Flavonoids show absorbance maxima at different wavelengths, so there is no single wavelength for all classes of flavonoids.

LC–UV with diode array detection (DAD) makes possible the chromatographic eluent to be scanned for UV–visible spectral data. The data are collected, and then can be compared with a library for peak identification. The information from the UV spectrum allows to identify the compound subclass or perhaps even the compound itself. Mabry et al. (1982) listed UV spectral data of 175 flavonoids in several solvents.

Robards and Antolowich (1997) showed that anthocyanins display band I and band II absorption maxima in the 265-275 and 465-560 nm regions, respectively. UV spectra of flavanones and isoflavones have mainly an intense band II peak, however a small band I peak since the conjugation between the A- and B- rings is little or absent (Mabry et al., 1970). Therefore, the catechins have small band I peaks due to this absence of conjugation and it can be found at 210 or 280 nm. Moreover, the absorption maxima characteristically are to be found at 270 and 330 to 365 nm for flavones and flavonols, at 290 nm for flavanones, at 236 or 260 nm for isoflavones (Merken and Beecher, 2000).

1.6. Plants Used for the Extraction of Flavonoids

1.6.1. *Laurus nobilis*

Laurus nobilis, is an aromatic evergreen tree or large shrub reaching 10–18 metres tall, native to the Mediterranean region, belongs to the Lauraceae family (Figure 1.8). It is also known as Bay Laurel, True Laurel, Sweet Bay, Laurel Tree, Grecian Laurel, Laurel, Bay leaf or Bay-Tree. It is known in Greek and Roman mythology as an emblem of victory and success. It is the only European representative of the Lauraceae family (Leung and Foster, 1999). It has found a cultivation place in many temperature and warm parts of the world, especially in the Mediterrian region which confines Greece, Spain, Morocco, and Turkey. Figure 1.9. shows the distribution of *Laurus nobilis* in Turkey.

Figure 1.8. Laurus nobilis Bay Laurel (Laurus nobilis) flower buds and leaves (Nikon D3000).

Laurus is widely utilized as a dried herb that contains a very fragrant and aromatic oil; it is utlilised a valuable spice and flavouring agent in the culinary and food industries and as an additive cosmetics (Conforti et al., 2006). The bay leaf is used in several types of cooking as well as in folk medicine for its antirheumatic properties, for the treatment of anal fistulas and various dermatoses and for its efficacy as a stomachic and carminative remedy in Tunisia. In addition, the decoct root was recognised for its expectorant properties. The drup was also used by the Jewish population of Jerba in the treatment of jaundice and rheumatic pain (Boukef, 1986).

Owing to the pharmacological properties and potential health benefits related to several compounds present in the plant, *Laurus nobilis* has taken renewed interest. In the fruit and leaves of *Laurus*, there are essential oils and fatty oils present. Recent studies have shown that biologically-active compounds from laurel leaves possess antimicrobial (De Corato et al., 2010; Derwich et al., 2009; Marzouki et al., 2009 a, b, and Castilho et al., 2007), antiproliferative (Afifi et al., 2010), antiviral (Loizzo et al 2008; Simic et al., 2004) and antioxidant activities (Misharina et al., 2009; Politeo et al., 2007, and Vasapollo et al., 2005). The phenolic constituents and bioactivities of organic and aqueous extracts from leaves have been studied extensively (Conforti et al., 2006; Dall' Acqua et al., 2009; De Marino et al., 2004; Liu et al., 2009; Papageorgiou et al., 2008; Skerget et al., 2005). However, vitamin E has been isolated only from leaves (Demo et al., 1998; Gómez-Coronado and Barbas 2003; Puoci et al., 2007) and fruits (Frega et al., 1982).

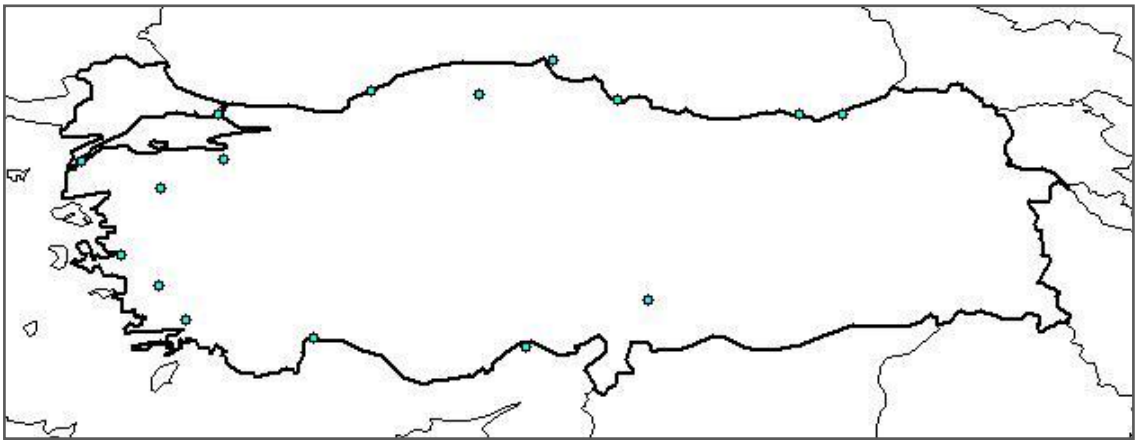

Figure 1.9. Geographical distribution of Laurus nobilis in Turkey
(Source: Turkish Plants Data Service (TÜBİVES))

Dorman and coworkers (2005) studied the isolation of flavonoids from Lamiaceae species. Aqueous-methanol extracts were prepared from basil (*Ocimum basilicum* L.), bay (*Laurus nobilis* L.), oregano (*Origanum vulgare* L.), rosemary (Rosmarinus officinalis L.), sage (Salvia officinalis L.), savory (Satureja hortensis L.) and thyme (Thymus vulgaris L.) by maceration and their phytochemical and antioxidant characteristics were assessed.

1.7. Aim of This Study

This research will comprise the study of flavonoids from the plant, namely, *Laurus nobilis*. According to the literature studies, flavonoids were involved in disease resistance in plants. This behaviour of the plants makes them important and since they can be used as potential drug candidates. The second aim of the present study is the synthesis of solid phase microextraction coatings for the extraction of flavonoids from plant(s). Another objective of this study is to characterize the solid phase microextraction coatings. Further, these coatings are used for the solid phase microextraction of isoquercitrin, apigetrin, eriodictyol, quercetin, luteolin, and apigenin.

CHAPTER 2

EXTRACTION OF FLAVONOIDS: METHOD DEVELOPMENT

2.1. Experimental

2.1.1. Preparation of Stock Solutions

Stock solutions of apigenin, apigetrin, eriodictyol, isoquercitrin, luteolin, and quercetin were prepared in methanol at the concentration of 100.0 µg/mL, and flushed with nitrogen gas. Stock solutions were then diluted to appropriate concentration with mobile phase before use. All stock and working standard solutions were stored in brown bottles at -20°C until used for analysis.

2.1.2. Plant Material

The leaves of *Laurus nobilis* were collected in the surroundings of Aydın, Turkey, in October 2011. The plant material was washed with ultra pure water (18MΩ) and dried at 60°C for 24 hour. Then, it was powdered and stored at -20°C until used for analysis.

2.1.3. Chemicals and Reagents

All standards and solvents were of HPLC grade. Ultra pure water (18MΩ) was used throughout the study. The chemicals and the reagents used were tabulated in Table 2.1.

Table 2.1. The properties of chemicals and reagents.

Item No	Reagent	Structure	Company	Product Code	Cas No	Purpose of Use
1	Apigenin (Flavone)	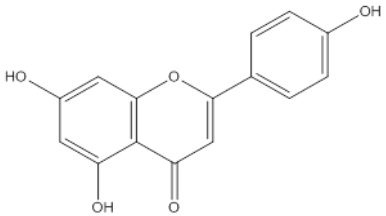	Fluka	10798	520-36-5	Standard
2	Apigetrin (Apigenin-7-O-glucoside)	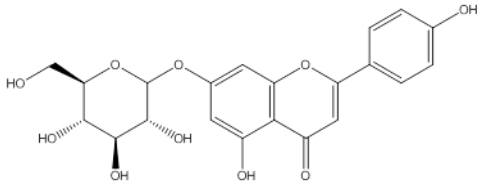	Fluka	44692	578-74-5	Standard
3	(-)-Catechin (Flavan-3-ol)	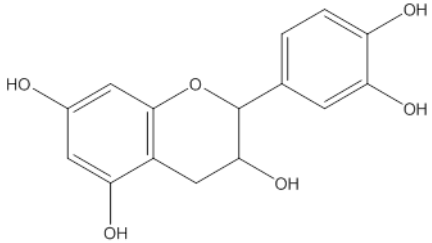	Sigma	C0567	18829-70-4	Standard

(cont. on next page)

Table 2.1. (cont.).

Item No	Reagent	Structure	Company	Product Code	Cas No	Purpose of Use
4	(+/-)-Eriodictyol (Flavanone)	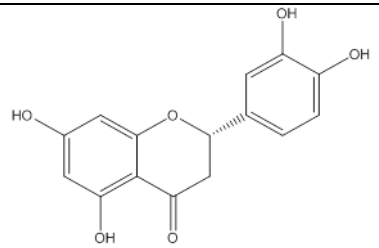	Sigma	94258	552-58-9	Standard
5	Isoquercitrin (Quercetin-3-O-glucoside)	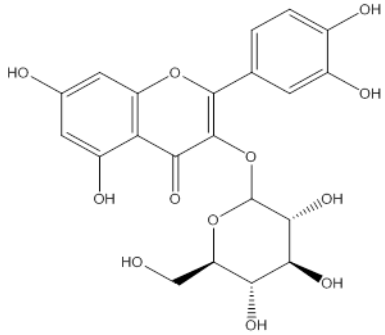	Fluka	17793	482-35-9	Standard
6	Luteolin (Flavone)	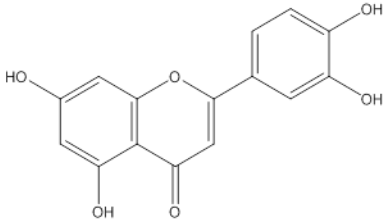	Sigma	L9283	491-70-3	Standard

(cont. on next page)

Table 2.1. (cont.).

Item No	Reagent	Structure	Company	Product Code	Cas No	Purpose of Use
7	Quercetin (Flavonol), ≥ 95% (HPLC)	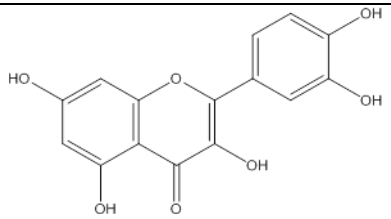	Sigma	Q4951	117-39-5	Standard, template molecule in the MIS synthesis
8	Methanol	-	Riedel	34885	67-56-1	Solvent, mobile phase
10	Hexane	-	Merck	1.04391	92112-69-1	Extraction solvent

2.1.4. Instrumentation and Apparatus

UV spectra of flavonoids were collected using Varian Cary Scan 50 UV-Visible spectrophotometer in the wavelength range of 200-600 nm. IKA (2930401, RO 10 power IKAMAG) multi position magnetic stirrer (Figure 2.4.) was used for the solid phase microextraction of the flavonoids.

SEM characterization of the silica samples were carried out using FEI Quanta 250 FEG prior to analysis.

Particle size distribution of polystyrene nanospheres were measured by Zetasizer Nano Series Particle Size and Zeta Potential Analyzer from Malvern Instruments.

A Perkin Elmer FT-IR System Spectrum BX with Pike Diffuse Reflectance Accessory was used to identify the functional groups present in the silica samples. The spectra of the silica samples were taken in a 4000.0 cm^{-1} – 400.0 cm^{-1} range with a scan number of 4.0 and a resolution of 4.0 cm^{-1}.

A Perkin Elmer Pyris Diamond TG/DTA Thermogravimetric Analyzer (TGA) (Boston, MA, USA) was used to follow the changes in the weight of silica samples as a function of temperature. The solid silica samples were heated from 25ºC to 750ºC in 10 minute intervals in N_2 atmosphere.

Chromatographic analysis was performed with an Agilent 1200 series consisting of an online vacuum degasser (model G1322A), a quaternary pump (model G1311A), a thermostated column compartment (model G1316A), manual injector (model G1328B), and a diode array detector (DAD) (model G1315DA). Standard solutions of compounds were dissolved in mobile phase to eliminate the peak fronting. Compounds were separated on a Zorbax Eclipse XDB-C18 column (150 mm x 4.6 mm, 5μm i.d., Agilent Co.). The mobile phase was degassed by ultrasonication under room temperature for 10 min. The mobile phase was consisted of methanol (A) and water containing 0.10 % acetic acid (B). Samples were eluted at a flow rate of 1.0 mL/min. Elution conditions applied were as follows: 0-10 min, linear gradient 35-45% A; 10-15 min, linear gradient 45-50% A; 15-20 min, linear gradient 50-55% A; linear gradient 55-60% A; 20-25 min. The column temperature was 25°C. The injection volume for all standards and samples was 20 μL. The detection wavelength for apigenin, apigetrin, eriodictyol, isoquercitrin, luteolin, and quercetin was 335 nm.

2.1.5. Extraction of Flavonoids

2.1.5.1. Ultrasonic Extraction

A 0.1 g amount of plant, namely, *Laurus nobilis*, was extracted in a glass container in an ultrasonic bath (Elmasonic S40H) with 10 ml methanol at 25°C for 30 min. This process was applied three times with the same plant material and the extracts were collected. The separation of extract from plant was achieved by filtration using 0.20 μm nylon membrane filter. The filtrate was washed with a 10.0 mL of hexane three times to eliminate the oil from the extract. The methanolic extract was concentrated under vacuum and diluted to 10 ml with methanol. The solution was filtered before being subjected to HPLC analysis. The same extraction procedure was perfomed with a 10 ml of methanol-water (80:20, v/v) mixture. Diluted samples of the extracts were prepared in mobile phase.

2.5.1.2. Soxhlet Extraction

A 0.5 g of the plant sample was subjected to soxhlet extraction using a 150ml Soxhlet extractor with a cellulose extraction thimble (Filterlab) for 6h. A 250 ml of methanol was used as an extraction solvent. After the extraction was completed, the extract was filtered through a 0.2μm nylon membrane filter. The methanolic extract was concentrated under vacuum and diluted to 25 ml with methanol. The methanolic extract was washed with a 20.0 ml of hexane three times to eliminate the oil from the extract. The solution was filtered before being subjected to HPLC analysis. Diluted samples of the extracts were prepared in mobile phase. The same extraction procedure was carried out with methanol-water (80/20; v/v) mixture.

2.5.1.3. Magnetic Stirring

A 0.1 g amount of plant, namely, *Laurus nobilis*, was extracted in a glass container with 10 ml methanol at 25°C for 24 h in the dark. The separation of extract from plant was achieved by filtration using 0.20μm nylon membrane filter. The filtrate

was washed with a 10.0 mL of hexane three times to eliminate the oil from the extract. The methanolic extract was concentrated under vacuum and diluted to 10 ml with methanol. The solution was filtered before being subjected to HPLC analysis. The same extraction procedure was performed with a 10 ml of methanol-water (80:20, v/v) mixture. Diluted samples of the extracts were prepared in mobile phase.

2.2. Results and Discussion

2.2.1. Elemental Analysis

The elemental composition of the plant used, *Laurus nobilis*, are given in Table 3.1. *Laurus nobilis* have carbon, hiydrogen, nitrogen and sulfur percentages as 47.39%, 6.96%, 1.86, and 0.15%, respectively. According to the results, the carbon is the highest percentage among the elements investigated.

Table 2.2. Elemental composition of *Laurus Nobilis* in terms of %C, %H, %N, and %S.

Plant	% C	% H	% N	% S
Laurus nobilis	47.39	6.96	1.86	0.15

2.2.2. UV Spectra of Flavonoids

Selection of an apropriate wavelength was of great importance to ensure precise detection of the analytes. For this reason, UV spectra of the flavonoids were detected and shown in Figure 3.1., 3.2., and 3.3. Two absorption bands are found between 250 and 380 nm in the UV spectrum of apigenin, apigetrin, luteolin, isoquercitrin, quercetin. However, catechin and eriodictyol show absorbance at 280 and 288 nm, respectively. Finally, 335 nm was chosen as the detection wavelength for flavonoids in this study.

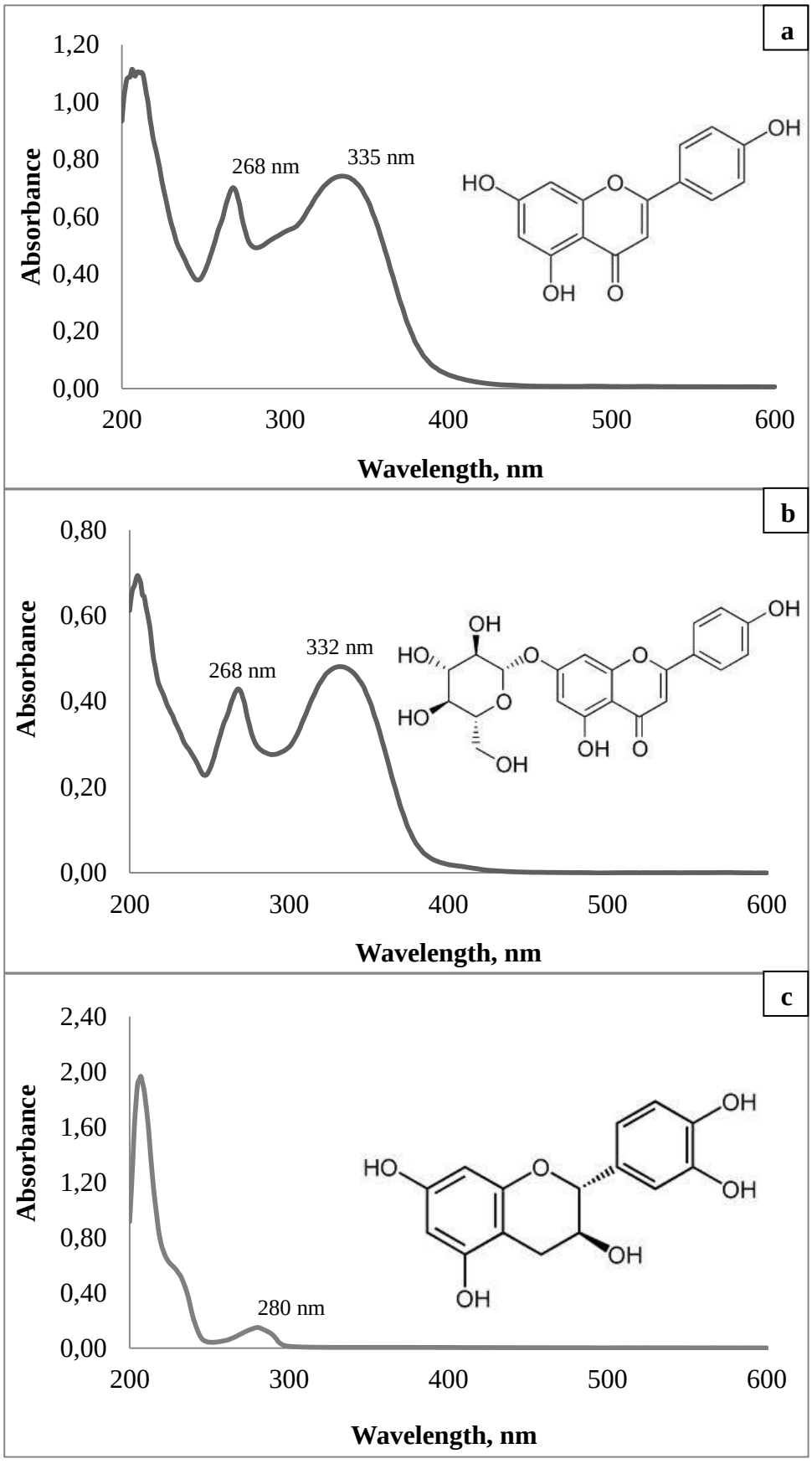

Figure 2.1. UV spectra of apigenin (a), apigetrin (b), and catechin (c) in methanol.

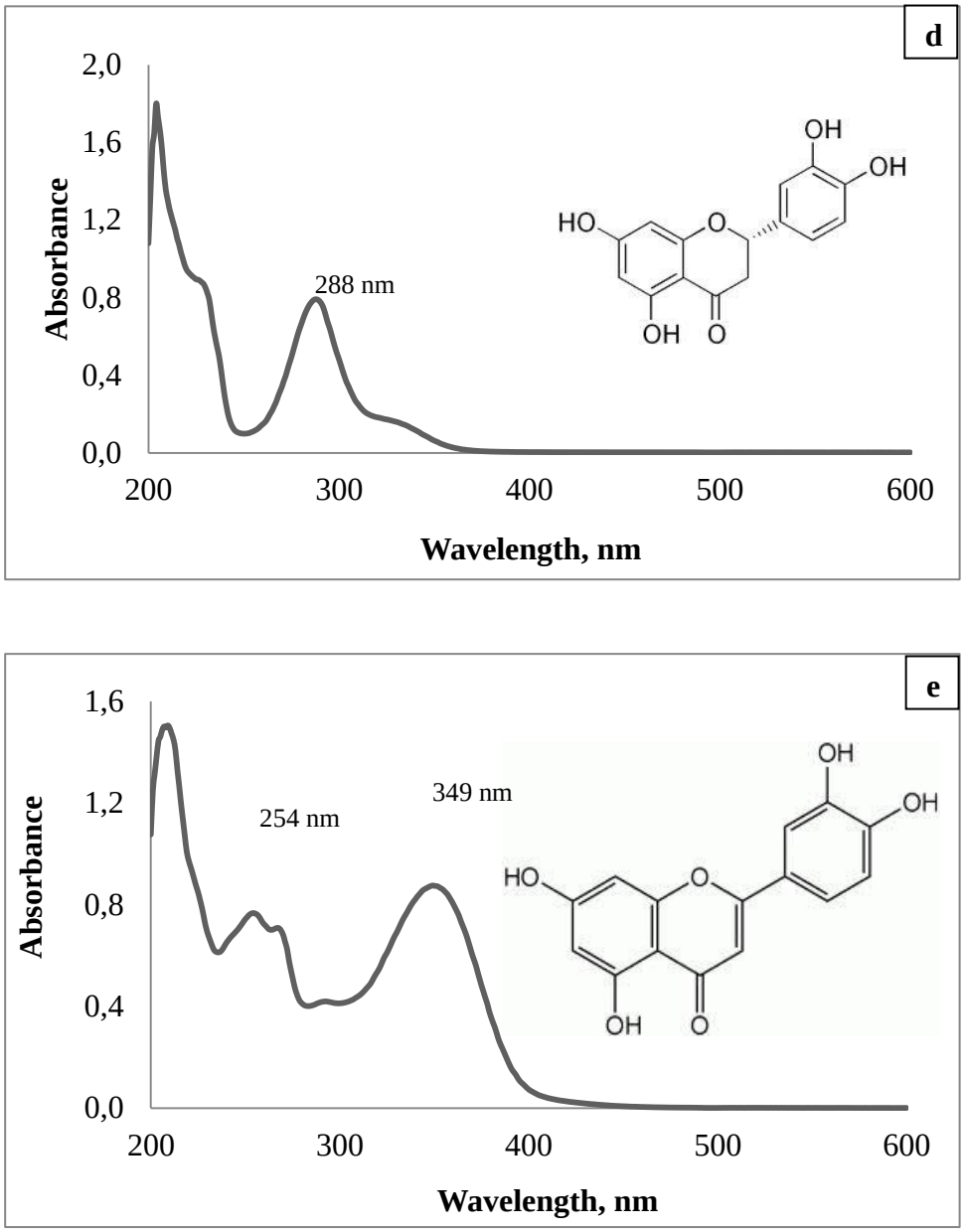

Figure 2.2. UV spectra of eriodictyol (d) and luteolin (e) in methanol.

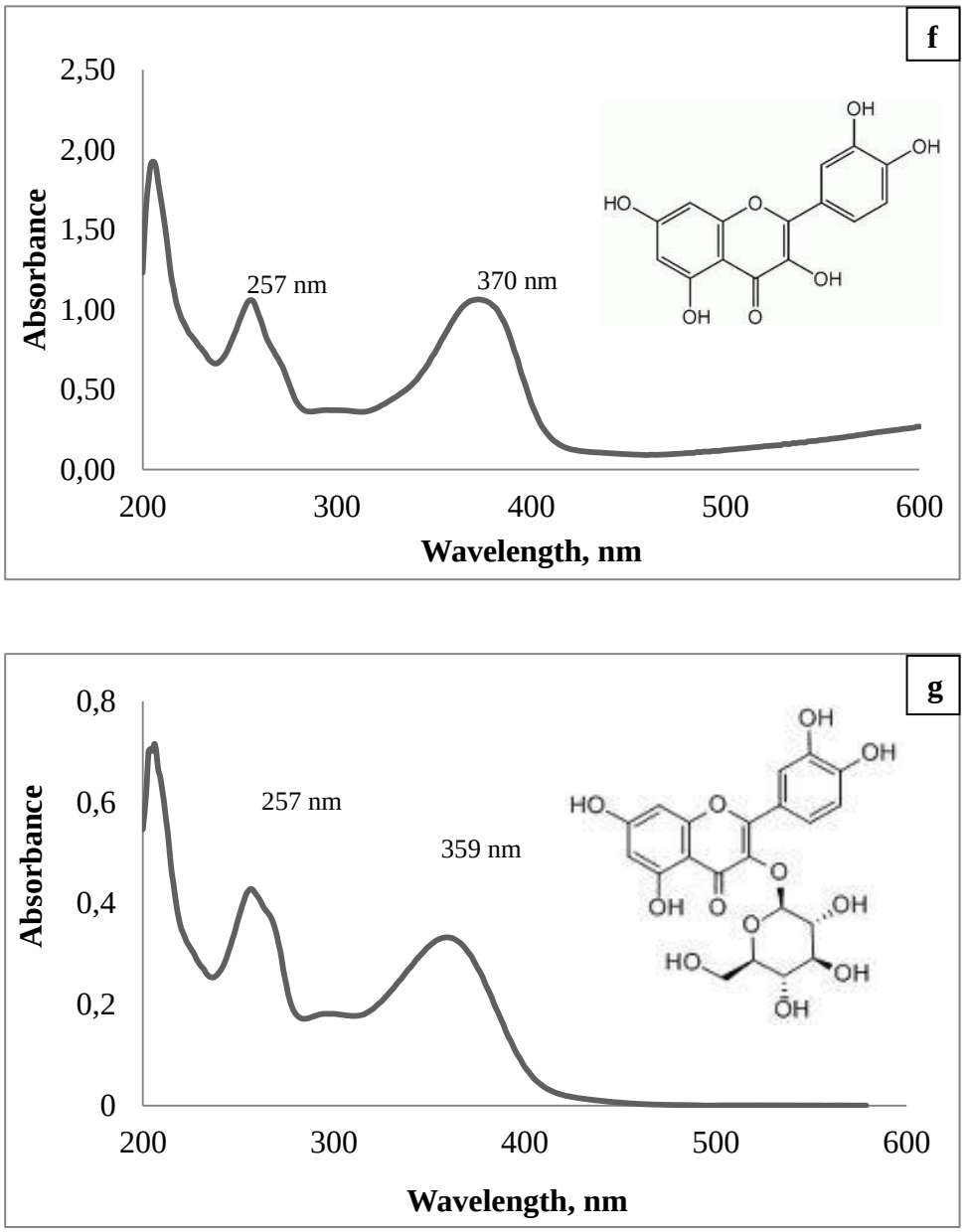

Figure 2.3. UV spectra of quercetin (f) and isoquercitrin (g) in methanol.

2.2.3. HPLC Analysis

The elution order of flavonoids is directly related to their structural properties. Figure 3.6. shows the HPLC separation of flavonoids studied (apigenin, apigetrin, eriodictyol, isoquercitrin, luteolin, and quercetin). Mostly, the retention times of the flavonoids follows the reversed-phase pattern: flavonoid glycosides elute earlier than flavonoid aglycone (Figure 1.7.). As the glycosylation of flavonoids increases their polarity and their movement enhances in reversed-phase HPLC (Andersen and

Markham, 2006). Apigetrin and isoquercitrin elutes before apigenin and quercetin. The retention time of eriodictyol is less than that of luteolin and apigenin, since the presence of unsaturation between positions 2 and 3 causes flavanones elute before their corresponding flavones (Andersen and Markham, 2006). Quercetin has three OH groups at 3, 3' and 4' position at is eluted first followed by luteolin (two OH groups at 3' and 4' positions) and apigenin (one OH group at 4' position).

In this work, three extraction methods were performed to evaluate their performance and they are namely, ultrasonic extraction, soxhlet extraction, and shaking in dark. The effect of extraction solvent was also investigated with the use of methanol and methanol-water (80:20, v/V). The results were listed in the Table 3.3. According to the results, the highest extraction yields were achieved by ultrasonic extraction. Moreover, the extraction of flavonoids by the methanol-water (80:20,v/v) mixture is more than that by methanol. In addition to these, the plant, namely, *Laurus nobilis*, contains the highest amount of eriodictyol among the compounds under investigation.

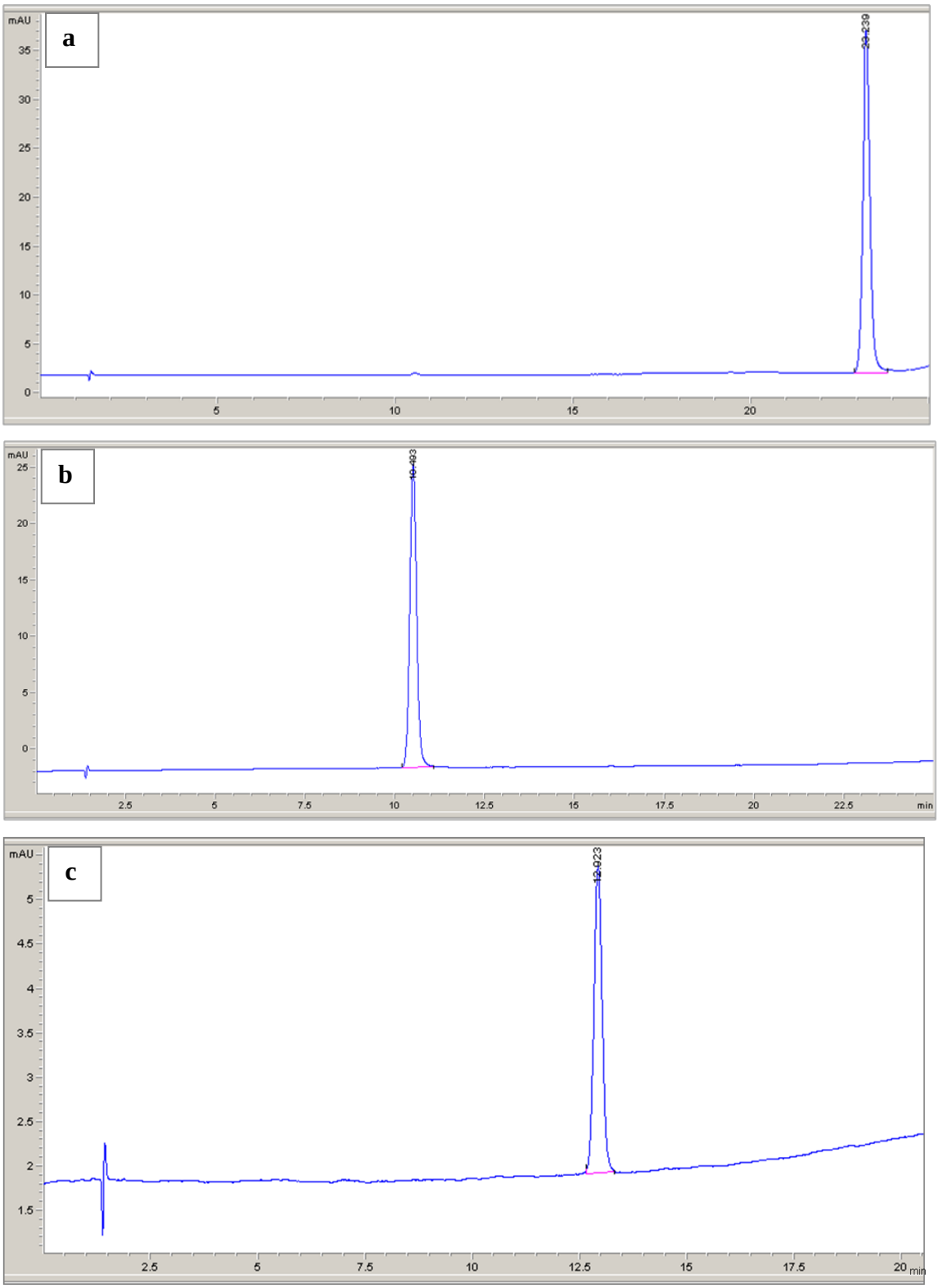

Figure 2.4. HPLC chromatogram of apigenin (a), apigetrin (b), and eriodictyol (c) (flavonoids dissolved in mobile phase).

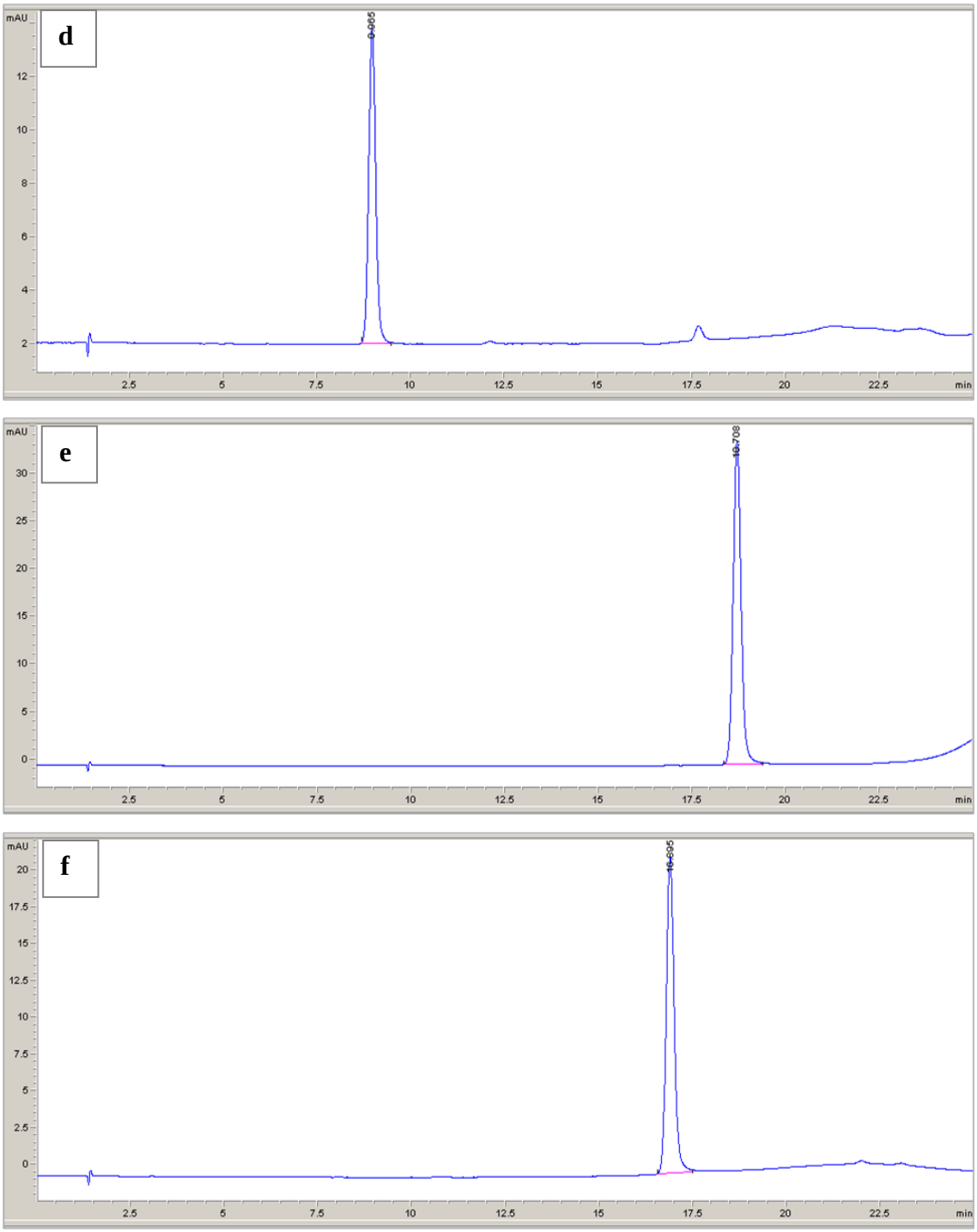

Figure 2.5. HPLC chromatogram of isoquercitrin (d), luteolin (e), and quercetin (f) (flavonoids dissolved in mobile phase).

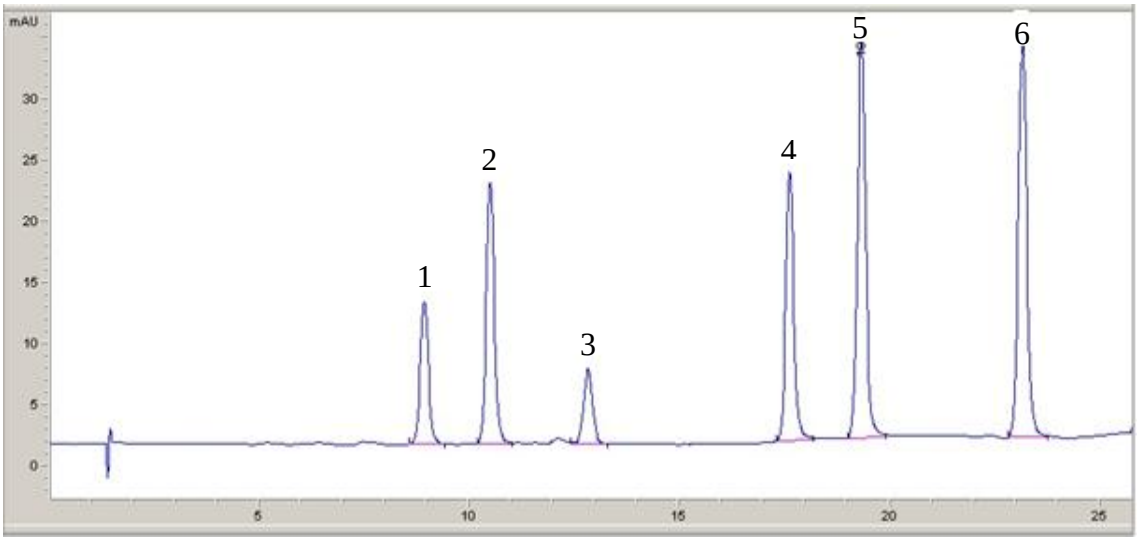

Figure 2.6. HPLC chromatogram of flavonoids (flavonoids dissolved in mobile phase) (isoquercitrin : 1, apigetrin : 2, eridictyol : 3, quercetin : 4, luteolin : 5, and apigenin: 6).

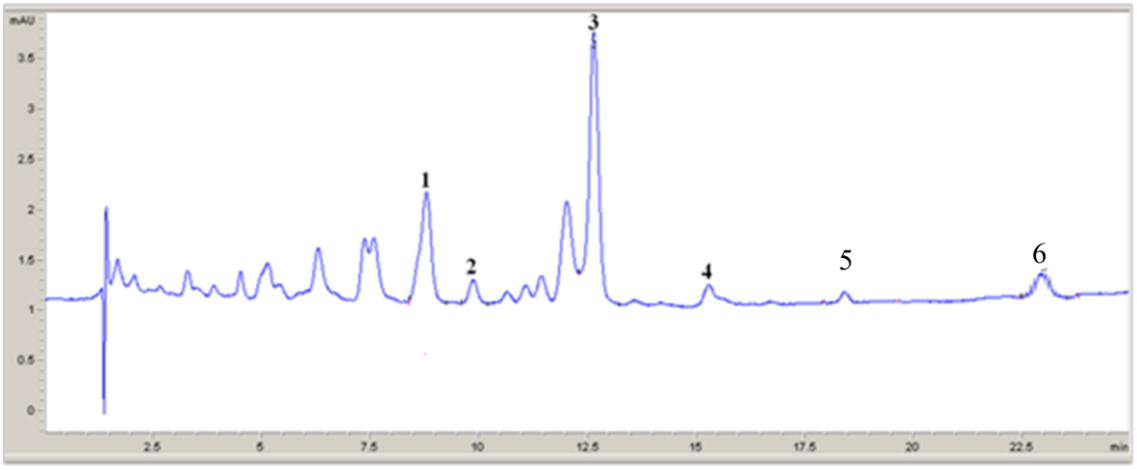

Figure 2.7. HPLC chromatogram of methanolic extract (flavonoids dissolved in mobile phase) (isoquercitrin : 1, apigetrin : 2, eridictyol : 3, quercetin : 4, luteolin : 5, and apigenin : 6).

2.2.4. Analytical Performance of the Method

Linearity of the calibration curves for the flavonoids studied was checked based on the values of correlation coefficients. The calibration curves (Figure 2.8) for

apigenin, apigetrin, eriodictyol, isoquercitrin, luteolin, and quercetin were linear in the range of 0.05-20.0 mg/L. They showed a linear response with $R^2 \geq 0.999$, in the selected range of standards. The LOD and LOQ values found for the flavonoids studied were tabulated in Table 2.3. Table 2.4 shows the amounts of flavonoids (mg of flavonoid / g of plant) extracted from *Laurus nobilis*, and the extraction results changed according to the extraction method and solvent.

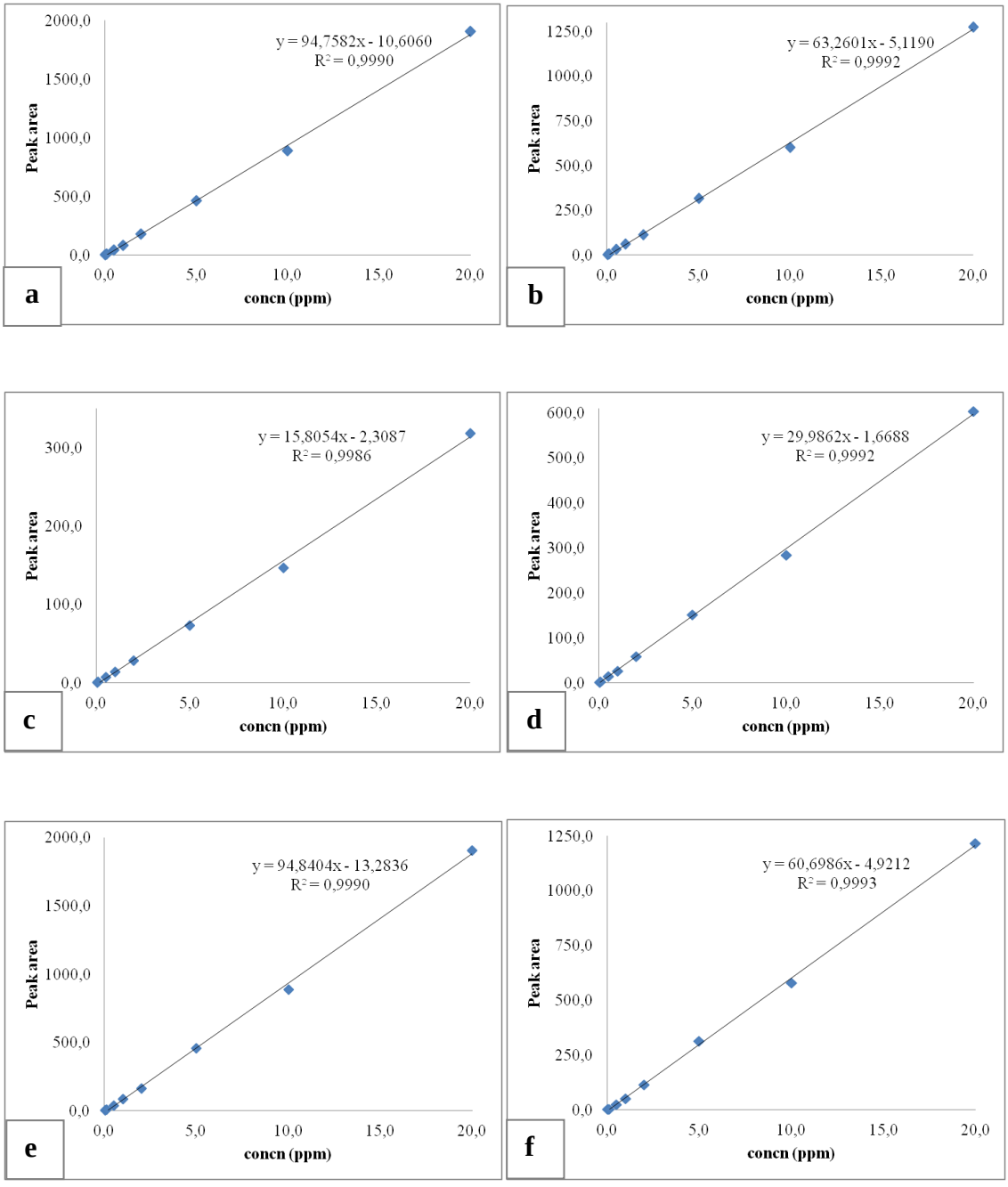

Figure 2.8. Calibration plots of the standards (apigenin (a), apigetrin (b), and eriodictyol (c), isoquercitrin (d), luteolin (e), and quercetin (f))

Table 2.3. Parameters of the analytical curves, LOD and LOQ for flavonoids quantification.

Flavonoids	**Linearity equation**	**Correlation coefficient, R^2**	**Linear Range (mg/L)**	**LOD (mg/L)**	**LOQ (mg/L)**
Apigenin	y = 94.7582x – 10.6060	R^2 = 0.9990	0.05-20.00	0.003	0.011
Apigetrin	y = 63.2601x – 5.1190	R^2 = 0.9992	0.05-20.00	0.004	0.013
Eriodictyol	y = 15.8054x – 2.3087	R^2 = 0.9986	0.05-20.00	0.009	0.030
Isoquercitrin	y = 29.9862x – 1.6688	R^2 = 0.9992	0.05-20.00	0.006	0.019
Luteolin	y = 94.8404x - 13.2836	R^2 = 0.9990	0.05-20.00	0.007	0.023
Quercetin	y = 60.6986x – 4.9212	R^2 = 0.9993	0.05-20.00	0.013	0.043

Table 2.4. Amounts of flavonoids (mg of flavonoid / g of plant) extracted from *Laurus nobilis* (n=3, except soxhlet extraction).

Extraction Type / Solvent		mg/g					
		Apigenin	Apigetrin	Eriodictyol	Isoquercitrin	Luteolin	Quercetin
Ultrasonic	MeOH	0.15 ± 0.03	0.12 ± 0.00	2.89 ± 0.01	0.73 ± 0.03	0.15 ± 0.01	0.09 ± 0.00
	$MeOH/H_2O$ (80/20)	0.13 ± 0.02	0.12 ± 0.01	2.88 ± 0.53	0.77 ± 0.16	0.15 ± 0.01	0.12 ± 0.03
Magnetic Stirring in the Dark	MeOH	0.13 ± 0.01	0.11 ± 0.02	2.86 ± 0.03	0.53 ± 0.19	0.15 ± 0.00	-
	$MeOH/H_2O$ (80/20)	-	0.13 ± 0.01	2.52 ± 0.42	0.66 ± 0.11	0.17 ± 0.12	-
Soxhlet	MeOH	0.08	0.07	2.82	0.74	-	-
	$MeOH/H_2O$ (80/20)	1.05	0.07	3.24	0.90	-	-

CHAPTER 3

NOVEL SOLID PHASE MICROEXTRACTION COATINGS FOR FLAVONOIDS: PART I: SOL-GEL COATINGS

3.1. Experimental

3.1.1. Chemicals and Reagents

The chemicals and the reagents used for the preparation of SPME fiber coatings with chloro- and amine, functionalization of thses coated fibers with imidazole and baicalin were listed in Table 3.1.

3.1.2. Preparation of SPME Fiber

The removal of the protective polyamide layer was achieved by immersing the piece of 7 cm cut fiber into acetone. Then, ultra-pure water was added to wash bare fibers. The following step is to enhance the content of silanol groups on bare silicate surface, and hence it is required to carry out the reaction. The activation of the silica surface was achieved by dipping segments of the bare silica fibers into 1.0 M NaOH solution for 60 min, and it was dipped into 0.1 M HCl solution for 30 min to neutralize the excess base. The activated silica fibers were washed with ultra pure water and they were dried for 24 h at 120°C. SPME fibers were produced in sol-gel based coatings (chloro- and amine- coating).

Table 3.1. The properties of chemicals and reagents.

Item No	Reagent	Structure	Company	Product Code	Cas No	Purpose of Use
1	(3-aminopropyl)trimethoxysilane **(**3-(Trimethoxysilyl)propylamine), 97%	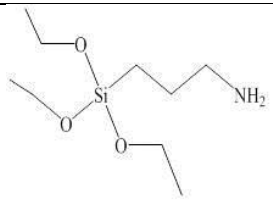	Aldrich	2811778	13822-56-5	Functionalization of silica fiber
2	(3-chloropropyl) trimethoxysilane	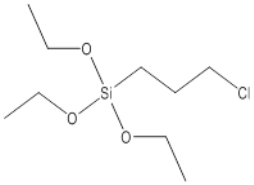	Aldrich	569615	5089-70-3	Functionalization of silica fiber
3	Poly(methylhydrosiloxane) (PMHS)	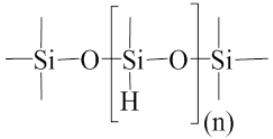	Aldrich	81330	9004-73-3	Deactivator in sol-gel process
4	Poly(dimethylsiloxane), hydroxy terminated (PDMS)	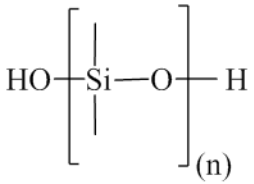	Aldrich	481939	70131-67-8	Organic polymer with sol gel active terminal for SPME coatings

(cont. on next page)

Table 3.1. (cont.).

Item No	Reagent	Structure	Company	Product Code	Cas No	Purpose of Use
5	THF		Sigma-Aldrich	87368	109-99-9	Solvent in sol-gel process
6	Dichloromethane		Riedel-de Haen	24233	75-09-2	Solvent in sol-gel process
7	TFA		Merck	76-05-1	808260	Catalyst in sol-gel prosess
8	Hydrochloric acid		Merck			Activation of silica surface
9	NaOH		Sigma			Activation of silica surface
10	Toluene		Merck	1.08325	108-88-3	Solvent in the ionic liquid synthesis
11	DMF		Merck		68-12-2	Solvent in the baicalin functionalization
12	Ethanol		Merck		64-17-5	Solvent

(cont. on next page)

Table 3.1. (cont.).

Item No	Reagent	Structure	Company	Product Code	Cas No	Purpose of Use
13	Methanol		Riedel	34885	67-56-1	Solvent, mobile phase
14	1-vinyl imidazole	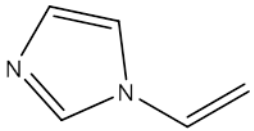	Sigma Aldrich	235466	1072-63-5	Ionic liquid precursor
15	1-methyl imidazole	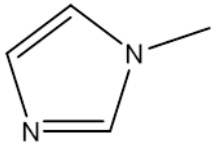	Merck	805852	616-47-7	Ionic liquid precursor
16	2-ethyl-4-methylimidazole, 95%	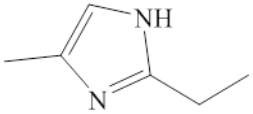	Aldrich	E36652	931-36-2	Ionic liquid precursor
17	Baicalin **(**Baicalein 7-*O*-β-D-glucuronide)	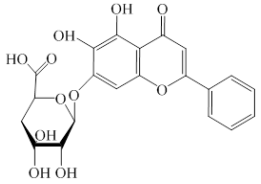	Aldrich	572667	21967-41-9	Baicalin functionalization of silica fiber and silica monolith

(cont. on next page)

Table 3.1. (cont.).

Item No	Reagent	Structure	Company	Product Code	Cas No	Purpose of Use
18	1-(3-dimethylaminopropyl)-3-ethylcarbodiimide hydrochloride (EDCl)	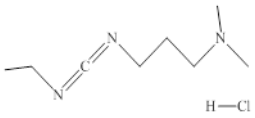	Sigma-Aldrich	E6383	6952-53-8	Cross linker in the baicalin-functionalized SPME fibers

(cont. on next page)

3.1.3. Chloro- and Amine- Coating of Bare Silica Fiber

Coating solutions with different precursors were prepared as follows; 100.0 µL PDMS (hydroxy terminated) and 150.0 µL THF were mixed in 1.5 mL vial. A precursor with 3-Chloropropyltrimethoxysilane (Cl-TMOS) or Aminopropyltrimethoxysilane (APTMS) of 50.0 µL was added into former solution; sequentially 25.0 µL of terminator (PMHS) was added to resulting solution. The sol-gel reaction was started after addition of 50.0 µL TFA (95v TFA+5v water) which was used to catalyze the reaction. The resulting solution was centrifuged for 10 min. Coating process was performed by the immersion of activated silica fiber into prepared solution for 30 min. After reaction period, coated fiber was dried at 60 ºC for 30 min. To achieve bulky coatings, the procedure can be repeated until desired thickness was obtained. Thermal curing at 120 ºC was applied for 24 h, which results in termination of the reactions.

The coating of the bare fibers was also performed with dip coater (Figure 2.1) for homogeneous surface coating. For the coating of the bare silica fiber, removal speed was selected as 10 mm/min.

3.1.4. Imidazole- and Baicalin- Functionalization of SPME Fibers

0.5 g of 2-ethyl-4-methylimidazole was added into 50.0 ml toluene, followed by the addition of TEA as a catalyst. Chloro- coated fibers were immersed into this solution, and refluxed for 24 h. After that, imidazole-functionalized SPME fibers were washed with successively, toluene, ethanol, and methanol, and dried at 60°C for 24 h (Row K.H., et al., 2010).

For baicalin functioanlization of amine- coated fibers; 0.10 g baicalin, 0.10 g EDCl were mixed in 50.0 ml DMF, and amine-coated fibers are dipped into this solution (L.-S. Qing et al. 2011). The solution was refluxed for 24 h in oil bath. The produced fibers were dried at 60°C for 24 h. The reaction for this modification is shown in Figure 2.2.

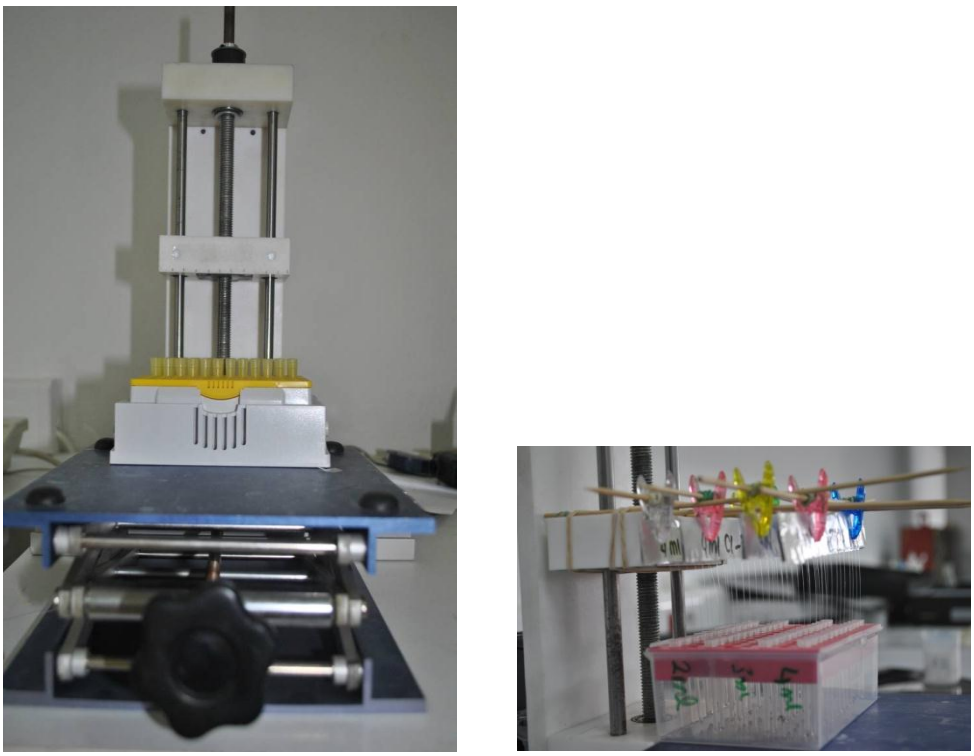

Figure 3.1. Dip coater (Nikon D3000).

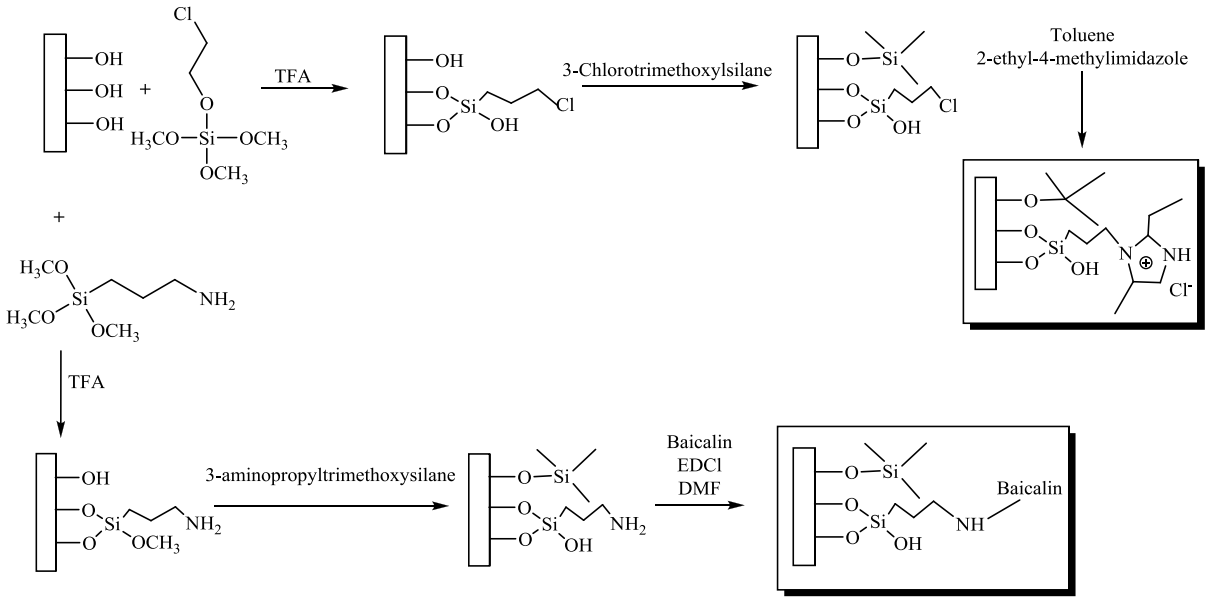

Figure 3.2. The reaction scheme for the preparation of imidazole- and baicalin-functionalized silica fibers.

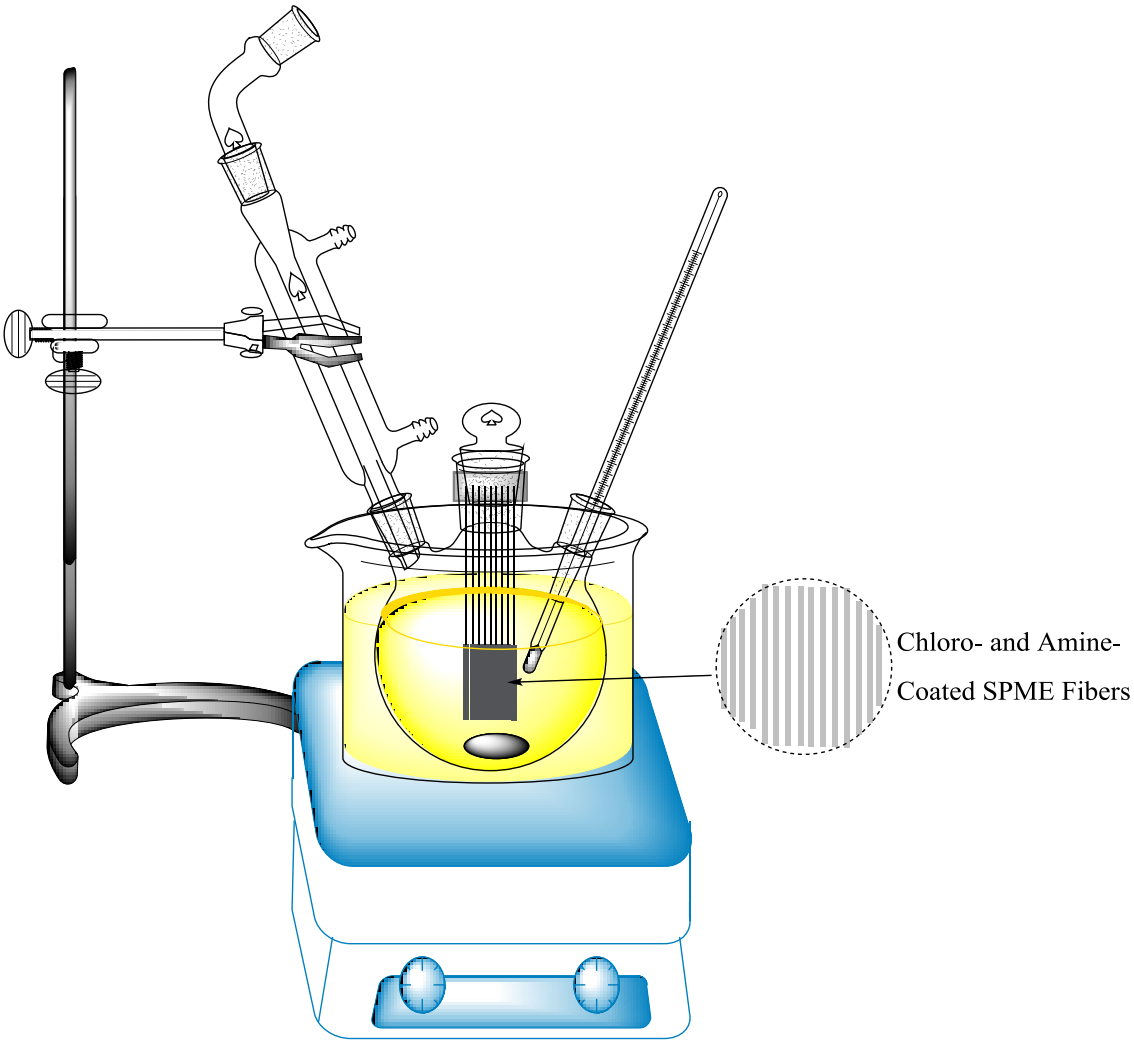

Figure 3.3. Experimental setup for the synthesis of baicalin- and imidazole-functionalized SPME fibers.

3.2. Results and Discussion

3.2.1. Characterization of SPME Fibers

3.2.1.1. SEM Results

SEM images of coated and bare silica fibers are displayed in Figure 3.4.- 3.26. SEM images of the bare silica fiber shows that the diameter of it is about 123.6µm. Then, these fibers were used in the coating processes. Both manually and by dip coater methods were applied for the production of coated fibers. SEM images show that manually coating produces SPME fibers that have lower surface roughness than dip

coater method. In the further stuides of SPME fiber coating dip coater method was utilized. In the early studies, different imidazole functionalized fiber produced with the presence and absence of PDMS. It is also done with for the baicalin functionalized fibers. In addition to these studies, more than one layer coated SPME fibers produced which have different diameters. Hence, we can control the coating thickness by increasing the number of coatings on the bare fiber. That is why, SPME coated fibers having different thickness can be produced which can be seen from the SEM images.

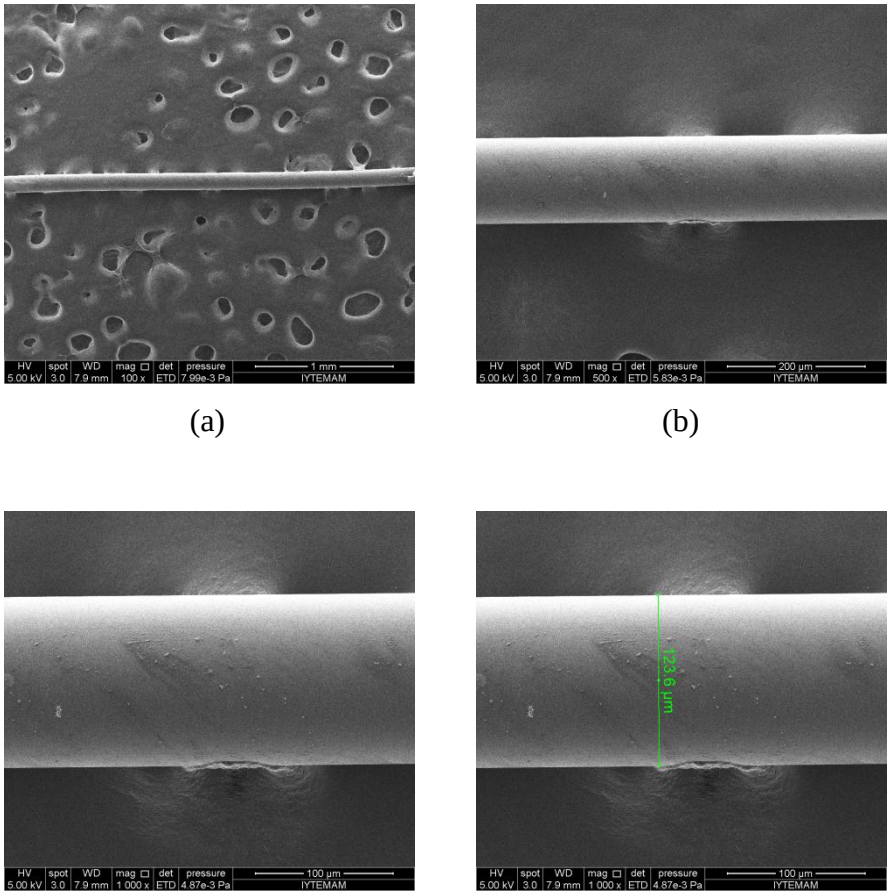

(a) (b)

(c) (d)

Figure 3.4. SEM images of bare fiber at varous maginifications (a) 100x, (b) 500x, (c) 1000x, (d) 1000x.

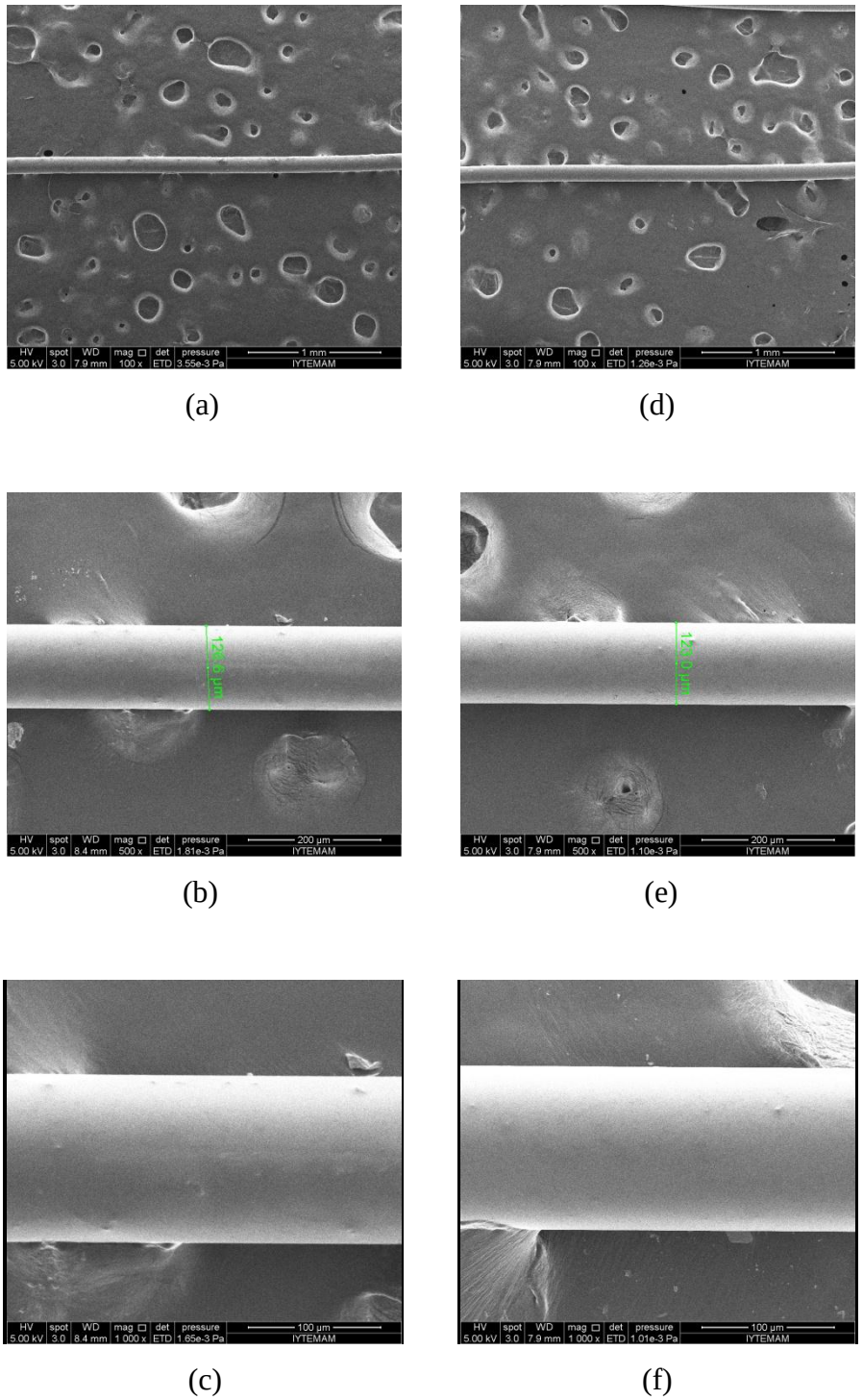

Figure 3.5. SEM images of manually single layer coated sol-gel based chloro-functionalized fibers (no PDMS) SPME fibers

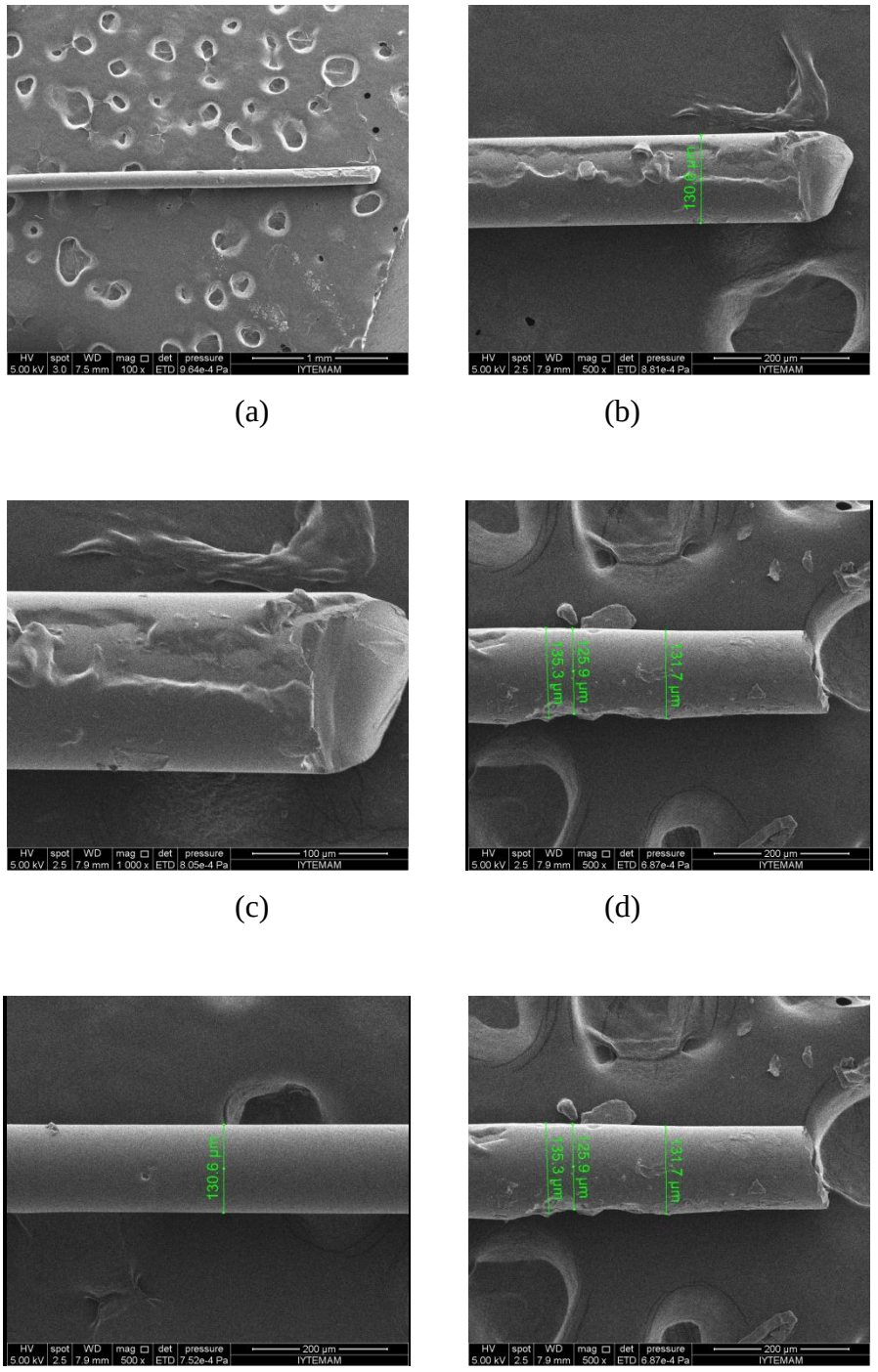

(a) (b)

(c) (d)

(e) (f)

Figure 3.6. SEM images of manually double layer coated sol-gel based chloro-functionalized (no PDMS) SPME fibers

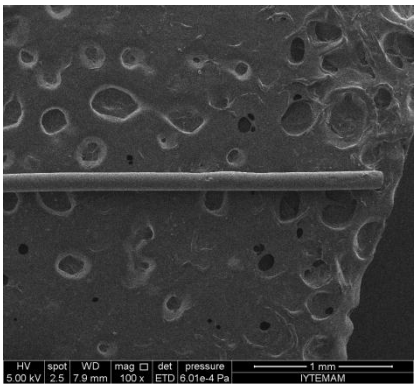

(a)

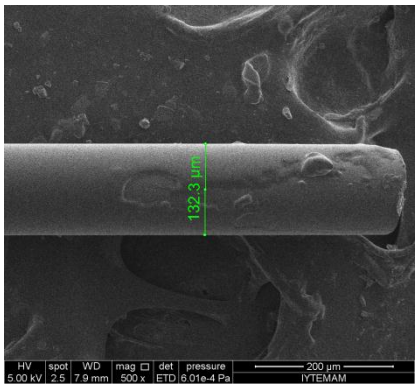

(b)

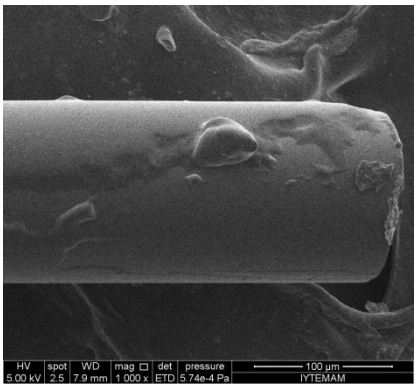

(c)

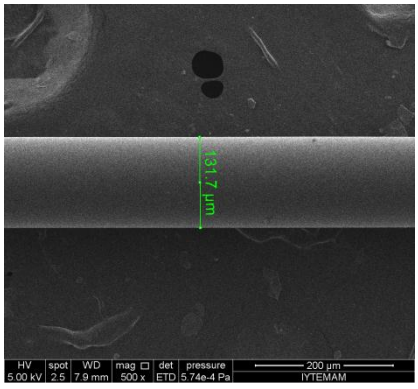

(d)

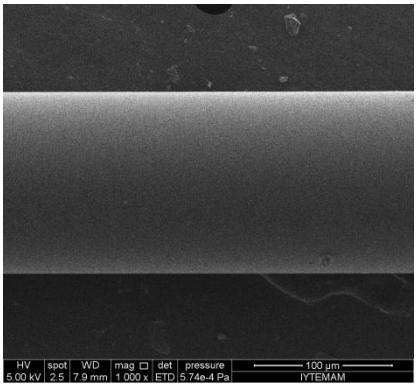

(e)

Figure 3.7. SEM images of manually double layer coated sol-gel based chloro-functionalized fibers (with PDMS) SPME fibers at various magnifications.

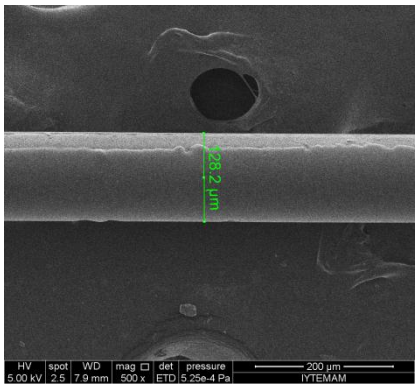

(f)

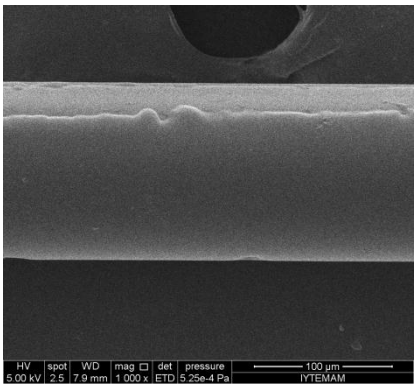

(g)

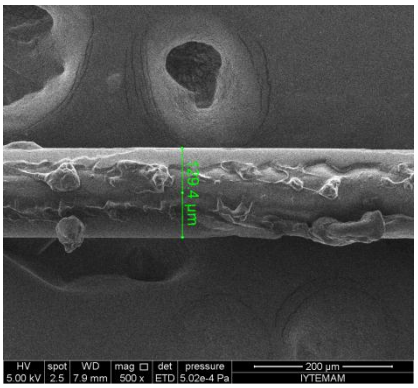

(h)

Figure 3.8. SEM images of manually double layer coated sol-gel based chloro-functionalized (with PDMS) SPME fibers (from a different parts of a fiber)

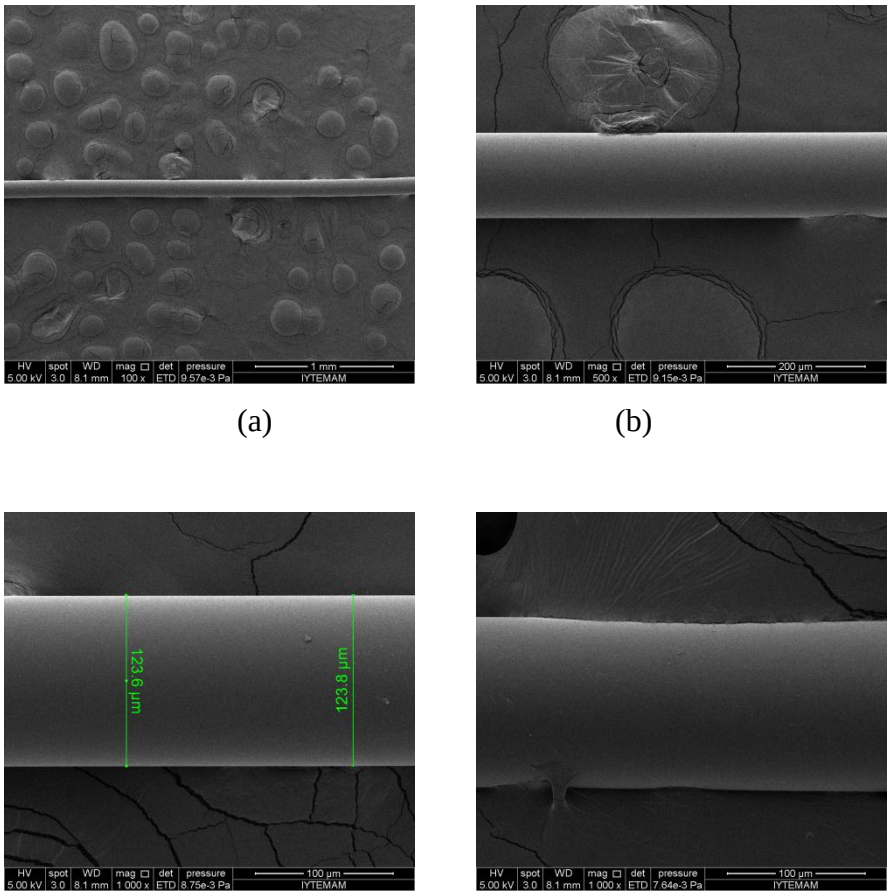

(a) (b)

(c) (d)

Figure 3.9. SEM images of manually coated 1-vinylimidazole modified SPME fibers after single layer coating of sol-gel based chloro-functionalization (no PDMS) at various magnifications.

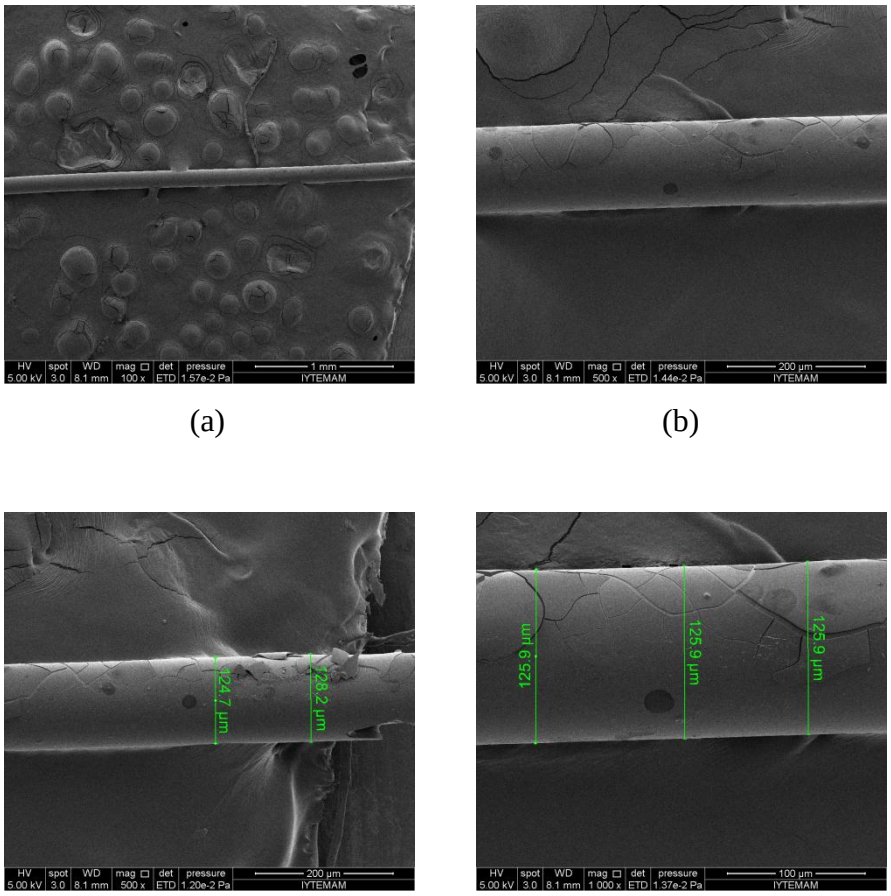

(a) (b)

c) (d)

Figure 3.10. SEM images of manually coated 1-vinylimidazole modified SPME fibers after double layer coating of sol-gel based chloro-functionalization (no PDMS) at various magnifications.

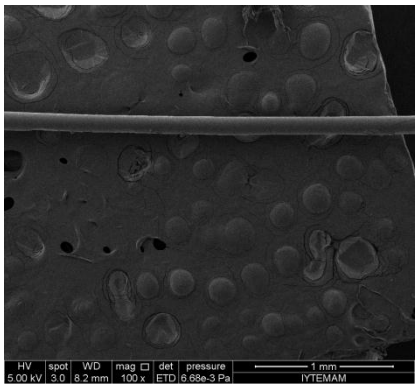

(a)

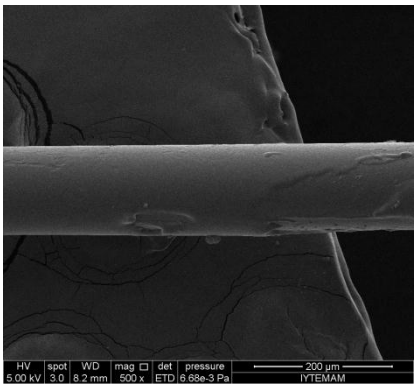

(b)

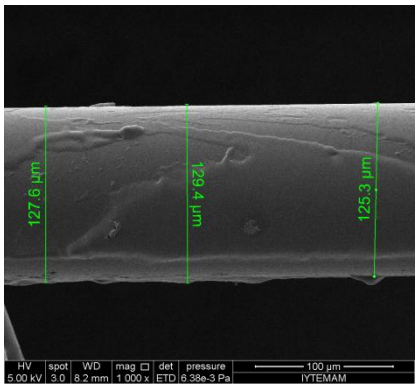

(c)

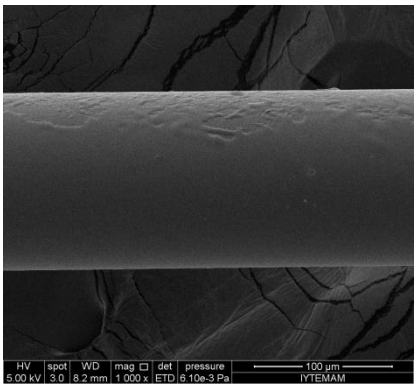

(d)

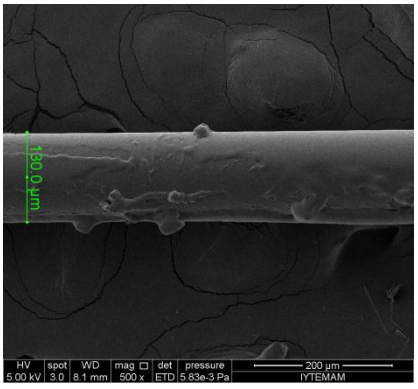

(e)

Figure 3.11. SEM images of manually coated 1-vinylimidazole modified SPME fibers after single layer coating of sol-gel based chloro-functionalization (with PDMS) at various magnifications.

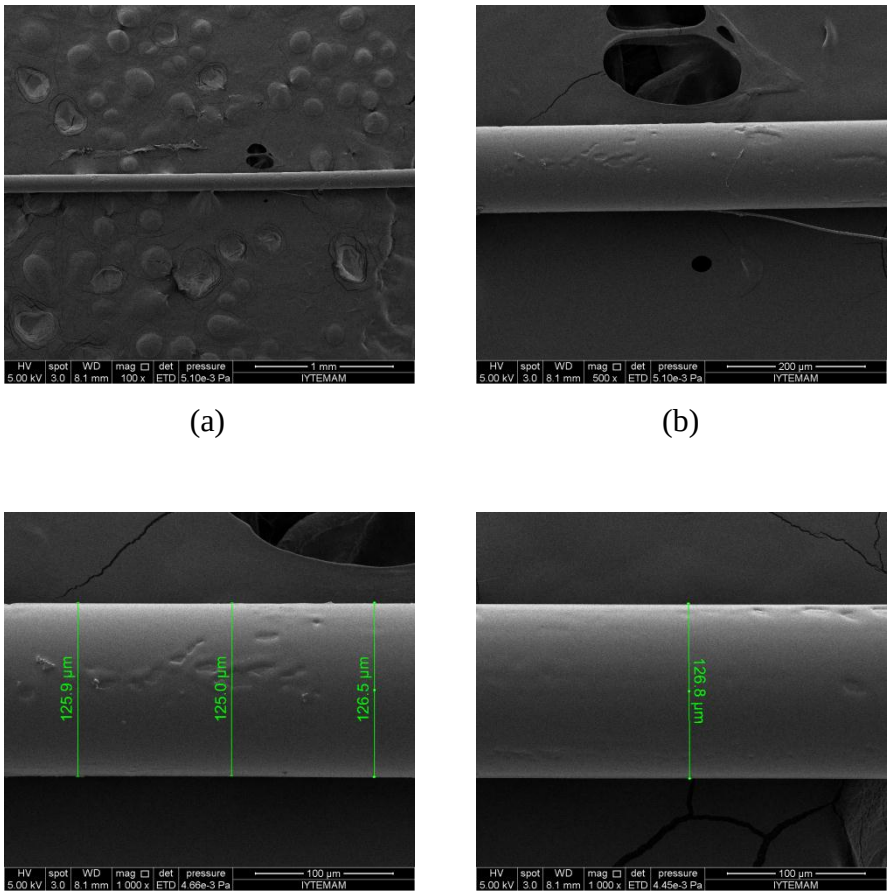

(a) (b)

(c) (d)

Figure 3.12. SEM images of manually coated 1-vinylimidazole modified SPME fibers after double layer coating of sol-gel based chloro-functionalization (with PDMS) at various magnifications.

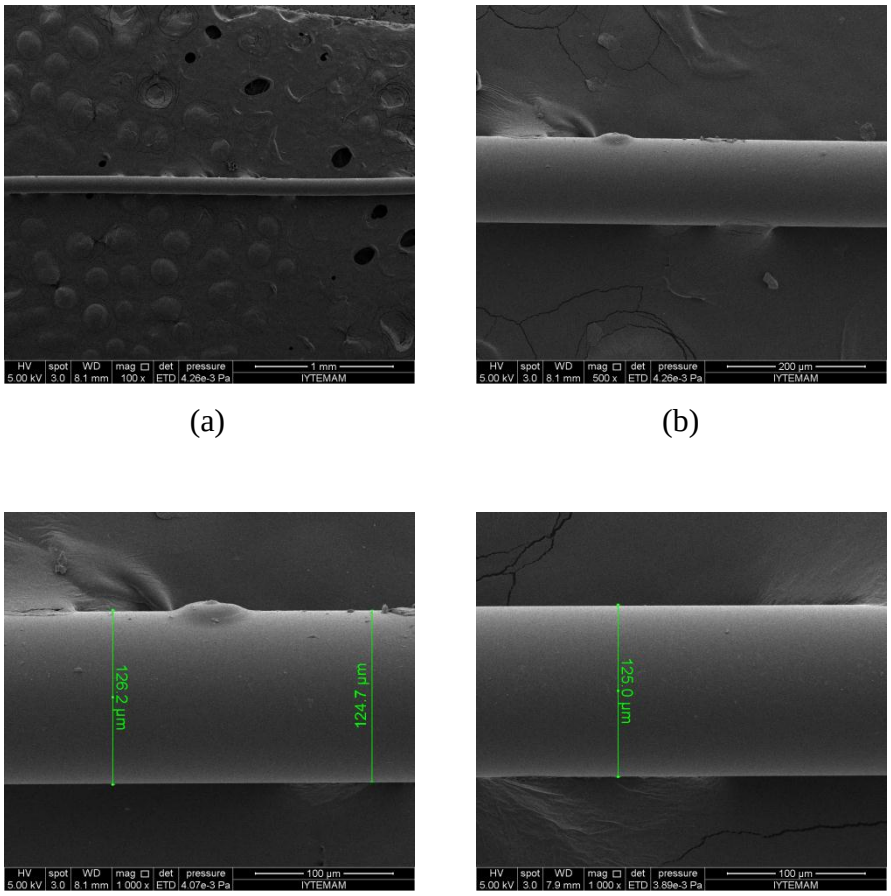

(a) (b)

(c) (d)

Figure 3.13**.** SEM images of manually coated 1-methylimidazole modified SPME fibers after single layer coating of sol-gel based chloro-functionalization (no PDMS) at various magnifications.

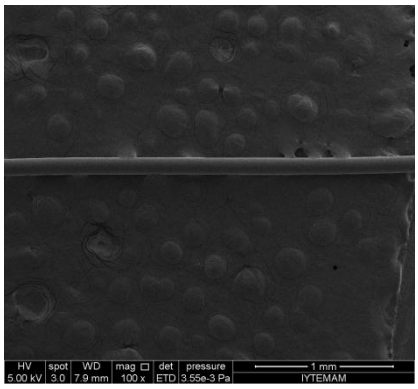

(a)

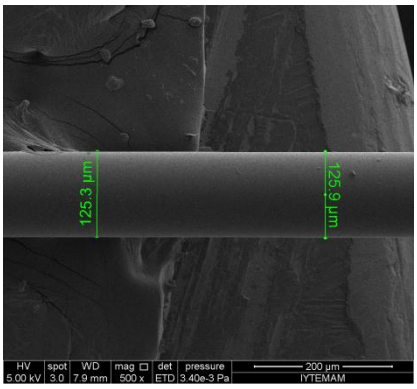

(b)

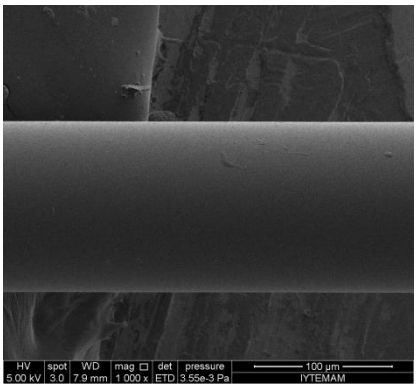

(c)

Figure 3.14**.** SEM images of manually coated 1-methylimidazole modified SPME fibers after double layer coating of sol-gel based chloro-functionalization (no PDMS) at various magnifications.

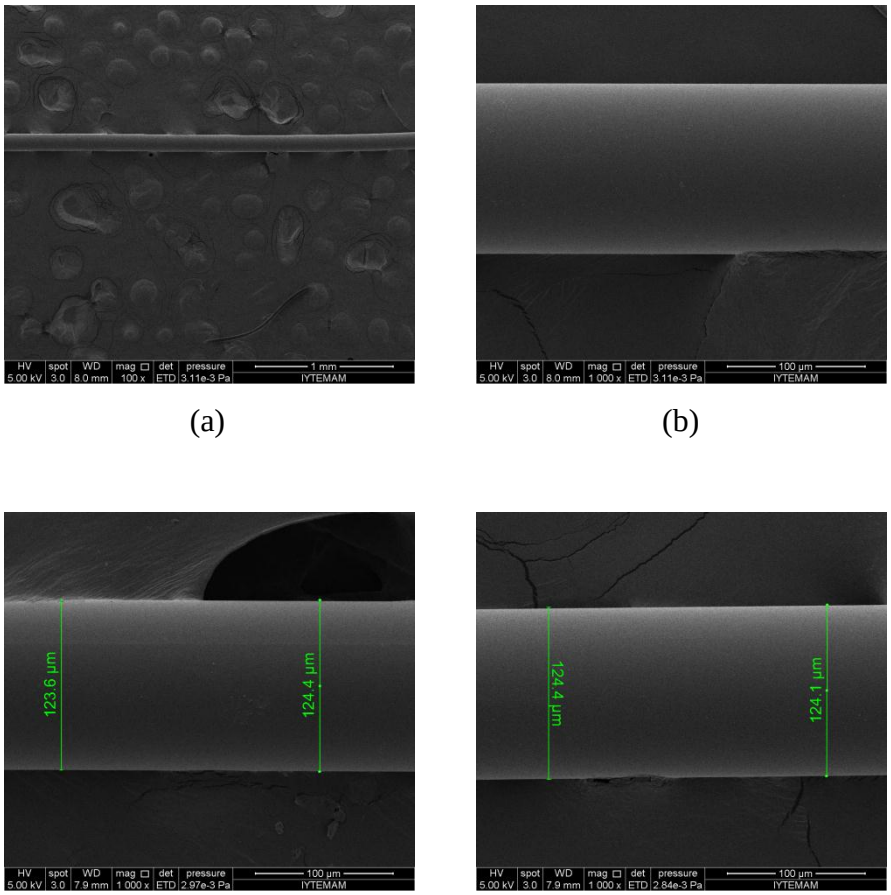

Figure 3.15. SEM images of manually coated 1-methylimidazole modified SPME fibers after single layer coating of sol-gel based chloro-functionalization (with PDMS) at various magnifications.

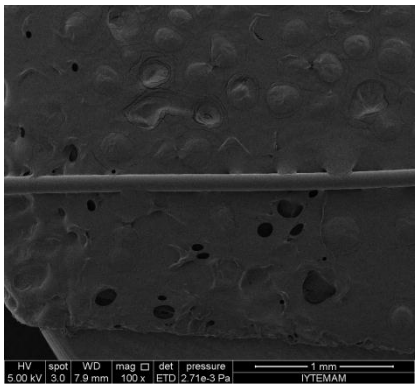

(a)

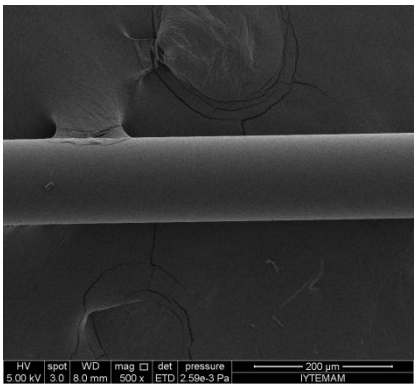

(b)

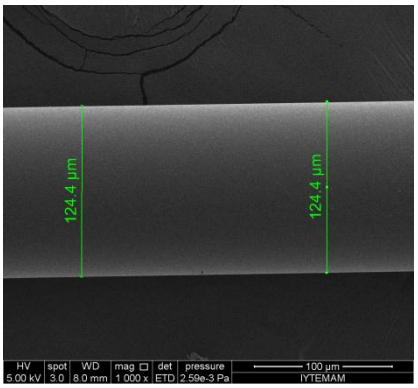

(c)

Figure 3.16. SEM images of manually coated 1-methylimidazole modified SPME fibers after double layer coating of sol-gel based chloro-functionalization (with PDMS) at various magnifications.

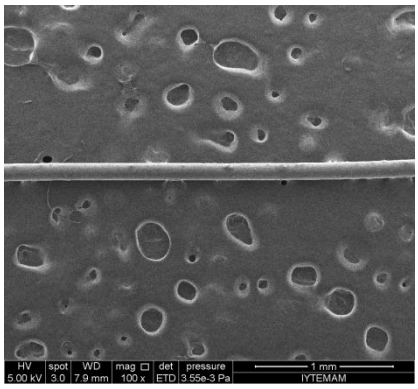

(a)

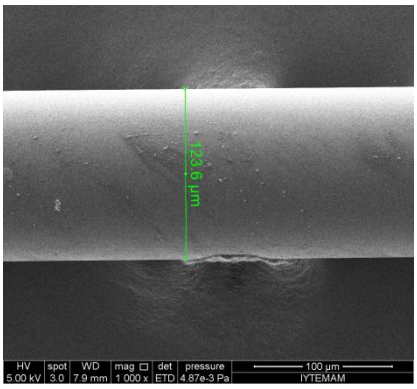

(b)

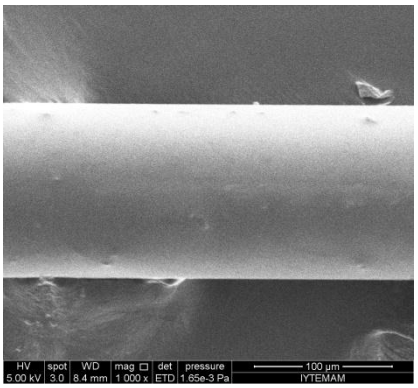

(c)

Figure 3.17. SEM images of sol-gel based chloro-functionalized fibers SPME fibers with dip coater: single layer coating ((a) 100x, (b) 500x, (c) 1000x)

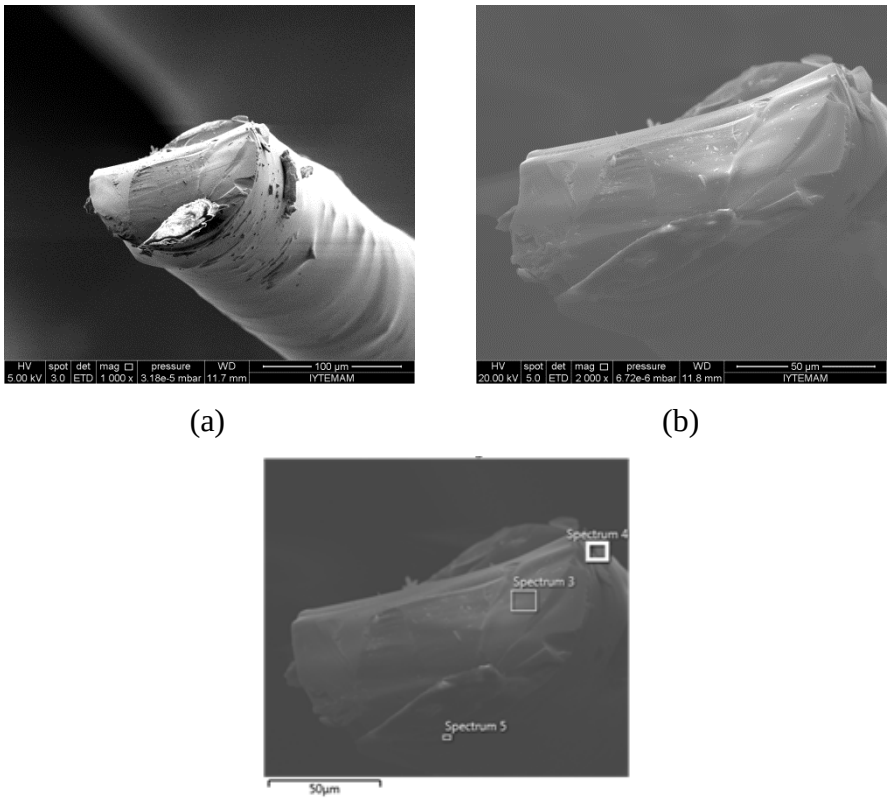

(a) (b)

(c)

Figure 3.18. SEM images of sol-gel based chloro-functionalized fibers with dip coater: double layer coating ((a) 1000x, (b) and (c) 2000x.

Table 3.4. Elemental composition of chloro-functionalized silica fibers (from SEM EDX results of Figure 3.23).

Element	Weight %		
	Spectrum 3	Spectrum 4	Spectrum 5
C	19.85	60.50	48.45
N	4.17	0.00	0.00
O	55.41	36.35	31.17
F	0.42	0.00	0.44
Si	19.14	0.04	15.90
Cl	1.01	3.12	4.04
Total:	100.00	100.00	100.00

In Figure 3.18., SEM image was taken from cut part of the coated fiber to show difference between inner part of silica fiber and coating layer. Then, SEM EDX spectra

were obtained different of cut surface of fiber. From these spectra, the elemental composition changed from the coating layer to inner surface of fiber. The similar results were obtained in Figure 3.19. and elemental composition for the selected areas in the image are listed in Table 3.4. Figure 3.19. also shows the coating process was not uniform, SEM EDX results (Table 3.5.) indicates the coating was achieved.

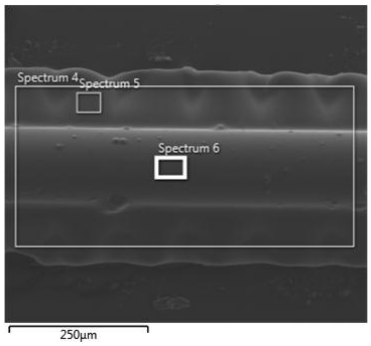

Figure 3.19. SEM images of sol-gel based chloro-functionalized fibers with dip coater: triple layer coating.

Table 3.5. Elemental composition of chloro-functionalized silica fibers (from SEM EDX results of Figure 3.23).

Element	Weight %		
	Spectrum 4	Spectrum 5	Spectrum 6
C	27.75	40.36	9.28
N	1.19	1.95	1.69
O	41.96	31.19	54.79
F	0.00	0.00	0.00
Si	23.75	19.18	33.75
Cl	5.36	7.31	0.50
Total:	100.00	100.00	100.00

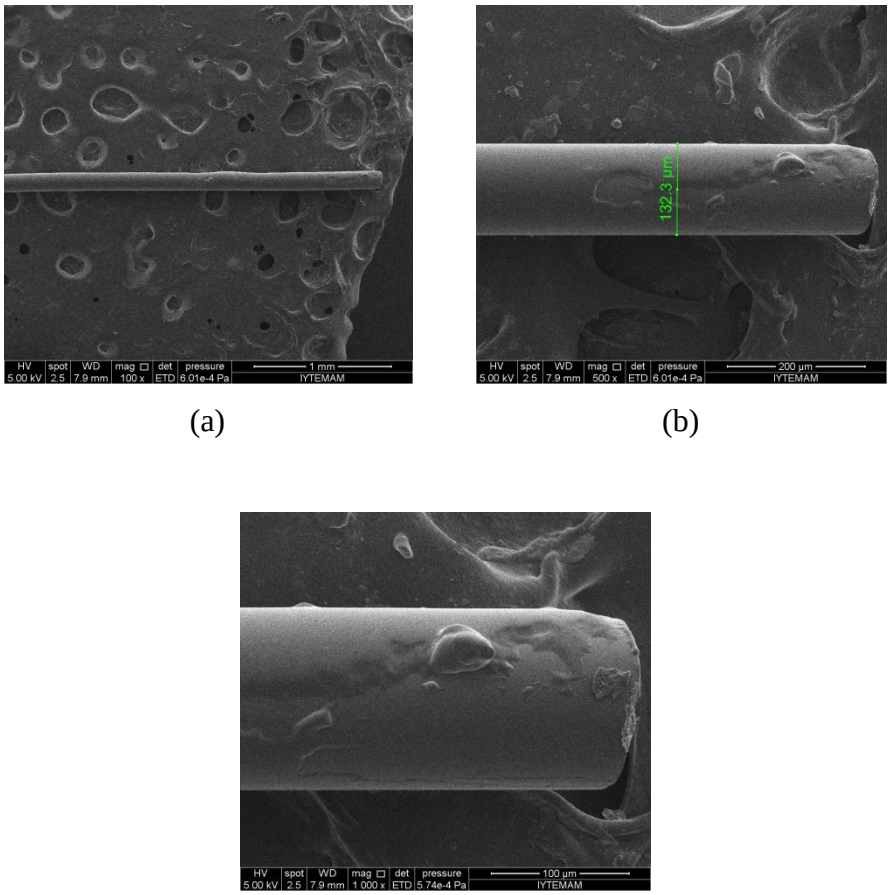

(a) (b)

(c)

Figure 3.20. SEM images of sol-gel based amine-functionalized fibers SPME fibers with dip coater: single layer coating ((a) 100x, (b) 500x, (c) 1000x.

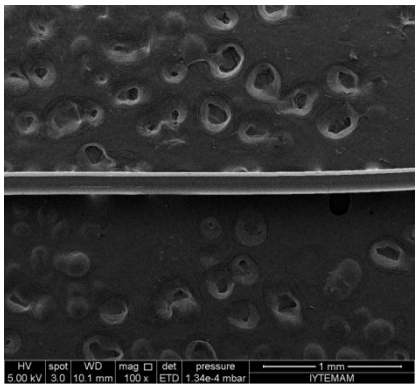

(a)

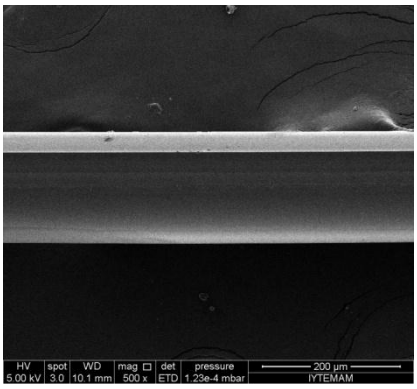

(b)

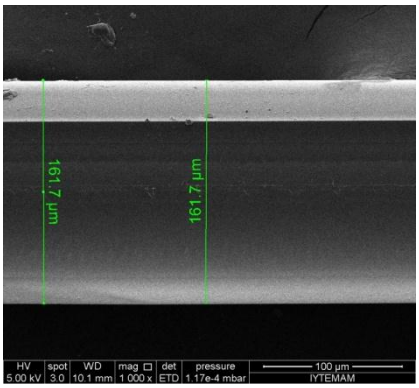

(c)

Figure 3.25. SEM images of imidazole-functionalized silica fiber (after triple layer chloride coating silica fiber) at various magnifications (6a) 100x, (6b) 500x, (6c) 1000x.

Figure 3.25. illustrates the effect of number of coating layer in the thickness of coated fibers. Imidazole-functionalized silica fiber after triple layer coating with Cl-TMOS was achieved with a thickness of fiber as 161.7 nm. The same trend was observed with an increase in the thickness of baicalin-functionalized silica fibers, for example, obtained thickness was around 206 nm (Figure 3.26.).

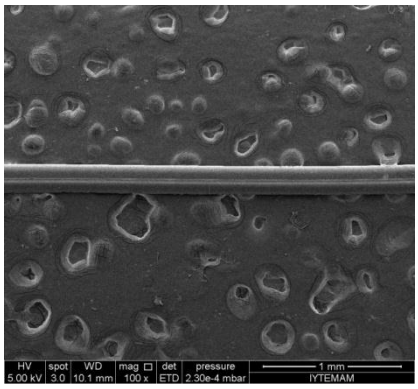

(a)

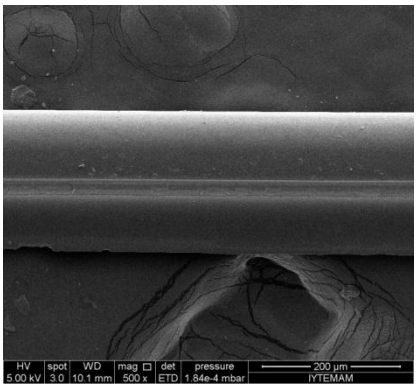

(b)

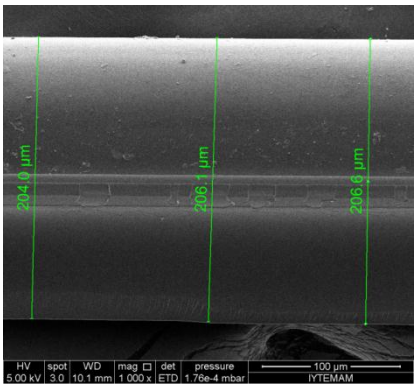

(c)

Figure 3.26. SEM images of baicalin-functionalized silica fiber (after triple layer amine coating of silica fiber) at various magnifications (a) 100x, (b) 500x, (c) 1000x.

CHAPTER 4

NOVEL SOLID PHASE MICROEXTRACTION COATINGS FOR FLAVONOIDS PART II: MONOLITHIC SILICA

4.1. Experimental

4.1.1. Chemicals and Reagents

The chemicals and the reagents used for the synthesis of polystyrene, monolithic silica and imidazole- and baicalin-functionalization of monolithic silica were tabulated in Table 4.1.

Table 4.1. The properties of chemicals and reagents.

Item No	Reagent	Structure	Company	Product Code	Cas No	Purpose of Use
1	Styrene (Phenylethylene, Vinylbenzene)	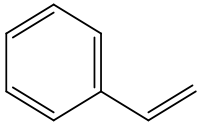	Sigma-Aldrich	S4972	100-42-5	Polystyrene synthesis
2	Sodium hydroxide					
3	Potassium persulfate	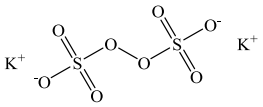	Sigma-Aldrich	216224		Initiator in the polystyrene synthesis
4	Tetramethyl orthosilicate	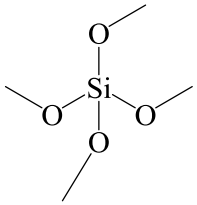	Merck	8.14178	1185-55-3	Silica source in monolithic silica synthesis
5	Pluronic F127	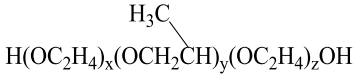	Sigma	P2243	9003-11-6	Triblock copolymer in the polystyrene synthesis
6	n-Pentane		Merck	107177	109-66-0	Cosurfactant in polystyrene synthesis
7	Hydrochloric acid		Merck	100317	7647-01-0	

(cont. on next page)

Table 4.1. (cont.).

Item No	Reagent	Structure	Company	Product Code	Cas No	Purpose of Use
8	Ethanol					Cosurfactant in polystyrene synthesis
9	(3-aminopropyl)trimethoxysilane (3-(Trimethoxysilyl)propylamine), 97%	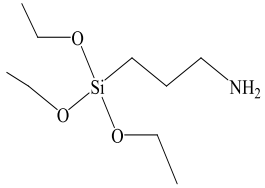	Aldrich	2811778	13822-56-5	Functionalization of silica fiber, functional monomer in the MIS synthesis
10	(3-chloropropyl) trimethoxysilane	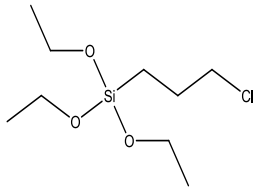	Aldrich	569615	5089-70-3	Functionalization of silica fiber
11	Toluene		Merck	1.08325	108-88-3	Solvent in the ionic liquid synthesis
12	Hexane	-	Merck	1.04391	92112-69-1	Solvent
13	Methanol		Merck	106007	67-56-1	Extraction solvent
14	DMF		Merck	103053	472-41-7	Solvent in the baicalin functionalization of monolithic silica

(cont. on next page)

Table 4.1. (cont.).

Item No	Reagent	Structure	Company	Product Code	Cas No	Purpose of Use
15	2-methyl-4-methylimidazole	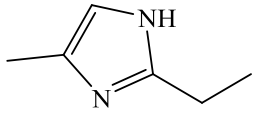	Aldrich	E36652	931-36-2	Ionic liquid precursor
16	Baicalin **(**Baicalein 7-*O*-β-D-glucuronide)	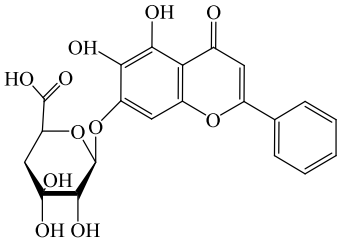	Aldrich	572667	21967-41-9	Baicalin functionalization of silica monolith
17	1-(3-dimethylaminopropyl)-3-ethylcarbodiimide hydrochloride (EDCl)	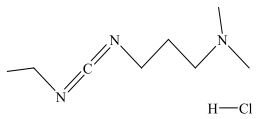	Sigma-Aldrich	E6383	25952-53-8	Cross linker in the baicalin-functionalized SPME fibers
18	Poly(methylhydrosiloxane) (PMHS)	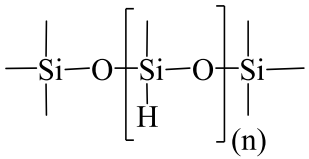	Aldrich	81330	9004-73-3	Deactivator in sol-gel process

(cont. on next page)

Table 4.1. (cont.).

Item No	Reagent	Structure	Company	Product Code	Cas No	Purpose of Use
19	Poly(dimethylsiloxane), hydroxy terminated (PDMS)	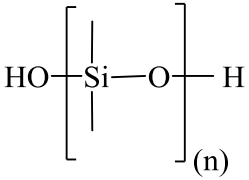	Aldrich	481939	70131-67-8	Organic polymer with sol gel active terminal for SPME coatings
20	THF		Sigma-Aldrich	87368	109-99-9	Solvent in sol-gel process
21	TFA		Merck	76-05-1	808260	Catalyst in sol-gel prosess

4.1.2. Synthesis of Polystyrene Templated Monolithic Silica

4.1.2.1. Synthesis of Polystyrene Macropore Template

Polystyrene nanospheres were synthesized according to the literature (Stein A. and co-workers et. al, 1999) by an emulsifier-free emulsion polymerization technique. A 105 mL of styrene was washed five times with 100 mL of 0.1 M NaOH (to remove the inhibitor 4-tert-butylcatechol in styrene). Washing was repeated with 100 mL water five times. Then, the color of styrene changed from colorless to pale yellow and that of NaOH solution changed from colorless to pink. For the synthesis of polystyrene macropore template, the experimental apparatus was given in Figure 2.5 and 2.6. (The polystyrene synthesis was performed with a three-necked flask). The system was purged with nitrogen for 2 h to eliminate radical scavenging oxygen from the reactor. A four-necked flask was filled with 850 mL degassed water and heated to 70°C, then 100 mL of washed styrene was added to this flask. Heidolph mechanical stirrer was used. A 0.3315 g of potassium persulfate initiator was added into a separate 200 mL polyethylene beaker containing 50 mL of water. The potassium persulfate solution was heated to 70°C. The reaction flask containing washed styrene was kept at 70°C, and the persulfate solution was introduced dropwise. The reaction flask was stirred at 300 rpm for 28 h at 70°C. The milky white final reaction mixture was obtained and poured into a polypropylene bottle and cooled to room temperature (before stored in a refrigerator at 4°C). The colloidal solution was centrifuged at 4000 rpm for 3h (for packing into a monolith structure), and the solid was dried at 60°C for 2h.

Figure 4.1. Change in the color of styrene during the extraction with NaOH.

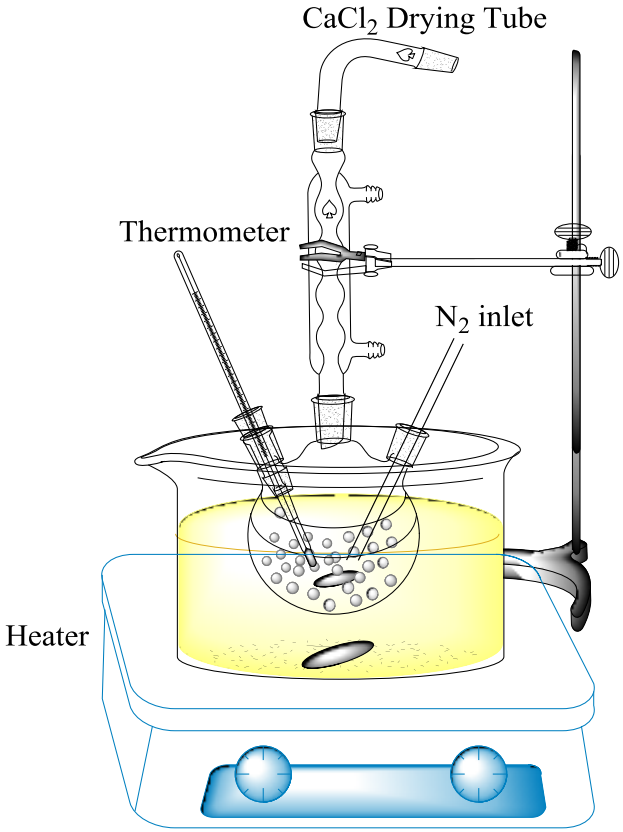

Figure 4.2. Set-up for the synthesis of polystyrene nanospheres

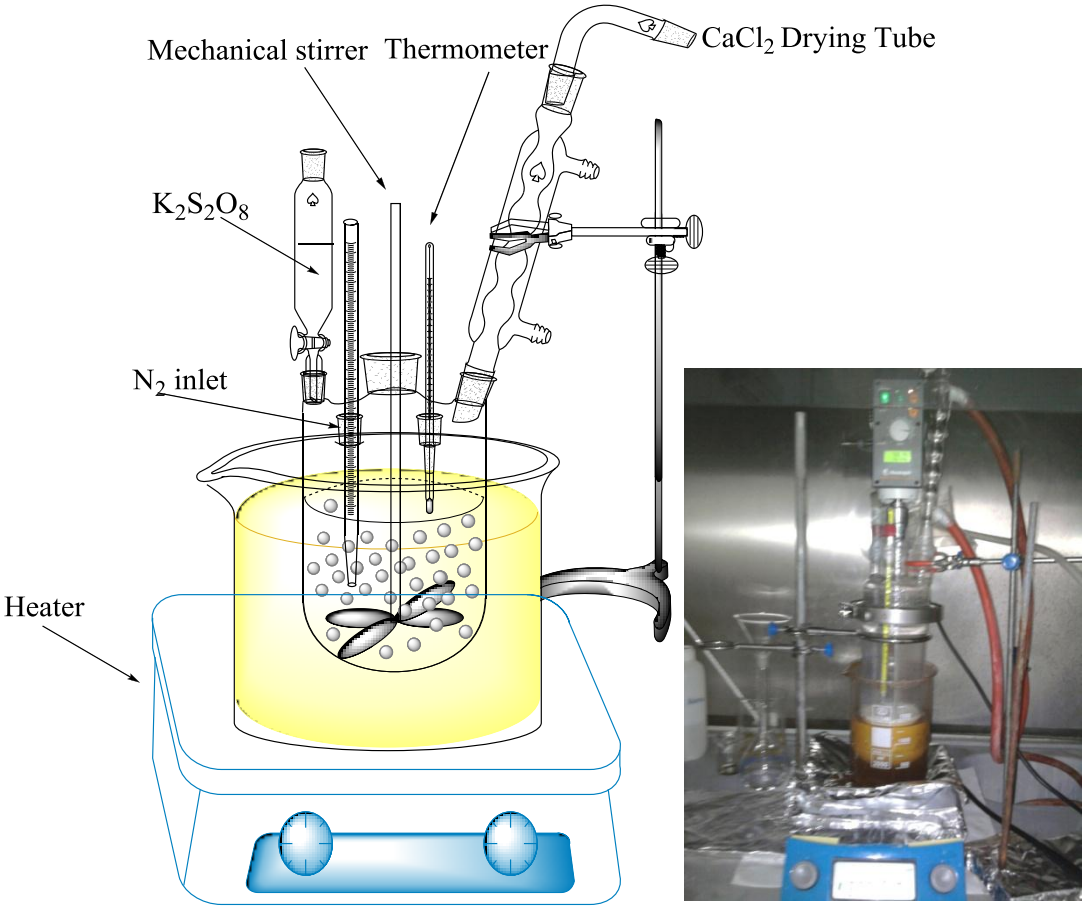

Figure 4.3. Set-up for the synthesis of polystyrene nanospheres.

4.1.2.2. Synthesis of Silica Monolith

Synthesis of silica monolith was performed by tetramethyl orthosilicate (TEOS) as a silica source, polstyrene spheres as a template, pluronic F127 as a block copolymer and ethanol or ethanol/n-pentane mixture as a cosurfactant (A.R. Loiola, et. al., 2008). First step is to prepare the acid-catalyzed sol-gel hydrolysis solution. For this, a 80.3 µL of concentrated HCl was added into a 250 mL polypropylene beaker containing 6.94 g of distilled water. Then, this solution was mixed with 18.16 g of TEOS for 15 min to start the acid catalyzed hydrolysis, stirring was continued until the temperature of the mixture was dropped to room temperature (Figure 2.10). In another polypropylene beaker, a 12.08 g of F127 and 6.0 ml of n-pentane or ethanol/n-pentane (1:1 mixture) were mixed to obtain clear solution. Next, the silicate and surfactant solutions were mixed for 15 min. After that, a 2.0 g of polystyrene spheres were added, and the final

solution was stirred for 1h. Then, the solution was centrifuged at 6000 rpm for 1h to remove the excess hydrolysis solution. After that, a hard gel was obtained. The obtained hard gel was first dried at 60°C for 2 h, then calcined at 550°C for 10 h at a heating rate of 1°C min^{-1}.

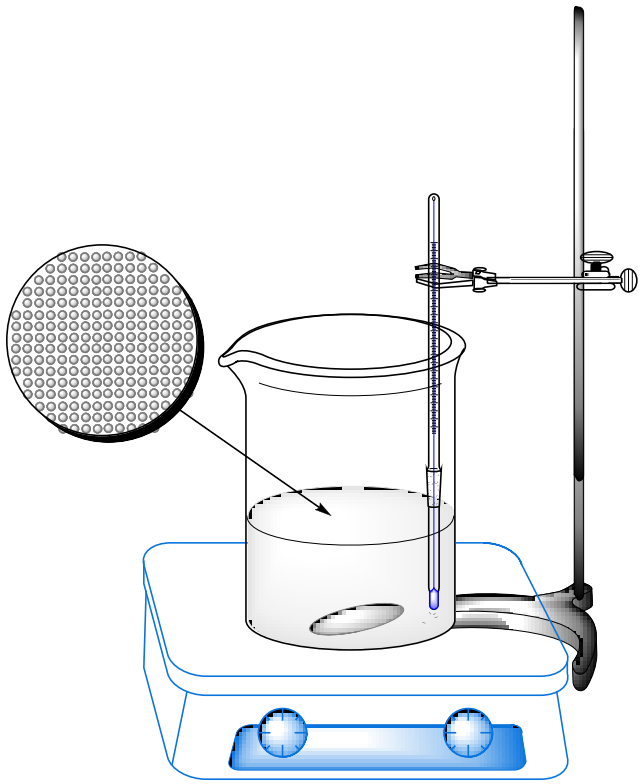

Figure 4.4. Set-up for the synthesis of silica monolith.

4.1.2.3. Imidazole Functionalization of Silica Monolith

Ionic liquid was synthesized according to the method applied by Row K.H and co-workers, 2010 (Figure 2.7. and 2.8.). It was prepared as, (3-chloropropyl)trimethoxysilane (24.5 mL, 0.102 mol) and 2-ethyl-4-methylimidazole (11.359 g, 0.103 mol) were placed into a 250- mL round-bottomed flask containing 40 mL of toluene. Temperature of the system (Figure 2.8.) was set to 100°C, and it was refluxed for 12 h. A slightly orange viscous oil was obtained, and the product was washed with cold hexane 3 times.

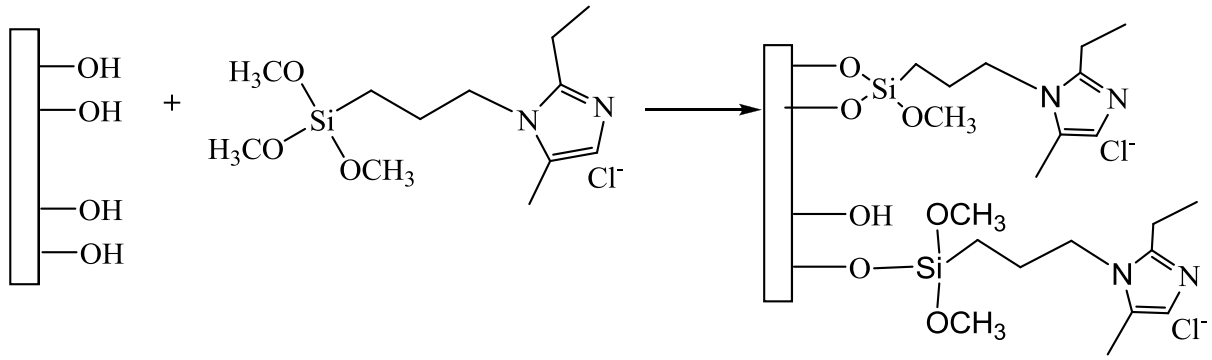

Figure 4.5. Reaction scheme for the preparation of imidazole-functionalized silica monolith.

The monolithic silica was first activated with a 50.0 mL solution of 0.01 M acetic acid for 1 h. Then, it was washed with ultrapure water. Washing was continued until a neutral filtrate was obtained. Activated monolithic silica was dried at 120°C for 24 h in an oven. A 0.235 g (0.67 mmol) of the product (ionic liquid) was added into 45 mL of toluene (Figure 2.3.). Activated monolithic silica were then added to this solution. This mixture was heated to 105°C, and then refluxed for 15 h (Figure 4.6). After that, imidazole-functionalized silica monolith were washed with successively, toluene, ethanol, and methanol, and dried at 60°C for 24 h (Row K.H., et al., 2010).

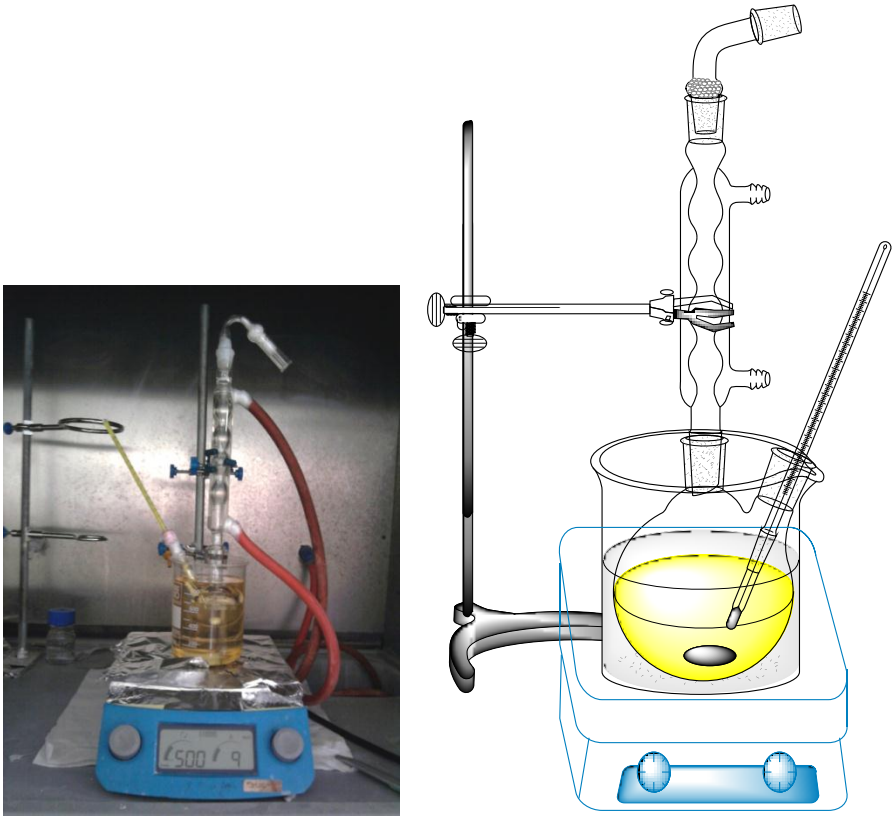

Figure 4.6. Experimental setup for the preparation of ionic liquid.

4.1.2.4. Baicalin Functionalization of Silica Monolith

The monolithic silica was first activated with a 50.0 mL solution of 0.01 M acetic acid for 1 h. Then, it was washed with ultrapure water. Washing was continued until a neutral filtrate was obtained. Activated silica was dried at 120°C for 24 h in an oven. Activated monolithic silica was modified first with amine, and then functionalized with baicalin. For the amine-modification of activated monolithic silica, 5.00 grams of activated silica, a 10.0 ml of toluene, and 3.0 mL of APTES were added into a two-necked flask. Experimental setup for this modification is shown in Figure 4.7. It was refluxed for 24 h at 110°C. Then, amine-modified monolithic silica was washed with acetone, toluene and dried at 60°C for overnight (Liu et al. 2002).

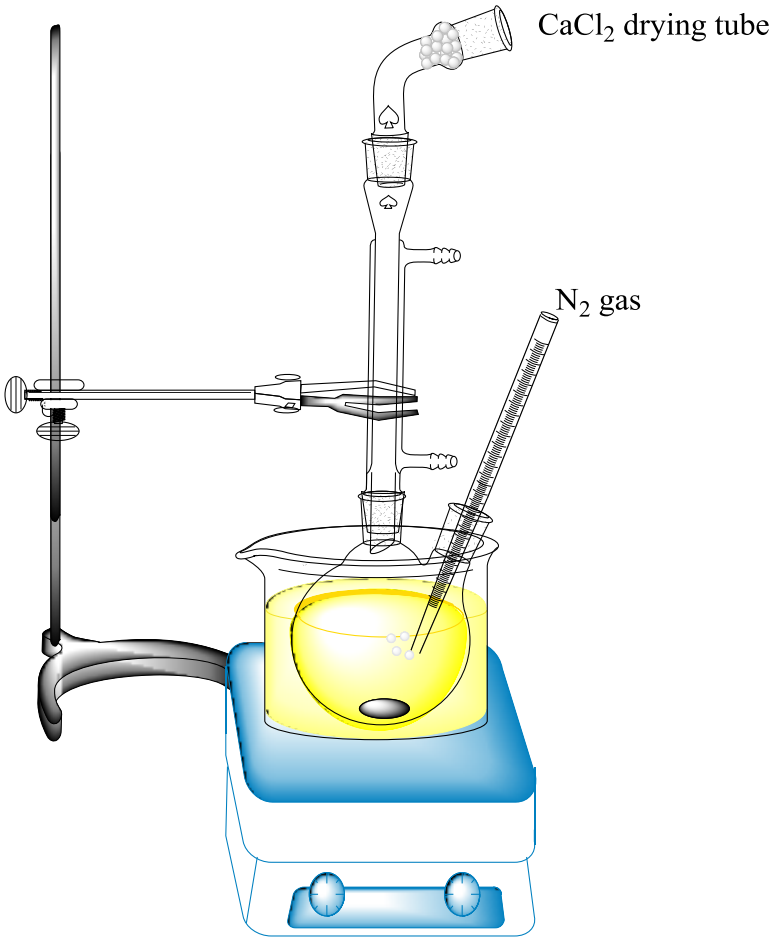

Figure 4.7. Experimental setup for the amine-modification of monolithic silica.

For the baicalin-functionalization of monolithic silica, the synthesis procedure was same as in the baicalin-functionalization of amine-coated silica fiber (Chapter 3).

4.1.2.5. SPME Fiber Coating with Imidazole- and Baicalin-Functionalized Monolithic Silica

Two methods were applied for the immobilization of imidazole- and baicalin-functionalized monolithic silicas on the surface of the bare silica fiber. First immobilization method was done by sol-gel solution. For this purpose, these modified silica samples were adhered onto the fiber surface by sol-gel coating solution. In this case, sol-gel solution behaves as a glue betwen a surface of a bare silica fiber and functionalized monolithic silicas. Sol-gel coating solution was prepared as: a 100.0 µL PDMS (hydroxy terminated) and a 150.0 µL THF were mixed in 1.5 mL vial. A

precursor with tetraethoxysilane (TEOS) of 50.0 µL was added into former solution; sequentially 25.0 µL of terminator (PMHS) was added to resulting solution. The sol-gel reaction was started after addition of 50.0 µL TFA (95v TFA+5v water) which was used to catalyze the reaction. The resulting solution was centrifuged for 10 min. Coating process was performed by the immersion of activated silica fiber into prepared solution for 30 min by a dip coater, and functionalized monolithic silicas were immobilized onto the surface of silica fiber.

The second immobilization method was the use of epoxy glue in the coating of stainless steel wire with imidazole- and baicalin-functionalized monolithic silicas. Before coating process, stainless steel wires were cleaned with acetone, ethanol, and methanol in ultrasonic bath for 30 min. Then, they were dried at 60°C for 24 h. Two-cm of the wire was limed with epoxy glue and imidazole- or baicalin-modified monolithic silica were immobilized on the surface of the wire. Next, coated wires were dried at 50°C for 24h. This coating was not used in the later studies. Since, the immobilized coatings did not extract the flavonoids studied. These could be due to blocking of functional groups which are responsible for the extraction of flavonoids. Hence, the first immobilization method (sol-gel solution as a glue) was used as the coating method throughout the study.

4.1.3. SPME Studies

A 10-mL aqueous solution of 0.10 mg/L flavonoids studied was transferred to a 20-mL amber glass vial containing a magnetic bar. The SPME extraction was performed with only baicalin-functionalized monolithic silica fiber for 5 min at room temperature with the solution being stirred at 300 rpm. After extraction, the extracted analytes on the SPME fiber were desorbed with 1.0 mL methanol in 5 min contact, and it was injected into the HPLC system for analysis.

4.2. Results and Discussion

4.2.1. Characterization of Polystyrene Nanosphers

4.2.1.1. SEM images

In Figure 4.8., the SEM images of the polystyrene nanospheres were shown. These nanospheres were synthesized by the experimental setup shown in Figure 4.2. In this case, magnetic stirring was followed and the particle size distributions of the polystyrene nanospheres were in the range of 160-400 nm which are not monodispersed.

The polystyrene nanospheres were also synthesized with another experimental setup (Figure 4.3.) which uses the mechanical stirring. The SEM images of the polystyrene nanospheres obtained with this approach was shown in Figure 4.9. It is indicated that mechanical stirring produces monodispersed polystyrene nanospheres. Moreover, the particle size of them ranges from 286 nm to 317 nm. In the following studies for the stynthesis of silica monolith this procedure were performed.

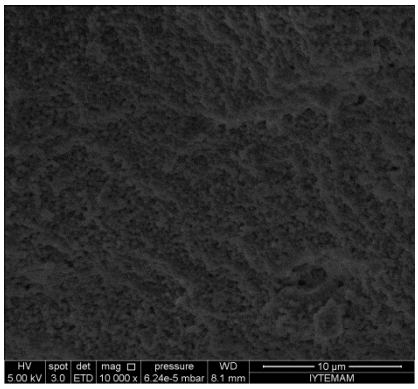

(a)

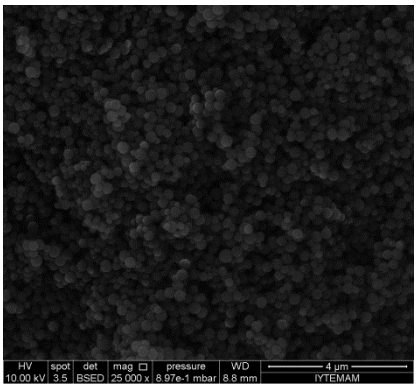

(b)

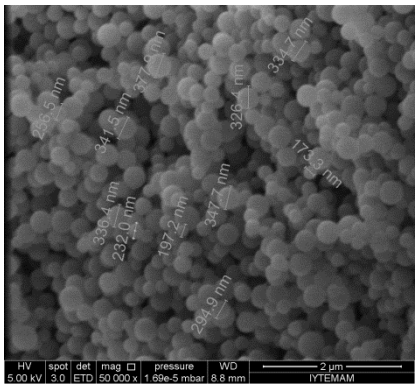

(c)

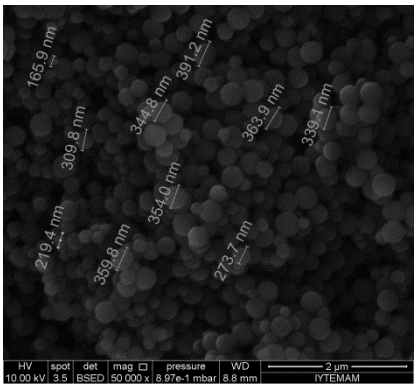

(d)

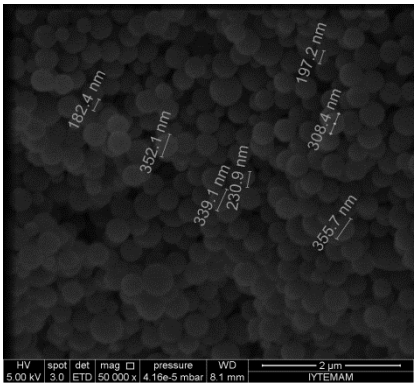

(e)

Figure 4.8. SEM images of polystyrene nanoparticles (synthesized by magnetic stirring)

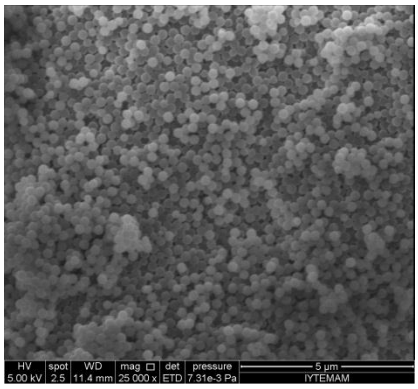

(a)

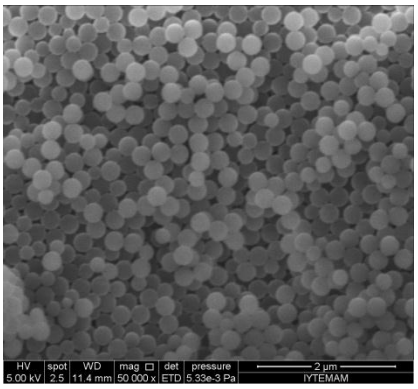

(b)

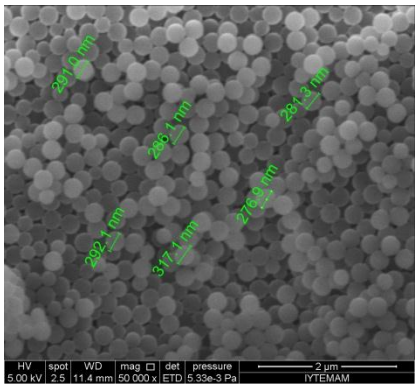

(c)

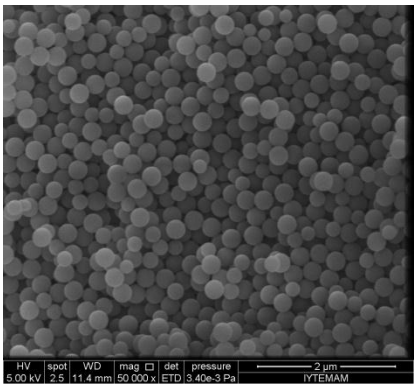

(d)

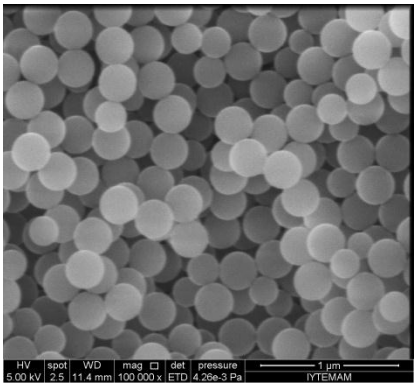

(e)

Figure 4.9. SEM images of polystyrene nanoparticles (synthesized by mechanical stirring)

4.2.2. Characterization of Monolithic Silica, and Functionalized Monolithic Silicas

The synthesized monolithic silica, baicalin- and imidazole- functionalized silica samples were characterized by SEM, FTIR, and elemental analysis.

4.2.2.1. SEM images

SEM images of monolithic silica samples at different magnifications are presented in Figure 4.10. and 4.11. These monolithic silicas were synthesized by polystyrene nanosphere template method (with mechanical strirring). It was demonstrated that all images have honeycomb-like structure in Figure 4.10. In this case, n-pentane was used as a cosurfactant in the silica monolith synthesis, and this helped to keep the monoliths as honeycomb-like structure. However, n-pentane/ethanol mixture was utilized as a cosurfactant, and it can be seen from the SEM images in Figure 4.11. honeycomb structure was not preserved, and there are still macropores present in the structure. Furthermore, the type of cosurfactant has an effect on the porosity of the monolith, that's why, in the following studies only n-pentane was used during the silica monolih synthesis. Figure 4.10 displays the magnified image of the macroporous monolith, and it can be seen that the diameter of the macropores lies between 210 and 220 nm. The main reason of this result is due to the usage of monodisperse polystyrene nanospheres during the synthesis. The same result is also seen from SEM images in Figure 4.11.

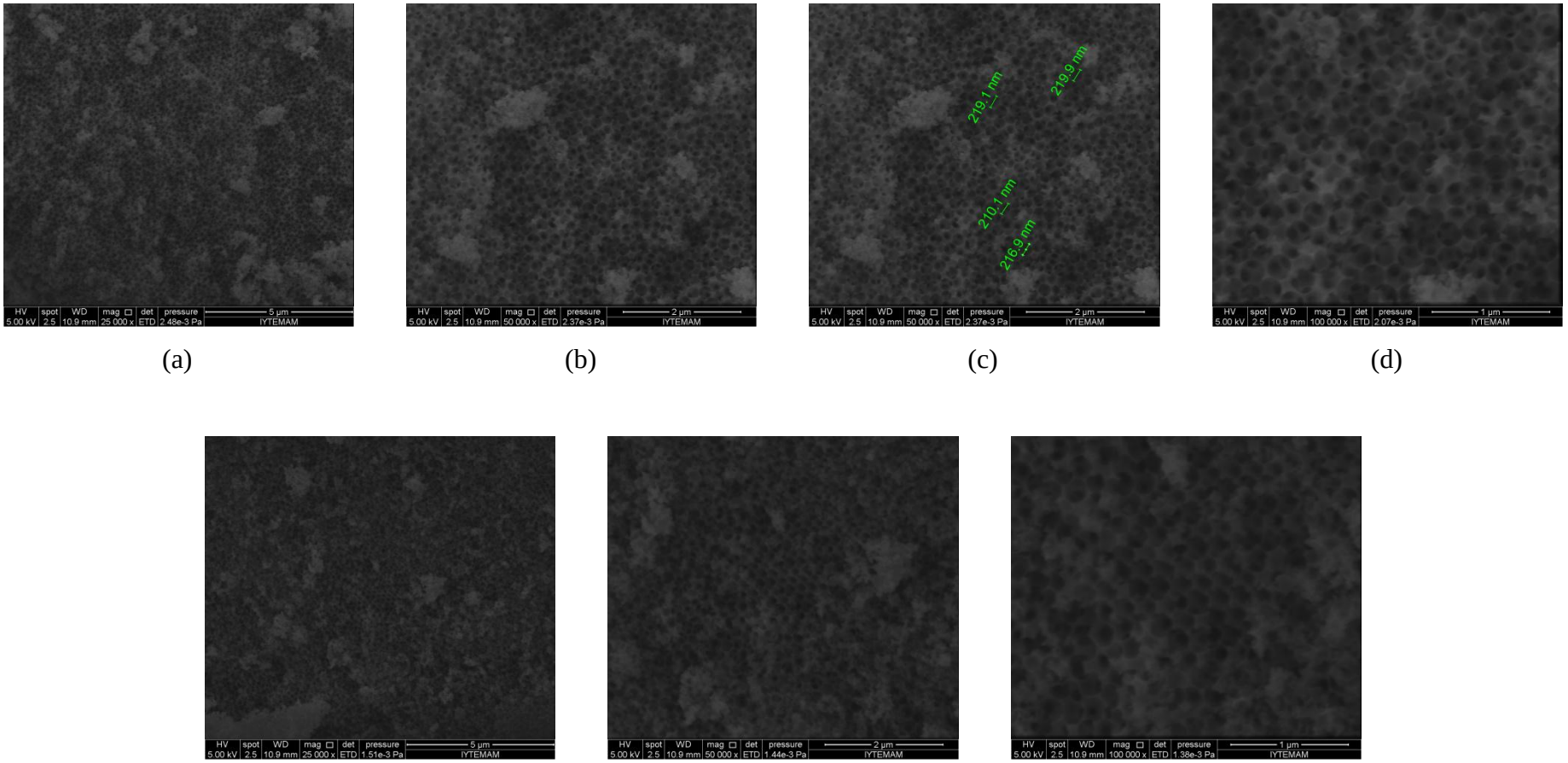

Figure 4.10. SEM images of silica monolith (n-pentane as a cosurfactant)

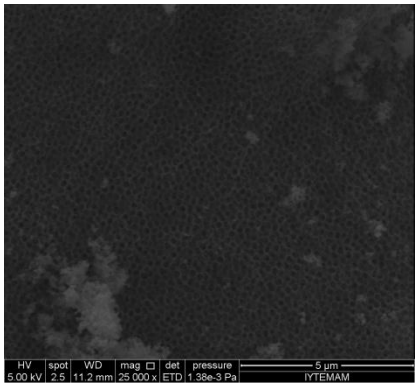

(a)

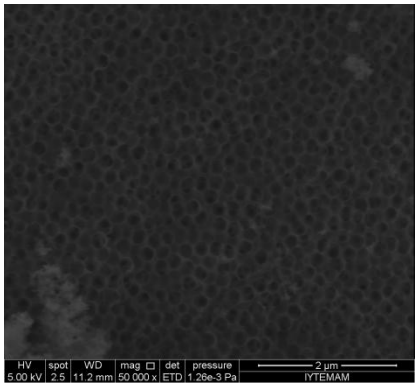

(b)

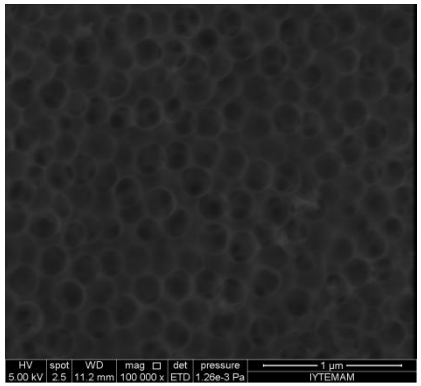

(c)

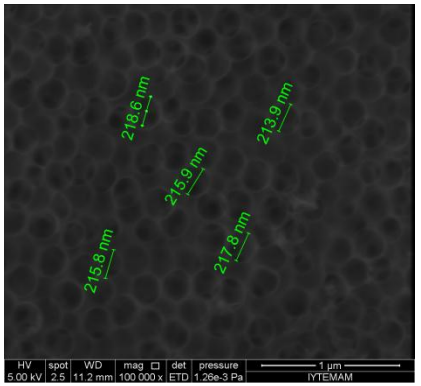

(d)

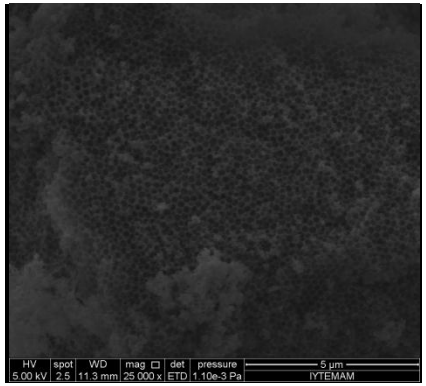

(e)

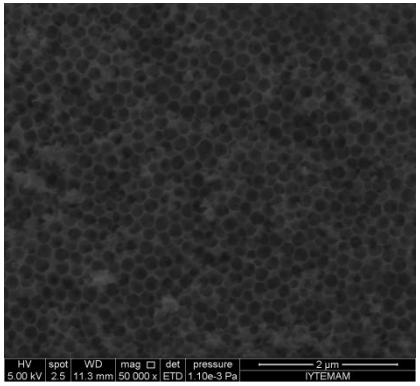

(f)

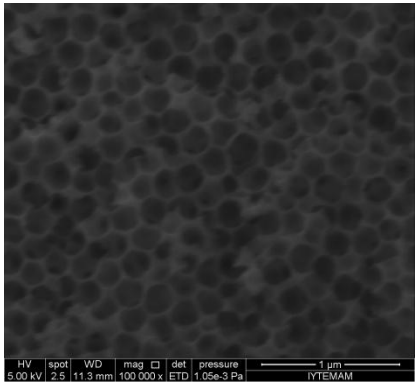

(g)

Figure 4.11. SEM images of silica monolith (n-pentane/ethanol mixture as a cosurfactant)

Figure 4.11. shows the SEM images of baicalin functionalized monolithic silica at different magnifications. It is clear that baicalin-functionalization of monolithic silica did not change or disrupt the honeycomb-like structure of monolithic silica. The main outcome of this result is that surface modification of silica monolith with baicalin without the loss of monolith structure.

SEM images of imidazole-functionalized silica can be seen in Figure 4.12. These images display that there is stil the presence of honeycomb-like structure of silica monolith, but some parts seem to be coated with the amorphous structure of silica. It may comes from the monolithic silica synthesis step. It is also possible that more than required amount sol-gel solution after the centrifugation step might remaint.

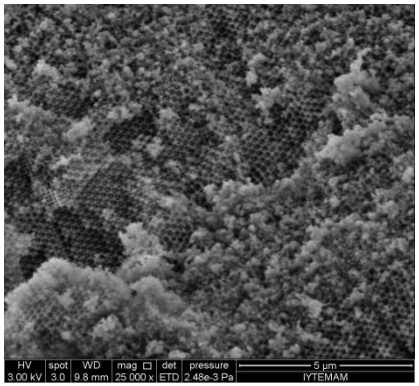

(a)

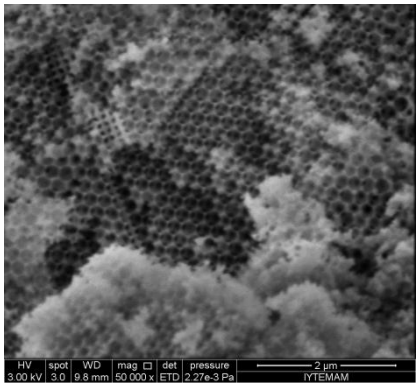

(b)

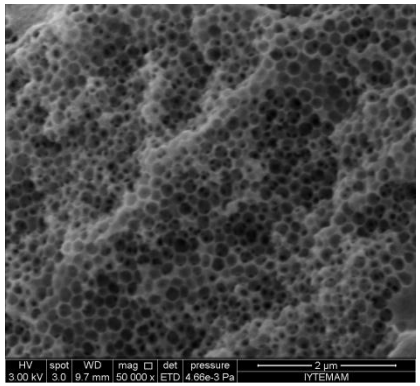

(c)

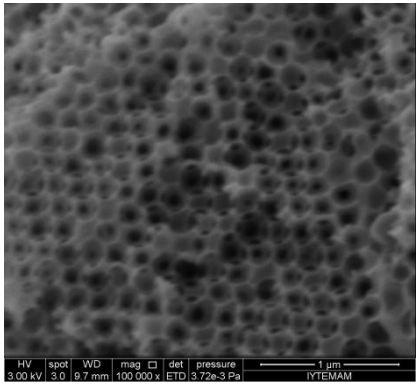

(d)

Figure 4.12. SEM images of baicalin functionalized silica monolith (a, b, c, and d) at different magnifications

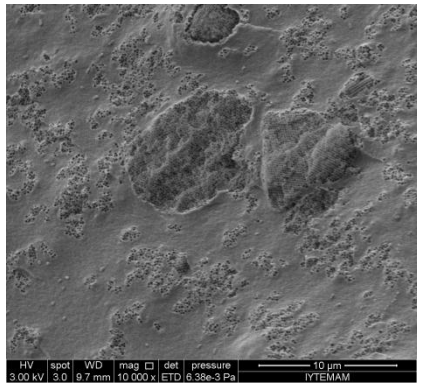

(a)

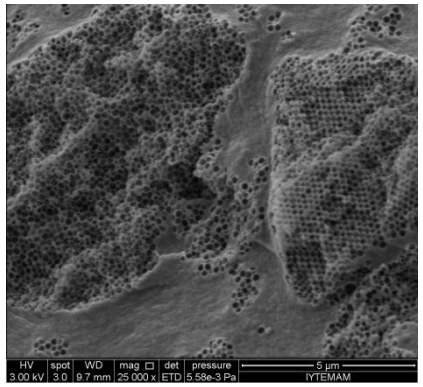

(b)

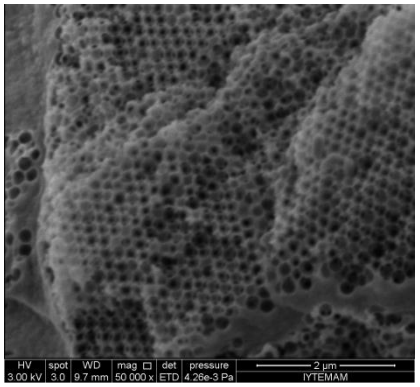

(c)

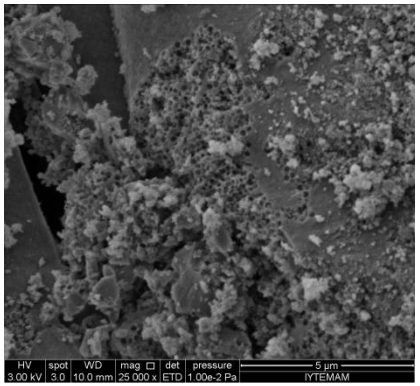

(d)

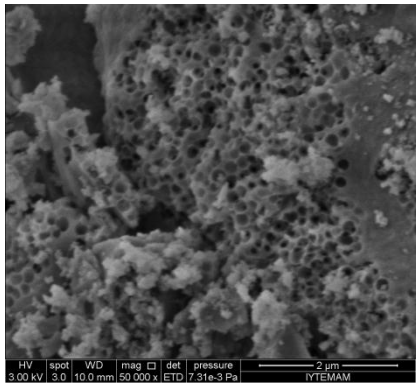

(e)

Figure 4.13. SEM images of imidazole functionalized silica monolith (a, b, c, d, and e) at different magnifications

4.2.2.2. FTIR Results

The functional groups in the monolithic silica and functionalized monolithic silicas obtained by FTIR are shown in Figure 4.15. These spectra were collected for monolithic silica, imidazole- and baicalin funtionalized monolithic silicas. These three spectra shows similar trend. The bands were intrinsic to the silica material, and the band was located at 3700-3200 cm^{-1} corresponds to the OH stretching vibrations of both the Si-OH group and carboxylic acid and OH groups in the baicalin structure. The asymmetrical stretching at 2360 cm^{-1} in only monolithic silica which can be arised from the presence of CO_2. The band at 1082 cm^{-1} indicates the strong Si-O bonds. In addition, Si-O-Si bending vibrations were located at 471 cm^{-1}. The peak at 2927 cm^{-1} shows C-H stretching of sp^3 hybridized C atoms. The difference in the monolithic silica and baicalin-functionalized monolithic silica could be seen from the peak at 1676 cm^{-1} which shows the presence of amine in the baicalin-functionalized monolithic silica. In addition, the peaks at 1388 and 1437 cm^{-1} are due to C-O stretching and C-N stretching vibrations, respectively. These peaks demonstrates the baicalin-functionalization of monolithic silica. In case of imidazole-functionalized-monolithic silica, the FTIR spectra were similar to the monolithic silica, and this shows the poor modification of the monolithic silica.

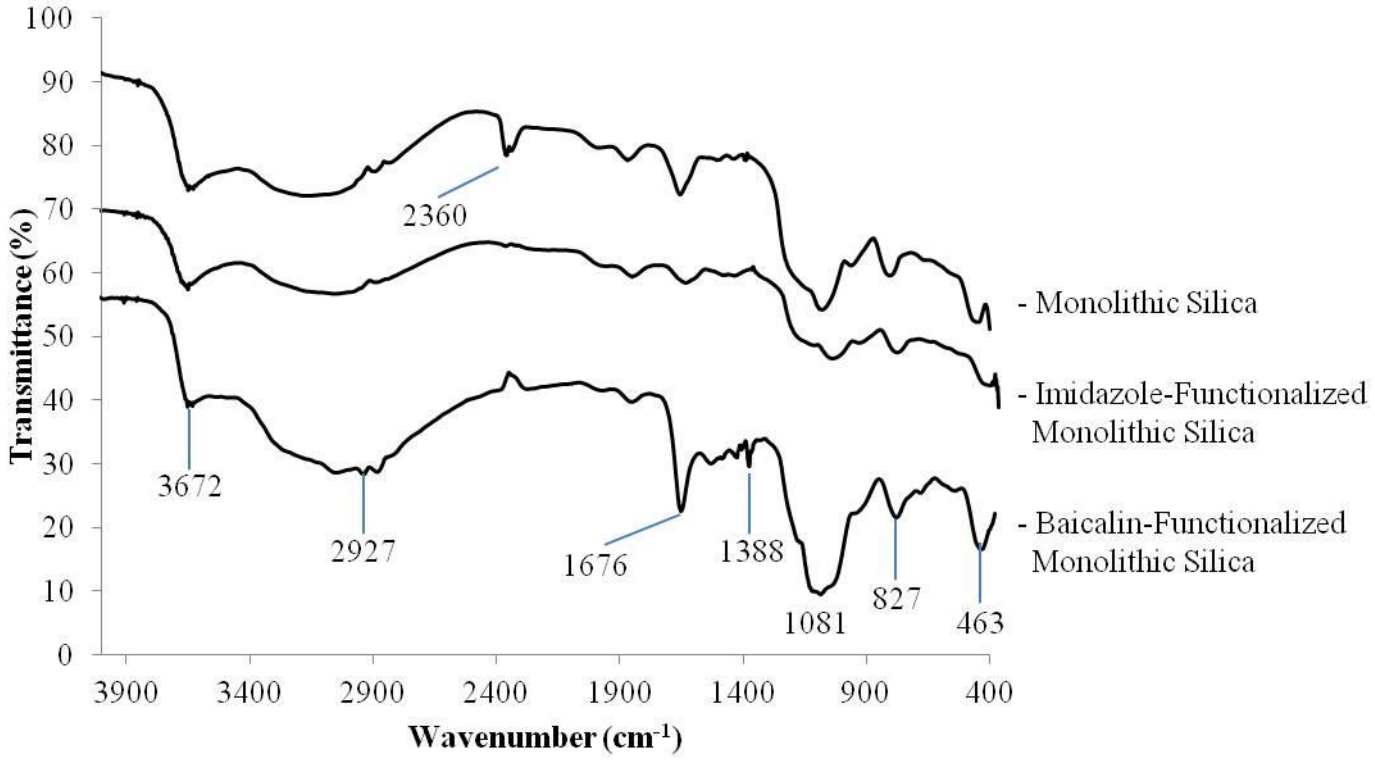

Figure 4.14. FTIR spectra of silica monolith, baicalin modified silica monolith, and imidazole modified silica monolith.

4.2.2.3. Elemental Analysis

Monolithic silica and functionalized monolithic silicas were also investigated in terms of their elemental composition, and the results were tabulated in Table 4.16. The percentage of C, H, N, S values changes from monolithic silica and functionalized monolithic silicas. Imidazole- and baicalin functionalized monolithic silica have higher carbon percentages as 3.025% and 10.360%, respectively than monolithic silica has. Baicalin-functionalized silica has highest C, H, N, and S percentages as 10.360%, 2.025%, 2.914%, and 0.121, respecttively among all. This results show that imidazole-functionalization of monolithic silica did not happened as expected, and it was also proved from the FTIR spectra of imidazole-functionalized monolithic silica.

Table 4.2. Elemantal composition of monolithic silicas.

Elements	**%C**	**%H**	**%N**	**%S**
* Monolithic silica	1.694	0.613	0.274	-
*Imidazole-functionalized monolithic silica	3.025	1.172	0.445	-
*Baicalin-functionalized monolithic silica	10.360	2.025	2.914	0.121

$$\text{Baicalin \%} = \left(\frac{\text{C \%}}{A_r(C)} - \frac{\text{N \%}}{A_r(N)} \times 3 \right) \times A_r(C) \div \left(\frac{A_r(C) \times 21}{M(C_{21}H_{18}O_{11})} \right)$$

Eqn. (4.1)

The mass percent of baicalin bound the monolithic silica can be determined with the aid of elemental analysis (Qing et al. 2011). It can be calculated by the Equation 4.1. In this equation, C% and N% are the content of carbon and nitrogen in baicalin-functionalized monolithic silica obtained from the elemental analysis. Ar(C), Ar(N), and Mr($C_{21}H_{18}O_{11}$) are the relative atomic mass of carbon and nitrogen, and relative molecular mass of baicalin, respectively. According to this method, the mass percent of baicalin was found as 5.068%. However, Qing and co-workers (2011) calculated the mass percent of baicalin loaded in baicalin-functionalized magnetic nanoparticles as

2.33%. This difference could be due to the monolithic structure synthesized in our study. Since, there are more active binding sites in the monolithic structure than the silica to be functionalized.

4.2.2.4. Thermal Gravimetric Analysis

Thermal stability of the monolithic silica and baicalin-functionalized monolithic silica was investigated, and the results were shown in Figure 4.15. The first mass loss is around 10% is due to the surface bound water molecules. In case, the second mass loss is due to the degradation of baicalin and APTES molecules in the baicalin-functionalized monolithic silica structure, and this can be seen in the range of 100-300°C temperature This behaviour was clearly illustrated in thermal decomposition curve (Figure 4.15).

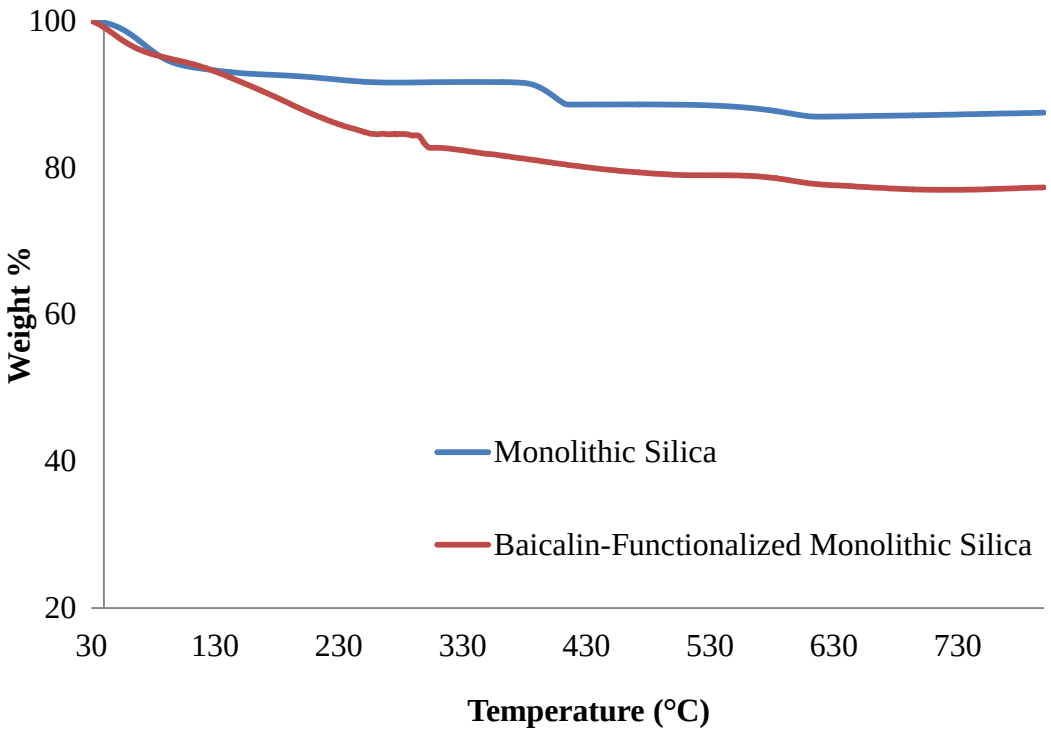

Figure 4.15. TGA decomposition curve of monolithic silica, and baicalin-functionalized monolithic silica

4.2.3. SPME of Flavonoids by Baicalin-Functionalized Monolithic Silica Fibers

Solid phase microextraction of these flavonoids were performed in aqueous solutions. Since, they are soluble in methanol, ethyl acetate, pyridine, slightly soluble in water, and practically insoluble in hexane and chloroform. For this reason, water was used as the extraction solvent, while methanol was utilized as the desorption solvent because of its high miscibility with water.

Extraction performance of the baicalin-functionalized monolithic silica coated fibers is presented in Figure 4.16. This results show that isoquercitrin, apigetrin, eriodictyol, quercetin, luteolin, apigenin was extracted by baicalin-functionalized monolithic silica fibers with higher percentage values. Extraction percentage of these flavonoids are almost 100.0%, while only eriodictyol was extracted as 79.33±5.93. From these results, it can be said that baicalin-functionalized monolithic silica adsorbed flavonoids from aqueous solutions. Sorption of flavonoids by baicalin-functionalized monolithic silica could be due to the the great conjugated system in baicalin molecules, and it has greater the charge transfer capacity through the increment of the electron density in the ring. In addition, it has hydrogen bonding capacity and π-π interaction (Qing et al. 2011). This properties thus makes the flavonoids to be extracted with the same skeleton (2-phenylchromone) of baicalin molecules. It could interact with the compounds possessing the same flavonoid skeleton. Hence, isoquercitrin and apigetrin seem to have similar structure with baicalin, since they are glucoside bound flavonoids, however quercetin, luteolin, and apigenin are the aglycones (having no glucoside in the structure. It has to be emphasized that they have differences in structures and polarities, whereas they all bound to baicalin-functionalized monolithic silica owing to posessing the same core flavonoid skeleton.

The extraction of these flavonoids in this study is higher than the literature study. Qing and co-workers synthesized baicalin-functionalized magnetic nanoparticles for selectively extracting flavonoids. In this study, they prepared iron nanoparticles and then coated with silica. Next, iron nanoparticles coated with silica was modified with baicalin. They reported that extraction efficiency of quercetin was 80.8±6.1%. In our study, the extraction efficiency has reached to 100.0%. This could be arised from the enhanced baicalin functionalization of monolithic silica surface. It correlates with the

elemental analysis results and baicalin loading in our study was calculated as 5.068%. Monolithic silica surface has more active binding sites to be functionalized, so the main outcome of this study is to use this property to extract flavonoids with higher amounts.

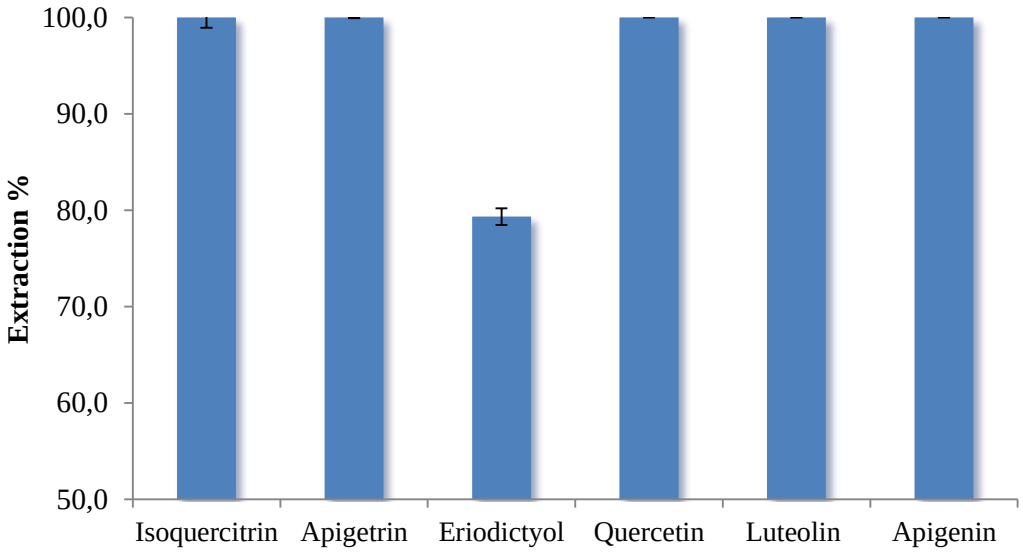

Figure 4.16. Extraction percentages of flavonoids (SPME conditions: 10.00 ml solution of 0.10 mg/L concentration, extraction time 5 min, stirring speed 360 rpm, at ambient temperature)

Isoquercitrin, apigetrin, quercetin, luteolin, and apigenin could be desorbed with methanol with higher amounts while eriodictyol is less (Figure 4.17.). This can be due to the lower extraction of eridocityol when compared with other flavonoids.

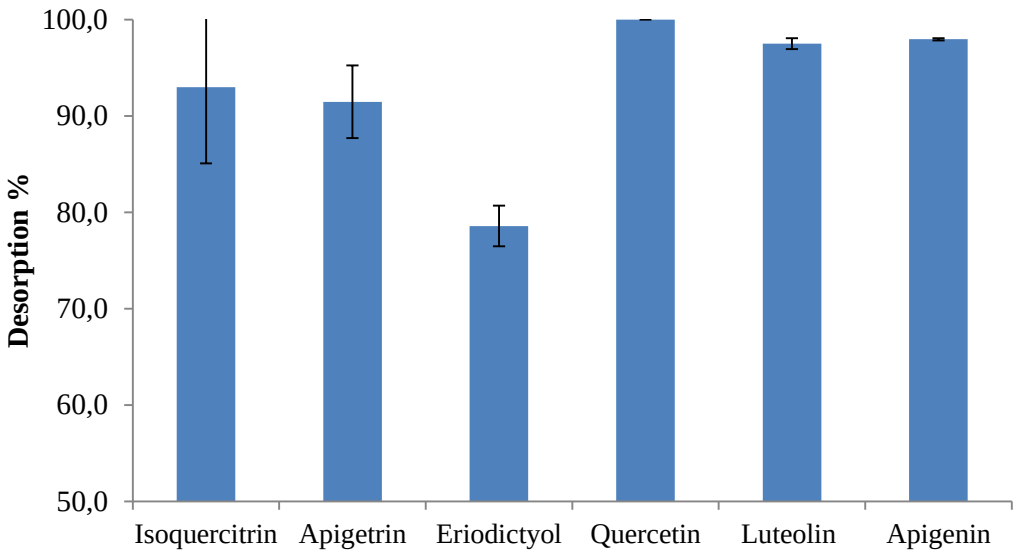

Figure 4.17. Desorption profile of flavonoids (SPME conditions: 10.00 ml solution of 0.10 mg/L concentration, extraction time and desorption time 5 min, stirring speed 360 rpm, at ambient temperature)

CHAPTER 5

NOVEL SOLID PHASE MICROEXTRACTION COATINGS FOR FLAVONOIDS PART III: MOLECULARLY IMPRINTED SILICA

5.1. Experimental

5.1.1. Reagents and Solutions

The chemicals and the reagents used for the synthesis of molecularly imprinted silica and molecularly imprinted silica coated fiber were indicated in Table 6.1.

5.1.2. Preparation of MIS SPME Fiber

A method from Dias and co-workers (2014) was used for the synthesis of the molecularly imprinted silica (MIS) mediated by Al^{3+}. In this method, quercetin as a template molecule, APTES as a functional monomer, TEOS as a crosslinker to form a polymeric network of a MIS, Al^{3+} as a Lewis acid site in the MIS structure were used to form a sol-gel. Figure 2.12. illustrates the preparation and the synthesis mechanism of MIS. To synthesize MIS, a 50.0 mg of quercetin was added into 10.0 mL of APTES at room temperature and it was dissolved completely. A 20.0 mL of TEOS and a 30.0 ml of 0.01 M of $AlCl_3$ were added to the solution above and it was stirred for 10 min. This stirring was done to complete the hydrolysis and polycondensation reaction. This homogenized solution became a gel. The gel was dried at 105°C for 2 h. To remove the quercetin from the MIS was first exposed to methanol-acetic acid (20:1, v/v) solution. Then, it was placed into the acetone, and waited for 6 h, and was dried at 60°C for 24 h. The obtained MIS was powdered, and it was used in the coating of bare silica fiber. The immobilization of the MIS was the same as in the baicalin-functionalized monolithic

silica, as the sol-gel solution became as a glue between the MIS silica and bare silica fiber surface (see .4.1.2.5.).

5.1.3. Extraction Studies

A 10.00 mL of ethanol-water (60:40, v:v) with a concentration of 0.10 mg/L flavonoids studied was transferred to a 20-mL amber glass vial containing a magnetic bar. The SPME extraction was performed with only baicalin-functionalized monolithic silica fiber for 5 min at room temperature with the solution being stirred at 300 rpm. After extraction, the extracted analytes on the SPME fiber were desorbed with 1.0 mL methanol in 5 min contact, and it was injected into the HPLC system for analysis.

Table 5.1. The properties of chemicals and reagents.

Item No	Reagent	Structure	Company	Product Code	Cas No	Purpose of Use
1	Quercetin (Flavonol), ≥ 95% (HPLC)	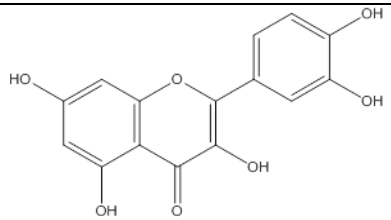	Sigma	Q4951	117-39-5	Standard, template molecule in the MIS synthesis
2	(3-aminopropyl)triethoxysilane	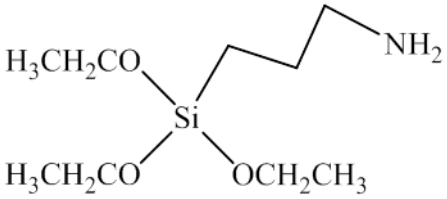			919-30-2	Functional monomer in the MIS synthesis
3	Tetraethylorthosilicate	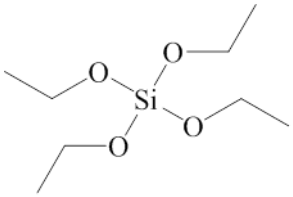	Merck	8.00658	78-10-4	Silica source in the MIS synthesis
4	Aluminum chloride, anhydrous, 98%		Merck	8.01081	7446-70-0	Lewis and Brønsted acid sites in the MIS synthesis

(cont. on next page)

Table 5.1. (cont.).

Item No	Reagent	Structure	Company	Product Code	Cas No	Purpose of Use
5	Methanol	-	Riedel	34885	67-56-1	Desorption solvent, mobile phase
6	Acetic acid		Merck	100056	64-19-7	Desorption solvent
7	Acetone		Merck	100020	67-64-1	Solvent for the complete removal of quercetin
8	Ethanol		Merck	111727	64-17-5	Extraction solvent

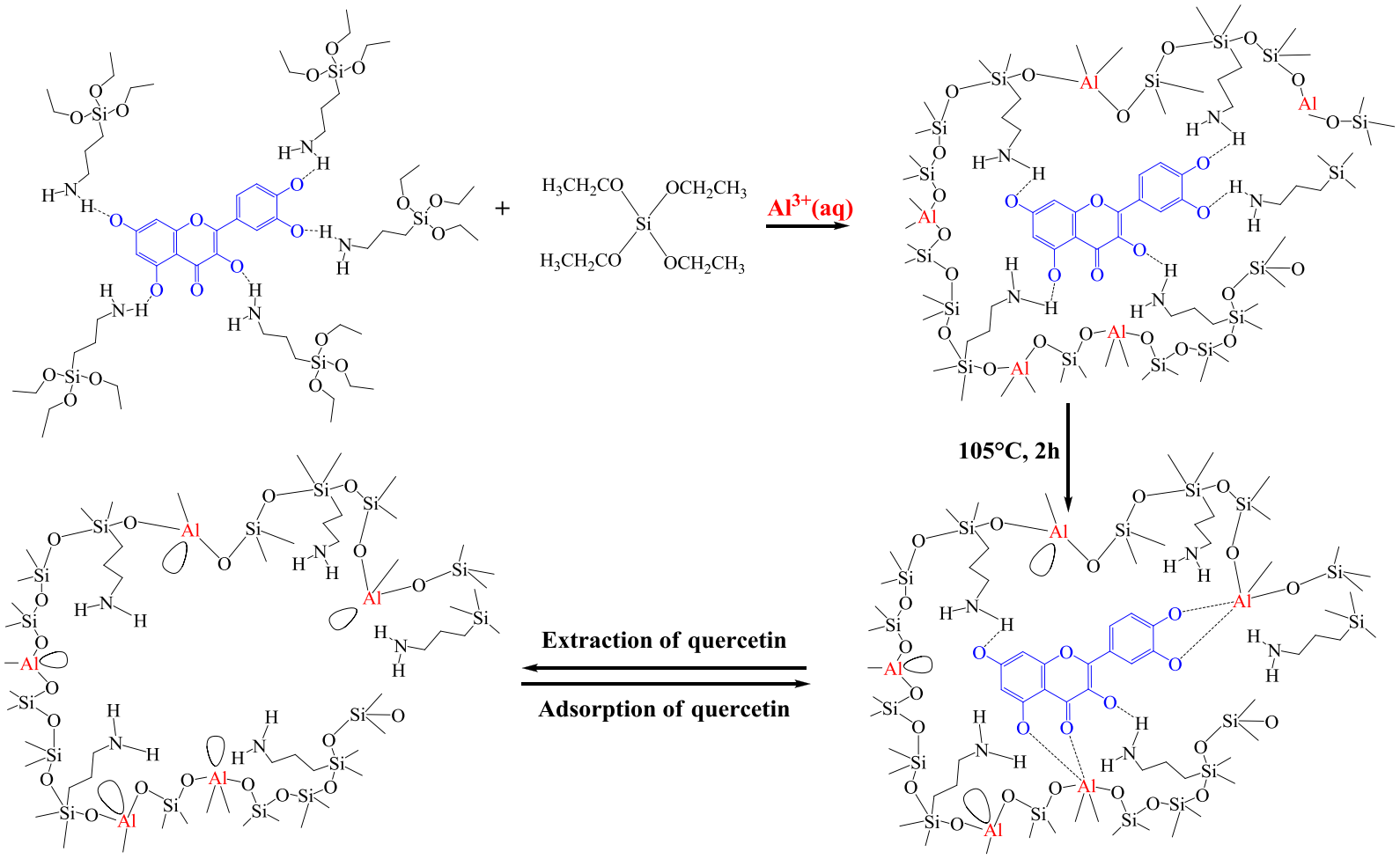

Figure 5.1. Mechanism proposal of MIS-Al synthesis
(Source: Dias A.C.B., 2014).

5.2. Results and Discussion

5.2.1. Characterization

5.2.1.1. SEM Images

Surface morhphology of molecularly imprinted silica prepared with 0.01 M and 0.10 M $AlCl_3$ was investigated by SEM images, and they are shown in Figure 5.2. and 5.3 with different magnifications and from different parts of the samples. All SEM images showed that molecularly imprinted silica samples have amorphous structure. SEM EDX results indicated the presence of aluminium in the silica structure (Figure 5.4. and Table 5.2.). The percentage of aluminium loaded in the molecularly imprinted silica prepared with 0.01 M $AlCl_3$ was found as 0.05%, while that prepared with 0.10 M $AlCl_3$ was 0.60% . Moreover, the increase in the concentration of aluminium came up with a conclusion with the higher aluminium percentage loaded in the molecularly imprinted silica. There were also increase in the chlorine percentages because of the higher concentration of $AlCl_3$ used during the synthesis. However, the percentages of C, N, O, and Si atoms seems to be unchanged for both molecularly imprinted silica samples.

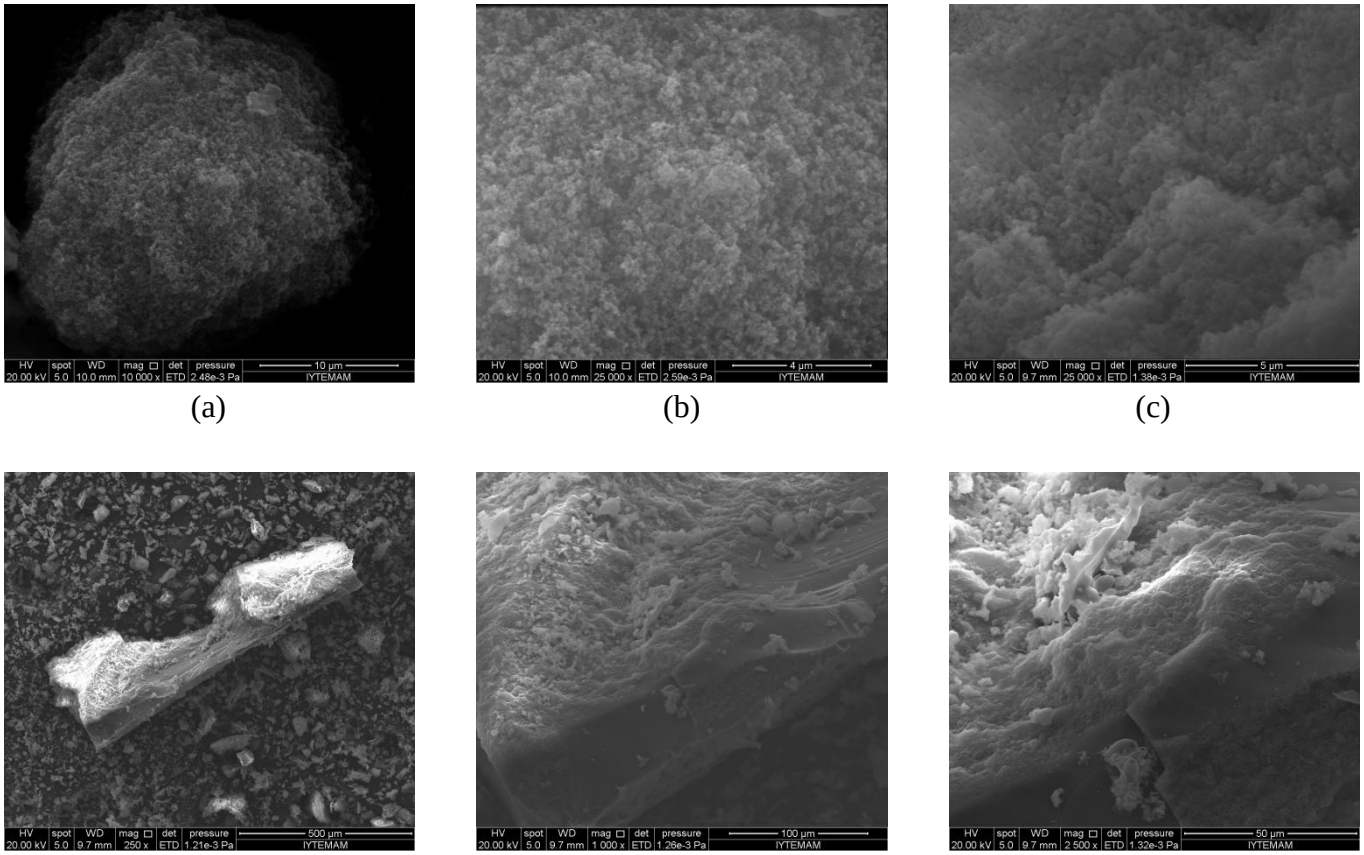

Figure 5.2. Sem images of MIS prepared with 0.01 M $AlCl_3$ (a, b, c, d, e, and f) at different magnifications

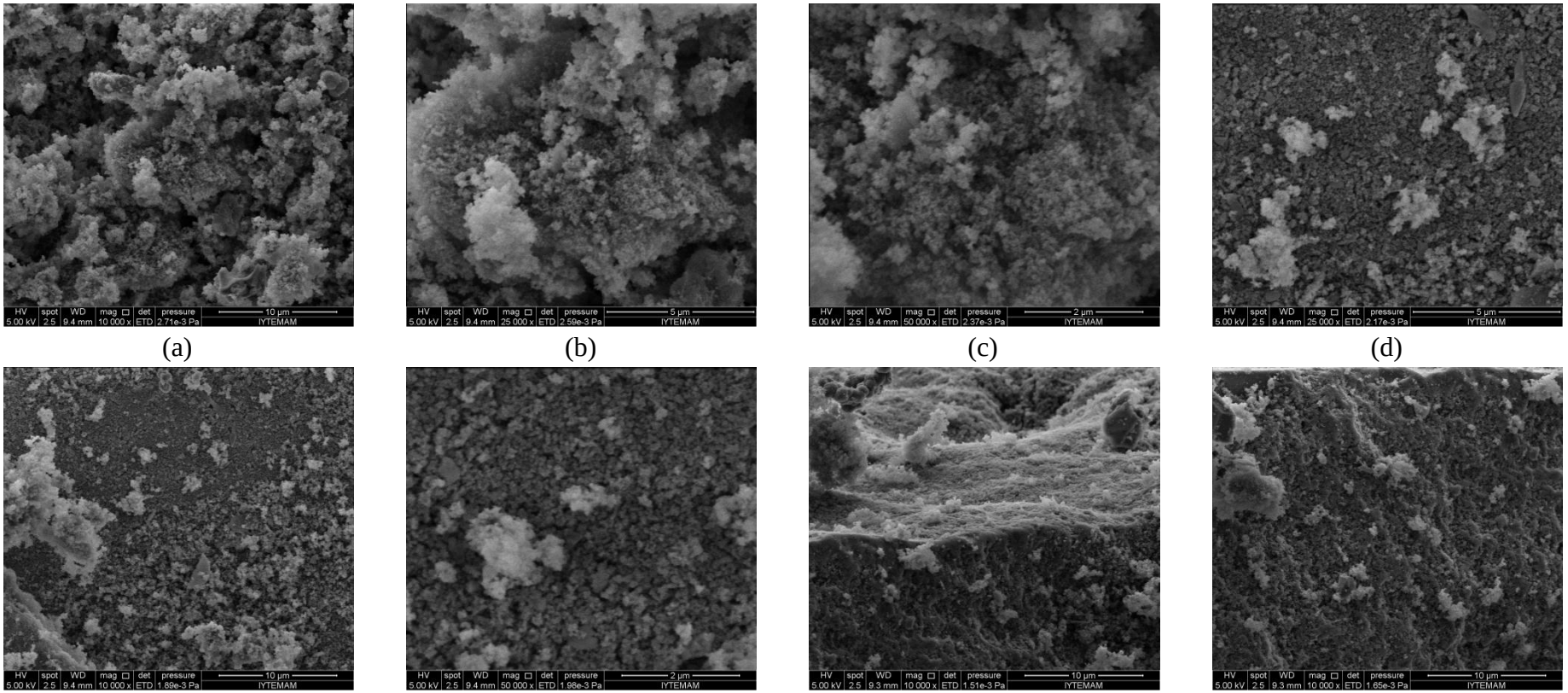

Figure 5.3. Sem images of MIS prepared with 0.1 M $AlCl_3$ (a, b, c, d, e, and f) at different magnifications

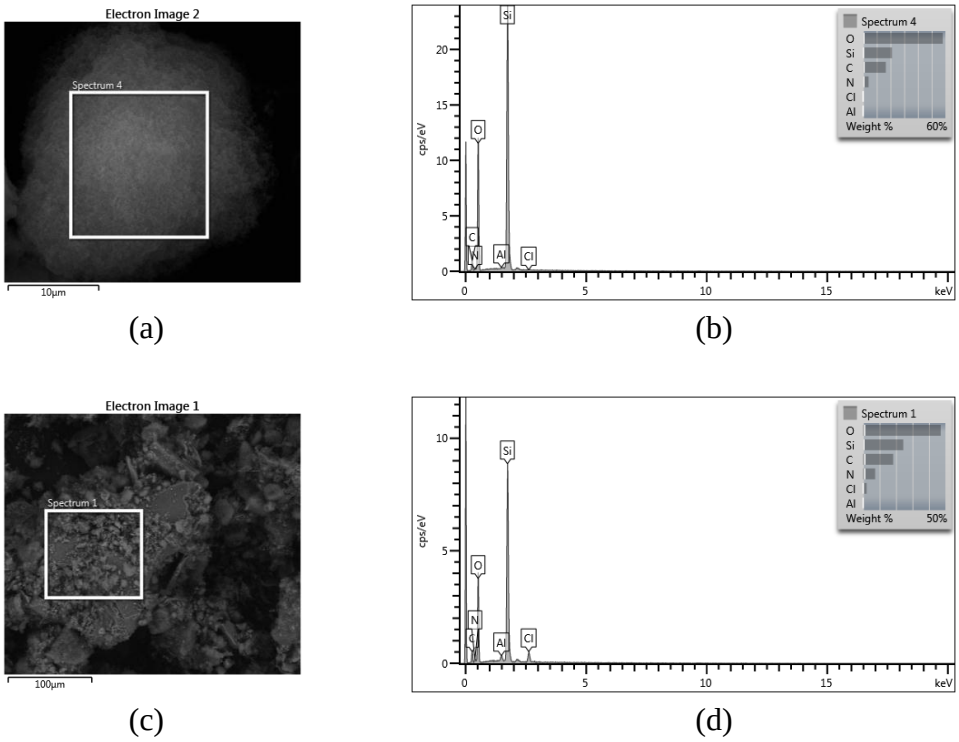

Figure 5.4. Sem EDX spectra of MIS prepared with 0.01 M $AlCl_3$ (a and b) and 0.1 M $AlCl_3$ (c and d)

Table 5.2. SEM EDX results of MIS

	Weight %	
Element	**0.01 M $AlCl_3$**	**0.1 M $AlCl_3$**
C	16.57	18.31
N	4.05	7.32
O	58.11	47.13
Al	0.05	0.60
Si	21.16	24.45
Cl	0.05	2.20

5.2.1.2. Elemental Analysis

Elemental composition of molecularly imprinted silica prepared with 0.01 M and 0.10 M $AlCl_3$ were determined, and are listed in Table 5.2. According to the results, the percentages of C, H, and N atoms were seemed to be unchanged, as the only change is that the concentration of $AlCl_3$ during sythesis. This change did not affect the elemental composition of these molecularly imprinted silica samples in terms of C%, H%, and N%. It was indicated that there is an agreement with the SEM EDX results and elemental analysis. For example, the percentages of C was determined as 16.57% with SEM EDX, and that was found as 12.790 with elemental analysis. The similar trend was seen in the N percentages (4.05% from SEM EDX and 4.062 from elemental analysis.

Table 5.3. Elemental composition of MIS in terms of %C, %H, %N, and %S.

Elements	%C	%H	%N	%S
MIS (0.01 M $AlCl_3$)	12.790	4.062	4.691	-
MIS (0.10 M $AlCl_3$)	12.960	4.382	4.718	-

5.2.1.3. FTIR Analysis

The functional groups in the molecularly imprinted silica obtained by FTIR are shown in Figure 5.5. These spectra were collected for molecularly imprinted silica prepared with both 0.01 M $AlCl_3$ and 0.10 M $AlCl_3$. These two spectra shows similar trend. The bands were intrinsic to the silica material, and the band was located at 3700-3200 cm^{-1} corresponds to the OH stretching vibrations of not only the Si-OH group but also Al-OH group, while that was at around 2920 cm^{-1} shows C-H stretching of sp^3 hybridized C atoms. The N-H stretching of the primary amine present in the functional monomer (APTES) was seen at 1561 cm^{-1}. The band at 1082 cm^{-1} indicates the strong Si-O bonds. In addition, Si-O-Si bending vibrations were located at 471 cm^{-1}.

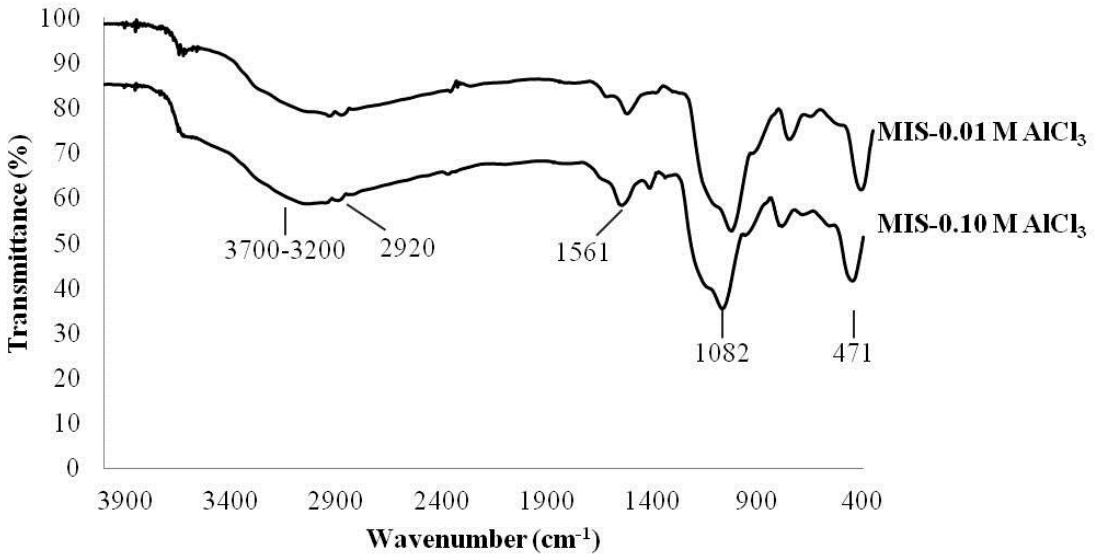

Figure 5.5. FTIR sectra of MIS prepared with 0.01 M $AlCl_3$ and 0.1 M $AlCl_3$

5.2.1.4. Thermal Gravimetric Analysis

TGA curves of molecularly imprinted silica which was prepared by 0.01 M and 0.10 M $AlCl_3$ are shown in Figure 5.6. The mass loss started below 130°C owing to the loss of water molecules bound in the molecularly imorinted silica. The weight loss continued until around 400°C which are the removal of the functional groups, OH, amine, ethyl groups in the molecularly imprinted silica. The similar thermal stability was seen from the molecularly imprinted silica samples prepared by different concentrations of $AlCl_3$. It is also clear that the thermal stability of the samples were not affected by the change in the concentration of $AlCl_3$.

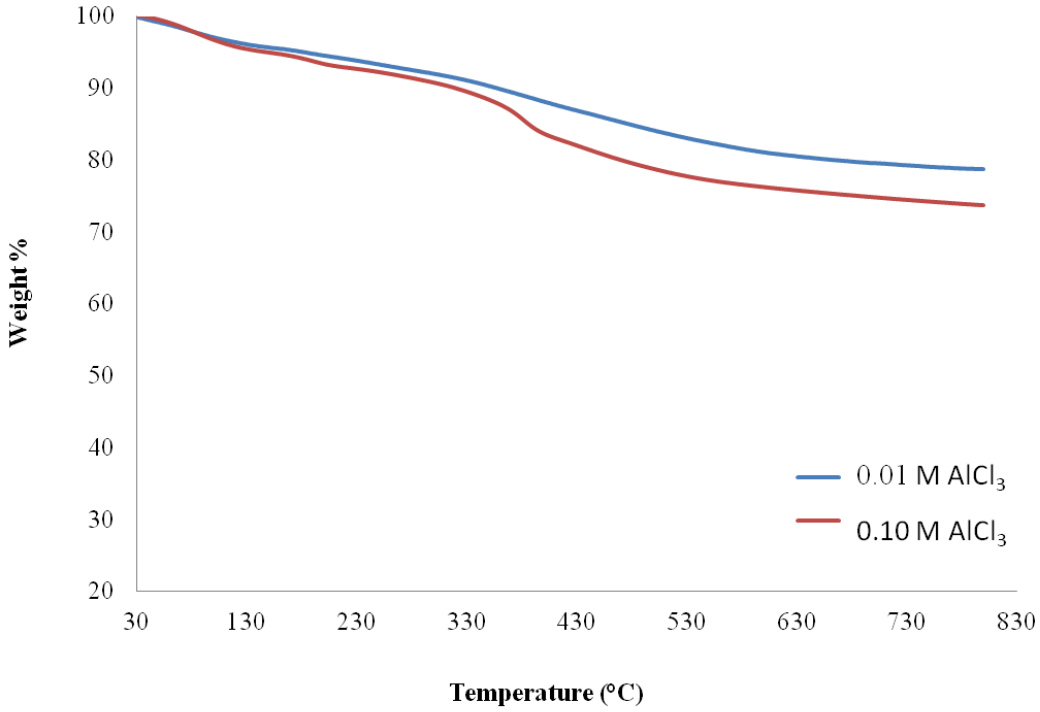

Figure 5.6. TGA decomposition curve of MIS prepared with 0.01 M $AlCl_3$ and 0.10 M $AlCl_3$

5.2.2. SPME of Flavonoids

The sorption behaviour of the MIS SPME fiber which relies on the molecular recognition of quercetin by MIS SPME fiber. This can be attributed to the two kinds of binding sites in the prepared MIS SPME fiber. First one is the interaction between the functional groups and hydroxyls (Lewis bases) of quercetin with the aluminum (complex formation). The second is the hydrogen bonds between the nitrogen atoms in the APTES (Dias et al. 2014). This characteristics of molecularly imprinted silica has an ability to extract quercetin, luteolin, apigenin, isoquercitrin, eriodictyol, and apigetrin with higher yields. The results are shown in Figure 5.7. In our study, the concentration of $AlCl_3$ was increased and the extraction of quercetin was reached to 100.0% once compared with the literature study (Dias et al. 2014). The number of complex formation of flavonoids with Al has enhanced by increasing the concentration of $AlCl_3$, and this may alter the extraction performance of molecularly imprinted silica in our study.

Figure 5.8. shows the desorption of flavonoids from the molecularly imprinted

silica. The desorption of flavonoids such as isoquercitrin, apigetrin, quercetin, luteolin, and apigenin ranges from 90.0 to 100.0%, where desorption of eriodictyol is 60.0 %.

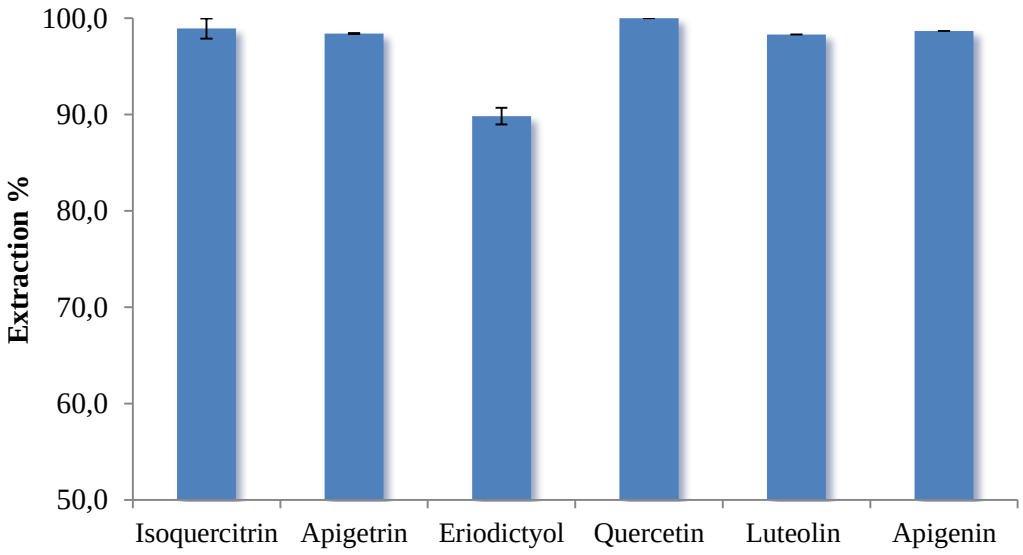

Figure 5.7. Extraction percentages of flavonoids (SPME conditions: 10.00 mL ethanol-water (60:40, v:v) solution of 0.10 mg/L concentration, extraction time 5 min, stirring speed 360 rpm, at ambient temperature)

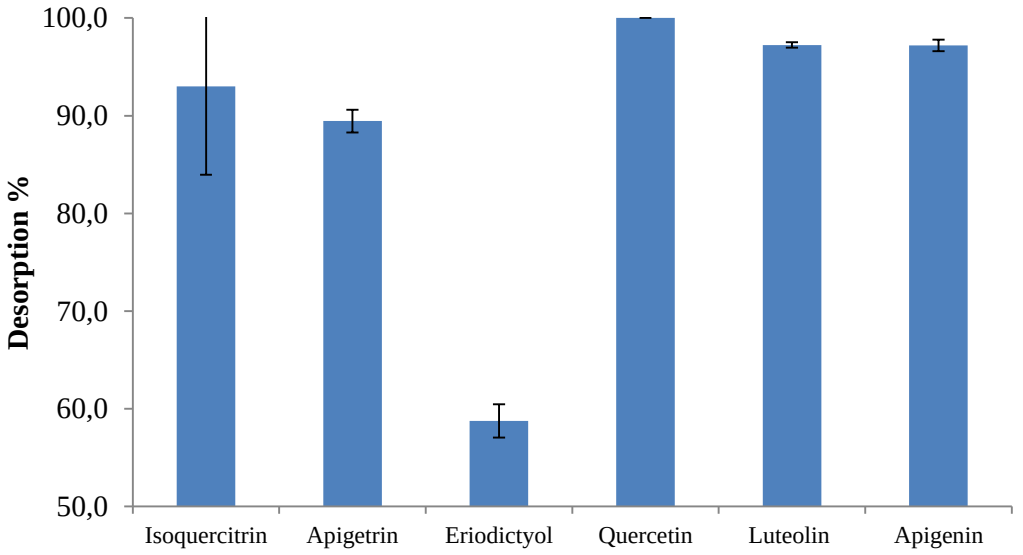

Figure 5.8. Desorption profile of flavonoids (SPME conditions: 10.00 mL solution of 0.10 mg/L concentration, extraction time and desorption time 5 min, stirring speed 360 rpm, at ambient temperature)

CHAPTER 6

CONCLUSION

This thesis study comprised of four parts: the first part is the method development. The method was developed for the separation of apigenin, apigetrin, eriodictyol, isoquercitrin, luteolin, and quercetin was performed by reversed-phase HPLC. The mobile phase was consisted of methanol and water containing 0.10 % acetic acid. The results obtained shows that the elution order of the compounds are as follows: isoquercitrin, apigetrin, eriodictyol, quercetin, and luteolin. Furthermore, their order of elution is based on the structural differences between them. Different wavelengths were obtained by UV spectra of flavonoids were used in the proper selection of detection wavelength. The practical detection wavelength was found to be 335 nm for all compounds studied.

Linearity, limit of detection (LOD), and limit of quantification (LOQ) were evaluated for quantitative purposes. The proposed method displayed a linear relationship between peak areas and concentrations for 0.05-20.0 mg/L for all compounds studied, with the correlation coefficient, $R^2 \geq 0.999$. The LOD and LOQ values for all compounds ranged from 0.003 to 0.013 and 0.011 to 0.043 mg/L, respectively.

Several extraction methods, like ultrasonic extraction, soxhlet extraction, and magnetic stirring (in the dark) have been performed. Eriodictyol extracted from *Laurus nobilis* is more than the other compounds studied. The higher quantities of flavonoids were extracted with ultrasonic extraction. Furthermore, two solvent systems were applied in the extraction, and the amount of flavonoids extracted using methanol- water (80:20, v/v) mixture is more than methanol.

The second part of the study is to prepare the solid phase microextraction coting with sol-gel method. The fibers were examined by scanning electron microscopy and the results show that dip-coating produced more homogeneous coatings. It is also shown that baicalin- and imidazole functionalization produced different layer thickness in the functionalized fibers.

The third part of the study is to synthesize baicalin- and imidazole-functionalized monolithic silicas and then used these as a solid phase microextraction coatings for flavonoids. The produced monolithic silicas were characterized by SEM, FTIR, elemental analysis, and TGA. SEM images showed that produced monolithic silica has honeycomb-like structure. Functionalization of monolithic silica has not an effect like deformation of honeycomb-like structure. Elemental composition of baicalin-functionalized monolithic silica showed that baicalin loading was increased with the use of monolithic silica as compared with literature study. This property makes the extraction performance of baicalin-functionalized monolithic silica coated fiber greater than the literature work. Thermal stability of monolithic silica and baicalin functionalized monolithic silica show differences.

In our study, the extraction efficiency has reached to 100.0%. This could be arised from the enhanced baicalin functionalization of monolithic silica surface. It correlates with the elemental analysis results and baicalin loading in our study was calculated as 5.068%. Monolithic silica surface has more active binding sites to be functionalized, so the main outcome of this study is to use this property to extract flavonoids with higher amounts. Isoquercitrin, apigetrin, quercetin, luteolin, and apigenin could be desorbed with methanol with higher amounts while eriodictyol is less. This can be due to the lower extraction of eridocityol when compared with other flavonoids.

In this work, the last part which includes the sythesis of molecularly imprinyted silica for the solid phase microextraction of isoquercitrin, apigetrin, eriodictyol, quercetin, luteolin and apğigenin. Surface morhphology of molecularly imprinted silica prepared with different concentration of M $AlCl_3$ was investigated by SEM images. All SEM images showed that molecularly imprinted silica samples have amorphous structure. SEM EDX results indicated the presence of aluminium in the silica structure . The percentage of aluminium loaded in the molecularly imprinted silica prepared with 0.01 M $AlCl_3$ was found as 0.05%, while that prepared with 0.10 M $AlCl_3$ was 0.60% . Moreover, the increase in the concentration of aluminium came up with a conclusion with the higher aluminium percentage loaded in the molecularly imprinted silica. There were also increase in the chlorine percentages because of the higher concentration of $AlCl_3$ used during the synthesis. However, the percentages of C, N, O, and Si atoms seems to be unchanged for both molecularly imprinted silica samples.

Elemental composition of molecularly imprinted silica prepared and according to the results, the percentages of C, H, and N atoms were seemed to be unchanged, as the only change is that the concentration of $AlCl_3$ during sythesis. This change did not affect the elemental composition of these molecularly imprinted silica samples in terms of C%, H%, and N%. It was indicated that there is an agreement with the SEM EDX results and elemental analysis. For example, the percentages of C was determined as 16.57% with SEM EDX, and that was found as 12.790 with elemental analysis. The similar trend was seen in the N percentages (4.05% from SEM EDX and 4.062 from elemental analysis.

The functional groups in the molecularly imprinted silica obtained by FTIR . FTIR spectra show the presence of Si-OH, Al-OH, amine groups. From the results, the thermal stability of the samples were not affected by the change in the concentration of $AlCl_3$.

The sorption behaviour of the MIS SPME fiber which relies on the molecular recognition of quercetin by MIS SPME fiber. This can be attributed to the two kinds of binding sites in the prepared MIS SPME fiber. First one is the interaction between the functional groups and hydroxyls (Lewis bases) of quercetin with the aluminum (complex formation). The second is the hydrogen bonds between the nitrogen atoms in the APTES. This characteristics of molecularly imprinted silica has an ability to extract quercetin, luteolin, apigenin, isoquercitrin, eriodictyol, and apigetrin with higher yields. In our study, the concentration of $AlCl_3$ was increased and the extraction of quercetin was reached to 100.0% once compared with the literature study. The number of complex formation of flavonoids with Al has enhanced by increasing the concentration of $AlCl_3$, and this may alter the extraction performance of molecularly imprinted silica in our study.

The desorption of flavonoids such as isoquercitrin, apigetrin, quercetin, luteolin, and apigenin ranges from 90.0 to 100.0%, where desorption of eriodictyol is 60.0 %.

REFERENCES

Afifi F.U., J.Z. Al-Kalaldeh, R. Abu-Dahab, 2010. Volatile oil composition and antiproliferative activity of *Laurus nobilis*, *Origanum syriacum, Origanum vulgare,* and *Salvia triloba* against human breast adenocarcinoma cells. *Nutrition Research* 30:271–278.

Andersen Ø.M. and K.R. Markham. 2006. Flavonoids. Chemistry, Biochemistry and Applications: CRC Press, Taylor and Francis Group: Baca Raton, Finland.

Aruoma O., T. Bahorun, L. Jen. 2003. Neuroprotection by Bioactive Components in Medicinal and Food Plant Extracts. *Mutation Research/ Reviews in Mutation Research* 544(2–3):203–215.

Boukef, M., K., 1986. Les plantes dans la médecine traditionnelle Tunisienne. Paris, Agence de coopération culturelle et technique.

Castilho P.C., J. Luna-Herrera, M. C. Costa, H. G. González, A. I. Rodrigues, 2007. Synergistic antimycobacterial activities of sesquiterpene lactones from *Laurus spp.* Journal of Antimicrobial Chemotherapy 59:548–552.

Cimpan G., S. Gocan. 2002. Analysis of medicinal plants by HPLC: recent approaches. *Journal of Liquid Chromatography and Related Technologies* 25:2225-2292.

Conforti, F., Statti, G., Uzunov, D., Menichini, F., 2006. Comparative chemical composition and antioxidant activities of wild and cultivated *Laurus nobilis* L. leaves and *Foeniculum vulgare* subsp. *piperitum* (Ucria) coutinho seeds. *Biological and Pharmaceutical Bulletin* 29:2056-2064.

Corradinia E.; P. Fogliaa; P. Giansantia; R. Gubbiottia; R. Samperia; A. Laganàa. 2011. Flavonoids: chemical properties and analytical methodologies of identification and quantitation in foods and plants. *Natural Product Research* 25(5):469-495.

Cuyckens F., A.A. Shahat, H. Van den Heuvel, K.A. Abdel- Shafeek, M.M. El-Messiry, M.M. Seif-El Nasr. 2003. The application of liquid chromatography–electrospray ionization mass spectrometry and collision-induced dissociation in the structural characterization of acylated flavonol O-glycosides from the seeds of Carrichtera annua. *European Journal of Mass Spectrometry* 9:409–420.

D'Archivio M., C. Filesi, R. Di Benedetto, R. Gargiulo, C. Giovannini, R. Masella. 2007. Polyphenols, dietary sources and bioavailability. *Annali dell'Istituto Superiore di Sanità* 43(4): 348-361.

Daher, S. and F:O: Gulacar. 2008. Analysis of phenolic and other aromatic compounds in honeys by solid-phase microextraction followed by gas chromatography-mass spectrometry. *J Agric Food Chem* 56 (14), 5775-80.

Dall'Acqua, S., Cervellati, R., Speroni, E., Costa, S., Guerra, M. C., Stella, L., Greco, E., Innocenti, G., 2009. Phytochemical composition and antioxidant activity of *Laurus nobilis L*. leaf infusion. *Journal of Medicinal Food* 12:869-876.

Dalluge J.J., B.C. Nelson, J. Brown Thomas, L.C. Sander. 1998. Selection of column and gradient elution system for the separation of catechins in green tea using high-performance liquid chromatography. *Journal of Chromatography A* 793:265-274.

De Corato U., O. Maccionia, M. T. G. Di Sanzo. 2010. Use of essential oil of *Laurus nobilis* obtained by means of a supercritical carbon dioxide technique against post harvest spoilage fungi. *Crop Protection* 29(2):142-147.

De Marino, S., Borbone, N., Zollo, F., Ianaro, A., Di Meglio, P., Iorizzi, M., 2004. Megastigmane and phenolic components from *Laurus nobilis L.* leaves and their inhibitory effects on nitric oxide production. *Journal of Agricultural and Food Chemistry* 52:7525-7531.

Demo, A., Petrakis, C., Kefalas, P., Boskou, D., 1998. Nutrient antioxidants in some herbs and Mediterranean plant leaves. *Food Research International* 31:351-354.

Derwich E., Z. Benziane,A. Boukir. 2009. Chemical Composition and Antibacterial Activity of Leaves Essential Oil of *Laurus nobilis* from Morocco. *Australian Journal of Basic and Applied Sciences* 3(4):3818-3824.

Dias A.C.B., L.R. Braga, A.A. Rosa. 2014. Synthesis and characterization of molecularly imprinted silica mediated by Al^{3+} for solid phase extraction of quercetin in *Ginkgo biloba L*. *Analytical Methods* . Accepted March 25, 2014. doi: 10.1039/C4AY00471J.

Djozan D., M. Mahkam, B. Ebrahimi, 2009. Preparation and binding study of solid-phase microextraction fiber on the basis of ametryn-imprinted polymer: Application to the selective extraction of persistent triazine herbicides in tap water, rice, maize and onion. *Journal of Chromatography A* 1216:2211-2219.

Djozan D., T. Baheri, 2007. Preparation and evaluation of solid-phase microextraction fibers based on monolithic molecularly imprinted polymers for selective extraction of diacetylmorphine and analogous compounds. *Journal of Chromatography A* 1166:16-23.

Djozan D., T. Baheri, M.H.P. Azar, M. Mahkam, 2007. Preparation of New Fibers on the Basis of Codeine Imprinted Polymer. *Materials and Manufacturing Processes* 22:758-763.

Dorman H.J.D., M. Koşar, R. Hiltunen. 2005. Effect of an acid treatment on the phytochemical and antioxidant characteristics of extracts from selected Lamiaceae species. *Food Chemistry* 91:525-533.

Feng Y.Q., H.J. Zhang, J.F. Huang, H. Wang, 2006. Determination of low-aliphatic aldehyde derivatizatives in human saliva using polymer monolith microextraction coupled to high-performance liquid chromatography. *Analytica Chimica Acta* 565:129-135.

Frega N., L. S. Conte, G. Lercker, P. Capella. 1982. Composition of drops of *Laurus nobilis Rivista Italiana delle Sostanze Grasse*. 59:329-333.

Gan F., L. Wang, G. Shao. 2012. Selectivity of two types of sulfadimidine-imprinted monolithic polymer-based fibers. *Journal of Separation Science* 35:816-822.

Gladstar R., P. Hirsch. 2000. Planting the Future. *Inner Traditions/Bear and Company*.

Gómez-Coronado D. J. M., C. Barbas. 2003. Optimized and validated HPLC method for α and γ-tocopherol measurement in Laurus nobilis leaves. New data on tocopherol content. *Journal of Agricultural and Food Chemistry* 51:5196-5201.

Hrazdina G. 1982. Anthocyanins, in J.B. Harborne and T.J. Mabry (eds.), The Flavonoids: Advances in Research, Chapman and Hall Ltd, Cambridge, Great Britain.

Hussein L., M.A. Fattah, E. Salem. 1990. Characterization of pure proanthocyanidins isolated from the hulls of faba beans. *Journal of Agricultural and Food Chemistry*. 38(1):95-98.

Iwashina T. 2003. Flavonoid function and activity to plants and other organisms. *Biological Sciences in Space* 17:24–44.

Justesen U., P. Knuthsen, T. Leth. 1998. Quantitative analysis of flavonols, flavones, and flavanones in fruits, vegetables and beverages by high-performance liquid chromatography with photo-diode array and mass spectrometric detection. *Journal of Chromatography A* 799:101–110.

Kataoka H. 2010. Recent developments and applications of microextraction techniques in drug analysis. *Analytical Bioanalytic Chemistry* 396:339-364.

Khorrami A.R., E. Narouenezhad, 2011. Synthesis of molecularly imprinted monolithic fibers for solid-phase microextraction of acetaldehyde from head-space of beverages stored in PET bottles. *Talanta* 86:58-63.

Kinoshita E., Y. Ozawa, T. Aishima. 1997. Novel tartaric acid isoflavone derivatives that play key roles in differentiating Japanese soy sauces. *Journal of Agricultural and Food Chemistry* 45:3753-3759.

Leung, A. Y., S. A. Foster. 1999. *Enciclopedia delle Piante Medicinali* Aporie: Roma: Italy.

Liu X.D., S. Tokurab, M. Harukia, N. Nishia, N. Sakairi. 2002. Surface modification of nonporous glass beads with chitosan and their adsorption property for transition metal ions. *Carbohydrate Polymers* 49(2):103–108.

Liu, M. H., N. Otsuka, K Noyori, S. Shiota,W. Ogawa, T. Kuroda, T. Hatano, T. Tsuchiya. 2009. Synergistic effect of kaempferol glycosides purified from *Laurus nobilis* and fluoroquinolones on methicillin-resistant Staphylococcus aureus. *Biological and Pharmaceutical Bulletin* 32:489-492.

Loiola A.R., L.R. D. da Silva, P. Cubillas, M.W. Anderson, 2008. Synthesis and characterization of hierarchical porous materials incorporating a cubic mesoporous phase. *Journal of Material Chemistry* 18:4985-4993.

Loizzo M. R., A. M. Saab, R. Tundis, G. A. Statti, F. Menichini, I. Lampronti, R. Gambari, J. Cinatl, H. W. Doerr 2008. Phytochemical Analysis and in vitro Antiviral Activities of the Essential Oils of Seven Lebanon Species. *Chemistry and Biodiversity* 5:461-470.

Mabry T.J., K.R. Markham, M. Thomas. 1970. The systematic identification of flavonoids. New York: Springer-Verlag.

Marzouki H, A. Khaldi, R. Chamli, S. Bouzid, A. Piras, D. Falconieri, B. Marongiu. 2009. Biological activity evaluation of the oils from Laurus nobilis of Tunisia and Algeria extracted by supercritical carbon dioxide. Natural Product Research 23(3):230-237.

Merken H.M. and G.R. Beecher. 2000. Measurement of food flavonoids by high-performance liquid chromatography: a review. Journal of Agricultural and Food Chemistry 48(3):577-579.

Misharina T. A., M. B. Terenina, and N. I. Krikunova. 2009. Antioxidant Properties of Essential Oils. *Applied Biochemistry and Microbiology* 45(6):642-647.

Monici M., P. Baglioni, P., N. Mulinacci, A. Baldi, F.F. Vincieri. 1994. A research model on flavonoids as photoprotectors: studies on the photochemistry of kaempferol and pelargonidin. *Acta Horticulturae* 381:340–347.

Mumper R.J. and J. Dai. 2010. Plant Phenolics: Extraction, Analysis and Their Antioxidant and Anticancer Properties. *Molecules* 15:7313-7352.

Papageorgiou, V., A. Mallouchos, M. Komaitis. 2008. Investigation of the antioxidant behaviour of air- and freeze-dried aromatic plant materials in relation to their phenolic content and vegetative cycle. *Journal of Agricultural and Food Chemistry* 56:5743-5752.

Pawliszyn J. 1999. Application of solid phase microextraction. *RSC Publication.*

Politeo O., M. Jukic, M. and Miloš, 2007. Chemical composition and antioxidant activity of free volatile aglycones from bay (*Laurus nobilis* L.) compared to its essential oil. *Croatia Chemica Acta* 80:121-126.

Prasad B.B., M.P. Tiwari, R. Madhuri, P.S. Sharma, 2011. Enantioselective separation and electrochemical sensing of d- and l-tryptophan at ultratrace level using molecularly imprinted micro-solid phase extraction fiber coupled with complementary molecularly imprinted polymer-fiber sensor. *Journal of Chromatography B* 879:364-370.

Puoci F, G. Cirillo, M. Curcio, F. Iemma,U.G. Spizzirri, N. Picci. 2007. Molecularly imprinted solid phase extraction for the selective HPLC determination of alpha-tocopherol in bay leaves. *Analytica Chimica Acta* 593:164-170.

Qing L-S., X. Liao, J. Xiong, Y. Xue, Yi-Ming Liu, B. Guang, Li-Sheng Ding. 2011. *J. Sep. Sci*., 34:3240–3245.

Robards K., M. Antolovich. 1997. Analytical chemistry of fruits bioflavonoids. *Analyst* 122:11–34.

Row K.H., Y. Wang, T. Zhu. 2010. Journal of Chromatographic Science, 48:690-693.

Sakakibara H., Y. Honda, S. Nakagawa, H. Ashida, K. Kanazawa. 2003. Simultaneous determination of all polyphenols in vegetables, fruits and teas. *Journal of Agricultural and Food Chemistry* 51(3):571-581.

Sargenti S.R. W. Vichnewski. 2000. Sonication and liquid chromatography as a rapid technique for extraction and fractionation of plant material. *Phytochemical Analysis*., 11(2):69-73.

Simic, A., M. Sokovic, M. Ristic, S. Grujic-Jovanovic, J. Vukojevic, P. Marin. 2004. The Chemical Composition of some Lauraceae essential oils and their antifungal activities. *Phytotherapy Research* 1:713-717.

Škerget M.; P. Kotnik, M. Hadolin, A.R. Hraš, M. Simonič, Ž. Knez. 2005. Phenols, proanthocyanidins, flavones and flavonols in some plant materials and their antioxidant activities. *Food Chemistry*.89:191-198.

Takeda K., Y. Tochika, R. Fukazawa, T. Mori. 1994. Flavonoids as UV-protectant. *Acta Horticulturae*. 381, 348–354.

Turkish Plants Data Service (TÜBİVES). http://turkherb.ibu.edu.tr/index.php (accessed June 3, 2011).

Vasapollo G., L. Longo. 2005. Anthocyanins from Bay (*Laurus nobilis L.*) Berries. *Journal of Agricultural and Food Chemistry* 53:8063-8067.

Veličković D.T., M.T. Nikolova, S.V. Ivancheva, J.B. Stojanović, V.B. Veljković. 2007. Extraction of flavonoids from garden (*Salvia officinalis* L.) and glutinous (*Salvia glutinosa* L.) sage by ultrasonic and classical maceration. *Journal of Serbian Chemical Society* 72(1):73–80.

Vuckovic D. 2013. High-throughput solid-phase microextraction in multi-well-plate format. *TrAC Trends in Analytical Chemistry* 45:136-153.

Walker J. B., K.J. Sytsma, J. Treutlein, M. Wink. 2004. '*Salvia* (Lamiaceae) is not monophyletic: implications for the systematics, radiation, and ecological specializations of Salvia and tribe Mentheae. *American Journal of Botany* 91:1115–25.

Wang Q., G.A. Baker,; S.N. Baker, L. A. Colón. 2006. Surface confined ionic liquid as a stationary phase for HPLC. *Analyst* 131 (9):1000-1005.

Wang Y., T. Zhu, K.H. Row. 2010. Preparation and Evaluation of Silica-Based Ionic Liquid-Modified Stationary Phase for HPLC. *Journal of Chromatographic Science* 48:690-693.

Wikipedia. http://en.wikipedia.org/wiki/Laurus_nobilis (accessed December 23, 2011).

Zhang G., H. Xua, S. Wanga, S. Huang, D. Songa, Y. Zhoua, G. Longa, 2011. A novel solid-phase microextraction method based on polymer monolith frit combining with high-performance liquid chromatography for determination of aldehydes in biological samples. *Analytica Chimica Acta* 690:86-93.

Zhang X., S. Xu, J.M. Lim, Y. Lee, 2012. Molecularly imprinted solid phase microextraction fiber for trace analysis of catecholamines in urine and serum samples by capillary electrophoresis. *Talanta* 99:270–276.

Zhang X., S. Xu, Y. Suna, D. Yua. 2013. Microwave-assisted preparation of monolithic molecularly imprinted polymeric fibers for solid phase microextraction. *Analyst* 138:2982–2987.

Zhang Y.P., Y.F. Jin, M.X. Huang, L.Y. Bai, M.L. Lee, 2013. A novel method to prepare monolithic molecular imprinted polymer fiber for solid-phase microextraction by microwave irradiation. *Journal of Separation Science* 36:1429-1436.

Zhang, Y.P., Y.F. Jin, N. Chen, R.Q. Liu, L.Y. Bai, J. Chen, 2013. Rapid Preparation of Monolithic Molecular Imprinted Polymer Fiber for Solid Phase Microextraction by Microwave Irradiation. *Journal of the Chinese Chemical Society* 60:1043-1049.

VITA

Name :Meral ESEN
Date and Place of Birth: 15.08.1981, İzmir
Nationality: Turkish (TC)
E-mail: karaca_meral@hotmail.com

EDUCATION

[2008-2014] Ph.D. İzmir Institute of Technology (Faculty of Science, Department of Chemistry)
Dissertation: Preparation of Novel Fiber Coatings for Solid Phase Microextraction of Flavonoids
[2005-2008] M.Sc. İzmir Institute of Technology (Faculty of Science, Department of Chemistry)
Dissertation: Biosorption of aqueus Pb^{2+}, Cd^{2+}, and Ni^{2+} ions by *Dunaliella salina, Oocystis sp., Porphyridium cruentum,* and *Scenedesmus protuberans* prior to atomic spectrometric determination
[1999-2005] B.Sc. İzmir Institute of Technology (Faculty of Science, Department of Chemistry)

ACADEMIC POSITIONS HELD

[2006 December-2014 June] Research Assistant
İzmir Institute of Technology
Faculty of Science, Department of Chemistry, İzmir, Turkey
Assisted undergraduate courses: General Chemistry, General Chemistry Laboratory I-II, Analytical Chemistry Laboratory I-II, Instrumental Analysis Laboratory, and Organic Chemistry Laboratory I-II.

WORK EXPERIENCE

Year Place Enrollment
2014 July-still continue Ege University, Faculty of Science, Department of Chemistry, İzmir, TURKEY, Chemist
2004 July-August Ministry of Justice, İzmir Institution of Forensic Medicine (Narcotic and Toxicology Laboratories), Trainee
2004 August-September Ministry of Health**,** İzmir Refik Saydam National Public Health Agency (Drinking Water and Waste Water Laboratories), Trainee

FOREIGN LANGUAGES

English (Advanced), German (Beginner), Italian (Beginner)

AWARDS

EXTECH 2012, 14th International Symposium on Advances in Extraction Technologies, 24-26 September 2012, Messina, ITALY - Best Poster Award (Royal Society of Chemistry sponsored)